COGNITIVE-MOTOR INTEGRATION IN NORMAL AGING AND PRECLINICAL ALZHEIMER'S DISEASE: NEURAL CORRELATES AND EARLY DETECTION

Kara M. Hawkins

A dissertation submitted to the Faculty of Graduate Studies in partial fulfillment of the requirements for the degree of

Doctor of Philosophy

Graduate Program in Kinesiology and Health Science
York University
Toronto, Ontario
May, 2015

ABSTRACT

The objectives of the studies included in this dissertation were to characterize how the ability to integrate cognition into action is disrupted by both normal and pathological aging, to evaluate the effectiveness of kinematic measures in discriminating between individuals who are and are not at increased Alzheimer's disease (AD) risk, and to examine the structural and functional neural correlates of cognitive-motor impairment in individuals at increased AD risk. The underlying hypothesis, based on previous research, is that measuring visuomotor integration under conditions that place demands on visual-spatial and cognitive-motor processing may provide an effective behavioural means for the early detection of brain alterations associated with AD risk. To this end, the first study involved testing participants both with and without AD risk factors on visuomotor tasks using a dual-touchscreen tablet. Comparisons between high AD risk participants (n = 22; mean age = 67.7 +/- 11.3) and both young (n = 22; mean age = 26.4 +/- 4.1) and old (n=22 mean age = 64.3 +/- 10.1) healthy control groups revealed significant performance disruptions in at-risk participants in the most cognitively demanding task. Furthermore, a stepwise discriminant analysis was able to distinguish between high and low AD risk participants with a classification accuracy of 86.4% (sensitivity: 81.8%, specificity: 90.9%).

Based on the prediction that the impairments observed in high AD risk participants reflect disruption to the intricate reciprocal communication between hippocampal, parietal, and frontal brain regions required to successfully prepare and update complex

reaching movements, the second and third studies were designed to examine the underlying structural and functional connectivity associated with cognitive-motor performance. Young adult (n = 10; mean age = 26.6 +/- 2.7), and both low AD risk (n = 10; mean age = 58.7 +/- 5.6) and high AD risk (n = 10; mean age = 58.5 +/- 6.9) older adult participants underwent anatomical, diffusion-weighted, and resting-state functional connectivity scans. These data revealed significant age-related declines in white matter integrity that were more pronounced in the high AD risk group. Decreased functional connectivity in the default mode network (DMN) was also found in high AD risk participants. Furthermore, measures of white matter integrity and resting-state functional connectivity with DMN seed-regions were significantly correlated with task performance. These data support our hypothesis that disease-related disruptions in visuomotor control are associated with identifiable brain alterations, and thus behavioural assessments incorporating both cognition and action together may be useful in identifying individuals at increased AD risk.

ACKNOWLEDGMENTS

I am incredibly lucky to have such a wonderful and loving family, making it very easy for me to honestly say that family comes first. So to start off I would like to thank my loving husband and best friend Gord, and my parents John and Debbie for their endless support. Thanks for always being there, no matter what. I would also like to thank my second set parents, Nancy and Ian, for their encouragement and understanding throughout this long process, including putting a roof over our heads when needed and even participating, along with my parents, as research subjects in my studies. My success is very much thanks to the intelligent, caring, and supportive families that I am surrounded by, including my brothers and extended family members. Thank you for both literally and figuratively helping us build a safe, warm, and beautiful home for the newest member of our family – Milla you light up our lives and we love you very much!

I would also like to thank my close friends for helping me keep an open-mind and providing me with a retreat from the often esoteric life of a graduate student. Last, but not least, I would like to thank my encouraging and understanding supervisor Dr. Lauren Sergio, my lab-mates (Patricia, Josh, Farah, David, and Diana), and those who have offered me guidance along the way (Dr. Guy Proulx, Dr. Will Gage, Dr. Denise Henriques, Dr. Gary Turner, Merv Mosher, Aman Goyal, Heather McGregor, and Rodrigo Perea). Lauren, thank you for the freedom, mentorship, and adventures that have helped me become more independent, competent, and confident. I will always be grateful for this experience!

TABLE OF CONTENTS

LIST OF TABLES

LIST OF FIGURES

Glossary of Abbreviations

Abbreviation	Non-Abbreviated Term
AD	Alzheimer's disease
ANCOVA	Analysis of covariance
ANOVA	Analysis of variance
ApoE	Apolipoprotein E
ApoE4	Apolipoprotein E epsilon 4
Aβ	Amyloid-beta
BA	Brodmann area
BOLD	Blood-oxygenation-level dependent
CC	Corpus callosum
CE	Constant error
CG	Cingulum bundle
CHT	Centre hold time
CPL	Corrective path length
CST	Corticospinal tract
DA	Axial diffusivity
DMN	Default mode network
DR	Radial diffusivity
DTI	Diffusion tensor imaging
EPI	Echo planar imaging
FA	Fractional anisotropy
FC	Functional connectivity
FDT	FMRIB's Diffusion Toolbox
FEAT	FSL's FMRI Expert Analysis Tool
FH+	Family history positive
FMa	Forceps major
FMi	Forceps minor
FMRIB	Functional Magnetic Resonance Imaging of the Brain
FOV	Field of view
FR	Feedback reversal
FSL	FMRIB Software Library
ICA	Independent component analysis
IFG	Inferior frontal gyrus
IFOF	Inferior fronto-occipital fasciculus
ILF	Inferior longitudinal fasciculus

IPL	Inferior parietal lobule
JHU	Johns Hopkins University
LFP	Local field potential
LOC	Lateral occipital cortex
M1	Primary motor cortex
MCI	Mild cognitive impairment
MD	Mean diffusivity
MFG	Middle frontal gyrus
MNI	Montreal Neurological Institute
MoCA	Montreal Cognitive Assessment
MPRAGE	Magnetization prepared rapid gradient echo
MRHH	Mackenzie Richmond Hill Hospital
MRI	Magnetic resonance imaging
MT	Movement time
MTG	Middle temporal gyrus
PCR	Polymerase chain reaction
PCUN	Precuneus
PD	Plane dissociated
PD+FR	Plane dissociated plus feedback reversal
PET	Positron emission tomography
PiB	Pittsburgh compound-B
PMv	Ventral premotor cortex
PPC	Posterior parietal cortex
rs-fMRI	resting-state functional magnetic resonance imaging
RT	Reaction time
S	Standard condition
SD	Standard deviation
SFG	Superior frontal gyrus
SLF	Superior longitudinal fasciculus
SPL	Superior parietal lobule
SPSS	Statistical package for the social sciences
TBI	Traumatic brain injury
TBSS	Tract-based spatial statistics
TE	Echo time
TFCE	Threshold-free cluster enhancement
THAL	Thalamus
THT	Target hold time

TMS	Transcranial magnetic stimulation
TMT	Total movement time
TOI	Tract of interest
TR	Repetition time
VE	Variable error
VR	Virtual reality
WM	White matter

Chapter One

General Introduction

1.1 Introduction

The underlying theory guiding this dissertation is that different types of visuomotor compatibility are processed in separate, but overlapping, parietofrontal networks, and that these separate networks are affected differently in healthy aging versus disease. Generally when reaching for an object in the environment the visual stimulus and its required motor action are in alignment. However, the evolution of the capacity for tool-use in primates has resulted in situations where the correspondence between vision and action is not direct. A common example is the use of a computer mouse to move a cursor on a monitor, which involves a decoupling, or dissociation, between the spatial location of the visual target and the spatial location of the movement goal. Such learned sensory- and/or cognitive-motor transformations underlie much of our everyday activities (including driving), yet the basic cortical mechanisms responsible for these behaviours remain unknown. Following damage to the cerebral cortex (e.g. neurodegeneration, stroke, traumatic brain injury), these complex visuomotor transformations may become impaired, and, in turn, the pattern of impairment may provide insight into the underlying neural mechanisms involved in this behaviour. The research projects presented here were designed to 1) characterize how the ability to integrate cognition into action is disrupted by Alzheimer's disease (AD) in its early stages, 2) to determine the predictive potential of kinematic measures in discriminating between high and low AD risk older adults, and 3) to examine the structural and functional neural correlates of cognitive-motor

integration in healthy aging and preclinical AD.

While the ability to directly interact with objects does not appear to be impaired in early AD relative to healthy aging, performance decrements have been observed when patients perform motor control tasks under conditions in which direct visual feedback is not provided (Ghilardi et al., 1999; Ghilardi et al., 2000; Tippett & Sergio, 2006; Tippett, Krajewski, & Sergio, 2007; Tippett, Sergio, & Black, 2012; Verheij et al., 2012). It has been suggested that these disruptions may result from functional (i.e. hypometabolism/ hypoperfusion) and structural (i.e. grey matter atrophy) alterations in posterior parietal association areas, which have been documented in preclinical AD (Jacobs et al., 2011; Schroeter, Stein, Maslowski, & Neumann, 2009). We further suggest that impairment in cognitive-motor integration may reflect early brain alterations disrupting the intricate reciprocal communication between hippocampal, parietal and frontal brain regions involved in successfully preparing, executing, and updating complex reaching behaviours. In support of this prediction, recent diffusion tensor imaging (DTI) studies in mild cognitive impairment (MCI) and AD have revealed disruption to the integrity of prominent parietal-frontal white matter tracts (Bosch et al., 2012), as well as projections from the hippocampus to the inferior parietal cortex (Villain et al., 2008). Ultimately, the projects in this dissertation are designed to demonstrate that using kinematic measures to evaluate cognitive-motor performance in older adults may provide a novel, simplified, and objective behavioural means through which to detect underlying brain alterations

associated with increased AD risk.

1.2 Visuomotor compatibility and visually-guided movements

Most reaching movements performed in daily life are referred to as standard visuomotor transformations. In this type of reach, the eyes are directed towards an object of interest and the hand moves to the same location in space as that acquired by the eyes. Many of the movements that we learn to perform, however, require non-standard visuomotor transformations, in which the motor system must integrate some form of cognitive information (e.g. visual-spatial, memory, rule-based, semantic) into the motor program. In a non-standard transformation the end effector must move to a spatial location that is not directly aligned with the location of the visual target. Two forms of non-standard transformational mapping have been described in the literature (Wise, di Pellegrino, & Boussaoud, 1996). The first form is referred to as a *sensorimotor recalibration* or *spatial realignment*. One situation in which this form of transformation is required is when the physical location of the visual stimulus is in a different plane relative to the movement required by the limb (e.g. moving a computer mouse or laparoscopic surgery). In this situation both vision and proprioception must be used to remap the visual location of the target and representation of the hand in one plane, onto the true location of the hand and target in the other plane (Bedford, 1993; Clower & Boussaoud, 2000; Lackner & Dizio, 1994). Furthermore, in order to sustain the motor plan throughout the course of the

movement, the current position of the actual hand relative to the actual reach target (both of which the eyes are not looking at) must be continuously updated. The second form is called *strategic control*; this occurs when a cognitive strategy is used to realign the required limb movement relative to the spatial location of the target (Redding & Wallace, 1996; Redding, Rossetti, & Wallace, 2005). For example, strategic control is required for anti-reaching tasks in which participants are asked to move in the opposite direction of a visual target, which is similar to incorporating the rule that moving a rudder to the left will move a boat to the right.

1.3 Parietofrontal networks for sensorimotor transformations

In order to reach accurately for an object one must transform sensory signals into a complex pattern of muscle activity, a process known as sensorimotor transformation. The neurological computations underlying this seemingly straightforward task are not yet completely understood. Reaching movements to visual targets rely on sensory information that is initially represented in retinocentric or eye-centered coordinates (i.e. the location of the target in space is internally represented in the brain using its position on the retina; Soechting & Flanders, 1992). In order to specify the kinematics and kinetics of the motor program, the retinocentric signal must be transformed into motor coordinates imposed by the joints and muscles of the arm. The cortical control of reaching movements has been described as a sequence of coordinate transformations

from retinocentric, to head-centered, then to body-, or shoulder-, centered coordinates by combining sensory signals in a serial manner, and comparing each with the body-centered location of the arm (Kalaska, Scott, Cisek, & Sergio, 1997). Numerous cortical areas appear to combine visual, proprioceptive, attentional, and biomechanical information. In particular, interconnected neuronal populations from parietal, premotor, and primary motor areas perform transformations from extrinsic spatial representations to intrinsic joint and muscle representations necessary for the generation of an accurate motor output (Battaglia-Mayer et al., 2000; Colby & Goldberg, 1999; Crawford, Henriques, & Medendorp, 2011; Crutcher & Alexander, 1990; Flash & Mussa-Ivaldi, 1990; Johnson, Ferraina, Bianchi, & Caminiti, 1996; Kalaska, Sergio, & Cisek, 1998; Sergio & Kalaska, 2003; Shen & Alexander, 1997; Zhang, Riehle, Requin, & Kornblum, 1997).

Much current research seeks to characterize the role of different frontoparietal networks in sensory-guided reaching, with an emphasis on the connectivity between these areas. However, there has been relatively little research on the neurophysiology of cognitive-motor integration, where rules dictate the relationship between perception and action (Bunge et al., 2005; Georgopoulos, 2000; White & Wise, 1999). Studies suggest that both superior and inferior parietal lobules (SPL, IPL) are involved in the early processing of sensory input for movement guidance. Neurons in the posterior parietal cortex discharge in response to both sensation and movement, and are thus considered

crucial in the transformation of visual information needed for motor behaviours (Blangero, Menz, McNamara, & Binkofski, 2009; Goodale, 1993; Kalaska, 1996). Further, cell activity in SPL, IPL, and the parietal-occipital junction is affected by attention, gaze, and tool use (Batista, Buneo, Snyder, & Andersen, 1999; Battaglia-Mayer et al., 2001; Buneo, Jarvis, Batista, & Andersen, 2003; Colby & Goldberg, 1999; Culham & Kanwisher, 2001; Dong, Chudler, Sugiyama, Roberts, & Hayashi, 1994; Ferraina et al., 2001; Inoue et al., 2001; Iriki, Tanaka, Obayashi, & Iwamura, 2001; Karnath & Perenin, 2005; Marzocchi, Breveglieri, Galletti, & Fattori, 2008; Mazzoni & Krakauer, 2006; Neggers & Bekkering, 2001; Prado et al., 2005; Snyder, Batista, & Andersen, 2000; Snyder, Calton, Dickinson, & Lawrence, 2002), all relevant to cognitive-motor integration. While the contribution of post-central cortical areas to rule-based nonstandard sensorimotor mapping is an open area of research, it is well known that higher cognitive functions are related to activity in frontal areas. Many studies have examined the degree to which cell activity in different frontal lobe regions covaries with the attributes of sensory input, motor output, and their various integrated combinations (Lamar & Resnick, 2004; Lu, Preston, & Strick, 1994; Mesulam, 1990; Mesulam, Nobre, Kim, Parrish, & Gitelman, 2001; Moscovitch, Kapur, Kohler, & Houle, 1995; Petrides, 1997). These characteristics of cells in parietal and frontal regions suggest relevance to the processing of visual input and the planning of limb movements requiring the integration of task-specific rules.

Previous neurophysiological research in our lab has specifically examined the involvement of parietal and premotor regions, at the single cell and cell assembly (local field potential - LFP) levels, during performance of standard relative to non-standard visuomotor transformation tasks (Hawkins, Sayegh, Yan, Crawford, & Sergio, 2013; Sayegh, Hawkins, Hoffman, & Sergio, 2013; Sayegh et al., 2014). The tasks used in these studies were similar to the dual touchscreen cognitive-motor assessment tasks developed for the aging and AD work described in this dissertation. Using single cell recordings in the SPL of rhesus macaque monkeys, we found a temporal activation profile supporting the role of the SPL in visually-guided reach planning and online monitoring, as well as significant differences in cell activation profiles during standard relative to non-standard task performance (Hawkins et al., 2013). These findings were taken to suggest that the SPL is involved in processing the non-standard nature of a motor task and contributes to the reciprocal parietal-frontal communication required to accurately transform incongruent sensory inputs into an appropriate motor action. Further support for the involvement of the SPL in non-standard visuomotor transformations was also found when analyzing LFPs within this region (Sayegh et al. 2014). Specifically, the onset of coordinated cell assembly oscillations within the beta range (10-20 Hz) occurred later in the planning phase of a non-standard relative to standard task. Furthermore, upon movement initiation, oscillations within both the low frequency (5-10 Hz) and gamma (30-40 Hz) ranges dominated during non-standard but not standard task performance.

These results were interpreted as reflecting a delay in top-down control over movement planning and increased reliance on proprioceptive inputs and online control mechanisms during non-standard reaching. Single cell and LFP recordings within the dorsal premotor cortex also revealed task-related differences in neural activation, including greater involvement of the rostral portion of the dorsal premotor cortex during rule integration and greater involvement of the caudal portion of the dorsal premotor cortex during online updating when performing a non-standard reaching task (Sayegh et al., 2013).

These fundamental studies have provided novel insight into our understanding of how the brain transforms visual information into an accurate motor output, specifically under conditions in which the correspondence between vision and action is not direct. Not only is this research relevant to the development of brain machine interfaces, it also supports the notion that manipulating visuomotor compatibility results in differential activation within parieto-frontal visuomotor networks. Furthermore, these findings have laid the foundation for our applied work, leading to the development of the hypothesis that the parieto-frontal networks underlying cognitive-motor integration are affected differently in healthy aging versus AD.

1.4 The effects of healthy aging on sensorimotor control

Changes in sensorimotor control with age have been well documented and involve alterations in both upper and lower limb function. Declines with age often include

increased variability, as well as slower reaction and movement times (Spirduso, 1975; Spirduso & Clifford, 1978; Yan, Thomas, Stelmach, & Thomas, 2000), irregular visually guided reach trajectories (Darling, Cooke, & Brown, 1989), and decreased postural stability and locomotor function (Alexander, Shepard, Gu, & Schultz, 1992; Woollacott, Shumway-Cook, & Nashner, 1986). Such well established age-related psychomotor slowing also contributes to less efficient movement planning (Haaland, Harrington, & Grice, 1993; Ketcham, Seidler, Van Gemmert, & Stelmach, 2002; Pratt, Chasteen, & Abrams, 1994) and online updating (Chaput & Proteau, 1996).

Studies examining the control of arm movements in older adults demonstrate increased reliance on visual feedback, which is often interpreted as compensation for deficiencies in central motor planning (Haaland et al., 1993; Ketcham et al., 2002; Pratt et al., 1994; Seidler-Dobrin & Stelmach, 1998). For example, Haaland et al. (1993) examined aiming movements with and without visual feedback in young and elderly adults. In doing so, they found that as target distance (i.e. movement amplitude) and size increased, older adults did not scale the velocity and distance of their initial movement to the same magnitude as young adults. Older adults were also less accurate at the end of the deceleration phase of the initial movement. Furthermore, older adults demonstrated larger increases in absolute error with increasing target distance in the non-visual condition. Based on these results, the authors suggest that the movement plans of older adults may be imprecise or incomplete, especially when movements are longer, thus resulting in

increased reliance on visual feedback.

On the other hand, some studies have also demonstrated that online corrective mechanisms may be less efficient in older individuals (Chaput & Proteau, 1996; Sarlegna, 2006). For example, Sarlegna (2006) compared the use of visual feedback regarding target position for the online correction of movement trajectories between young and older adults. Targets were either stationary or displaced at movement onset (so-called "double-step" paradigm), thus requiring efficient use of online visual feedback to adjust movement trajectories during trials in which target displacement occurred. Older adults displayed significantly later and less accurate trajectory corrections compared to young adults on target-jump trials. The authors suggest that the efficient use of visual information (either perceived, or not – e.g. when target jumps occur during saccadic suppression) for large online corrections, such as those required in a double-step task, likely involves the posterior parietal cortex (PPC). Evidence for the role of PPC in online updating comes from studies in which PPC activity is disrupted through transcranial magnetic stimulation (TMS) or lesion. Both of these manipulations result in impairment to the trajectory corrections normally observed during visual target displacement tasks (Desmurget et al., 2001; Pisella et al., 2000). Thus, age-related declines in information processing speed, particularly in posterior parietal regions responsible for the integration of somatosensory information into movements (Ashe & Georgopoulos, 1994; Ferraina & Bianchi, 1994; Kalaska, Cohen, Prud'homme, & Hyde, 1990; Rizzolatti, Luppino, &

Matelli, 1998), may result in delayed online updating in older individuals.

Similar age-related changes as those involved in the planning and online correction of arm movements have also been observed in the planning and guidance of foot placement during locomotion. Specifically, when stepping over obstacles or onto targets, older individuals fixate the target earlier and longer than young individuals before initiating their step (Chapman & Hollands, 2006a; Chapman & Hollands, 2006b; Chapman & Hollands, 2007). Thus, there appears to be a common age-related increase in the reliance on visual information for both upper and lower limb motor control. To examine the use of vision by young and older adults during locomotion, Chapman and Hollands (2006a) experimentally controlled for the availability of visual information during the stance and swing phases of the step cycle. In this study, the authors demonstrated that older participants exhibit significantly larger foot placement errors when vision is unavailable during both the stance and swing phases, while young adults are not affected by the visual manipulations. These results were taken to suggest that older adults have a reduced ability to efficiently use vision for feed-forward planning during locomotion.

The complex inter-limb coordination patterns required for locomotion have also been examined in older adults (Heuninckx, Wenderoth, Debaere, Peeters, & Swinnen, 2005; Heuninckx, Wenderoth, & Swinnen, 2008). Using cyclical flexion-extension movements of the right wrist and ankle, that were either isodirectional (both limb segments moved in the same direction) or non-isodirectional (both segments moved in opposite directions),

Heuninckx et al. (2005) have demonstrated that coordination performance is less stable in older adults, even after correcting for task difficulty by slowing the cycling frequency. Using functional magnetic resonance imaging (fMRI), these authors have also shown that in both isodirectional and non-isodirectional coordination tasks elderly participants exhibit additional activation of brain areas involved in sensory processing and integration (including the supramarginal gyrus, secondary somatosensory area, precuneus, frontal operculum, and anterior insula), as well as cognitive monitoring of motor performance (including the pre-supplementary motor area, pre-dorsal motor areas, prefrontal cortex and rostral cingulate). Furthermore, during the more complex non-isodirectional task, elderly participants exhibited additional activation of brain regions known to be involved in inhibitory control and the suppression of prepotent responses (i.e. the anterior rostral cingulate and the dorsolateral prefrontal cortex). These results, along with the finding that increased activation is associated with improved performance in the elderly (Heuninckx et al., 2008), suggest that additional recruitment in the aging brain is compensatory in nature. In other words, enhanced attentional deployment and cognitive monitoring may reconcile age-related deficits in more automatic sensorimotor processing (Wu & Hallett, 2005).

1.5 Visuomotor deficits in Alzheimer's disease and lesion studies

Although AD is most commonly associated with memory and other cognitive

impairments, deficits in purposeful movements (i.e. apraxia) have been identified later in the course of the disease (Parakh, Roy, Koo, & Black, 2004). Furthermore, recent studies have demonstrated subtle deteriorations in the performance of non-standard sensorimotor transformation tasks in early AD (Ghilardi et al., 1999; Ghilardi et al., 2000; Tippett & Sergio, 2006; Tippett et al., 2007; Tippett et al., 2012; Verheij et al., 2012). These studies have shown increases in reaction time, movement time, and task performance errors in AD patients compared to age-match controls when they are required to perform reaching tasks that do not allow for continuous visual monitoring of the hand. Standard reaches, on the other hand, do not show impairment in patient groups (Tippett et al., 2007). The authors of these studies suggest that structural degradation of parietal and prefrontal areas, as well as the cortico-cortical connections between them (Braak & Braak, 1991; Ghilardi et al., 2000), may be responsible for the observed impairments in non-standard visuomotor transformations. Ghilardi and colleagues (1999) suggest that the increased movement times and fragmented velocity profiles observed in their study indicate a strong reliance on continuous visual monitoring of the moving hand in AD patients. Furthermore, better accuracy in initial movement direction, relative to end point accuracy, suggests that these patients can generate a motor plan, but are unable to sustain the motor plan throughout the course of the movement. In other words, the internal feedback loop required to update the current location of the hand relative to the position of the target, which relies on intact parietal-frontal connections, may be disrupted in these

patients. Based on the observation that hypoperfusion of parietal areas correlates with clinical evidence of apraxia in AD patients (Foster et al., 1984), it has also been suggested that visuomotor transformation deficits observed in early AD may reflect early deterioration of the neural networks involved in praxic functions. Although clinically obvious apraxia is often not present until the later stages of AD, subtle apraxic deficits have been observed early in the disease process, and may actually be an early feature of the disease (Crutch, Rossor, & Warrington, 2007a; Crutch, Rossor, & Warrington, 2007b; Kluger et al., 1997; Salek, Anderson, & Sergio, 2011; Willis, Behrens, Mack, & Chui, 1998; Yamaguchi et al., 2011).

Research into the neural basis of praxic function suggests an important role for inferior parietal-frontal regions. A recent lesion subtraction analysis compared left brain-damaged patients with impaired purposeful limb movements (i.e. ideomotor limb apraxia), to left brain-damaged patients without these impairments (Pazzaglia, Smania, Corato, & Aglioti, 2008). The results suggested that limb apraxia is associated with lesions to the inferior parietal cortex, as well as the inferior frontral gyrus extending into ventral premotor cortex (PMv) (i.e. an inferior parietal-frontal network). Lesion studies by Buxbaum and colleagues (Buxbaum, Sirigu, Schwartz, & Klatzky, 2003; Buxbaum, Johnson-Frey, & Bartlett-Williams, 2005; Buxbaum, Kyle, Grossman, & Coslett, 2007) have presented similar findings. These studies have demonstrated that left hemisphere patients who exhibit apraxic deficits (such as abnormal hand posture responses to meaningful

objects/tools, impaired object recognition, and/or impaired functional hand-object interactions) present with lesions including Brodmann areas (BA) 39 and/or 40 (i.e. angular and supramarginal gyri of the IPL), whereas lesions in patients who do not exhibit apraxia rarely include inferior parietal regions. Based on these findings, Buxbaum et al. (2007) have suggested that the IPL maps between representations of object identity processed by the ventral stream (i.e. in the nearby temporal lobe) and spatial representations of the body processed by the dorsal stream (i.e. in the nearby SPL), thus allowing for the integration of object-based knowledge and action representations, which can then be transformed into a motor program by premotor cortex. Interestingly, Buxbaum et al. (2003) have also demonstrated that apraxic patients are able to perform normally at recognizing appropriate hand postures for interacting with novel objects. Thus, these authors have suggested that motor responses to novel objects may be mediated by intact superior parietal-frontal pathways concerned with spatial-to-motor computations that do not require access to stored representations. It has been suggested that these superior networks may be mainly responsible for processing more rapid, online visuomotor transformations (Rossetti et al., 2005). Accordingly, damage to superior parietal areas results in a different neurological impairment known as optic ataxia.

Optic ataxia is defined as a disorder affecting the accuracy and co-ordination of rapidly executed reaching and grasping movements under visual control, especially when the target object is in peripheral vision (Karnath & Perenin, 2005). This disorder is not

related to visual acuity or motor execution deficits, that is, patients can perceive objects and produce movements, but they exhibit difficulty formulating accurate visually guided limb trajectories. Using a lesion subtraction method, Karnath and Perenin (2005) compared a group of patients who sustained parietal damage and exhibited optic ataxia, with a group of patients who sustained similar parietal damage, but did not exhibit optic ataxia. Their lesion overlap findings revealed that optic ataxia appears to be associated with lesions close to the parieto-occipital junction, centering on the precuneus at the medial cortical aspect of the hemisphere.

These patient studies illustrate the important role of the posterior parietal cortex in visuomotor control, and support the notion of two functionally distinct parietal-frontal streams (Rizzolatti & Matelli, 2003): the so-called "dorsal-dorsal" stream responsible for the online control of motor actions, and the so-called "ventral-dorsal" stream subserving space perception, action organization and action understanding. When lesions are relatively isolated to one stream or the other they result in the ideomotor apraxia/optic ataxia dichotomy described above. The visuomotor deficits observed in early AD, however, are less well understood. Recently, studies using brain-imaging techniques to examine the functional and structural changes associated with AD (see section 1.7) have provided some insight into this behaviour. Specifically, these studies have demonstrated that along with structural hippocampal atrophy, compromised parietal-frontal and cingulum bundle white matter tracts, as well as posterior parietal

hypometabolism/hypoperfusion and reduced resting-state functional connectivity in early AD may lead to disruption in hippocampal-parietal and parietal-frontal visuospatial and visuomotor networks. In other words, disconnection across cortical regions, as oppose to isolated atrophy within specific brain regions, may underlie the observed visuomotor deficits in early AD.

1.6 Typical clinical manifestation of Alzheimer's disease and biomarkers for early detection

The major neuropathological changes associated with AD have been identified (i.e. amyloid-beta accumulation and neurofibrillary tangles), however the underlying cause is largely unknown. Typically, the initial clinical manifestation of AD dementia involves short-term memory deficits, which eventually progress and are accompanied by more global and pronounced cognitive impairments. A diagnosis of probable AD involves several steps to rule out other potential causes of dementia, including evaluation of mental status, medical history, clinical examination, and laboratory tests. While AD is the most common cause of dementia (50-60% of cases), there are many other disorders that can simulate or cause dementia, some of which are responsive to treatment (e.g. depression, medication-induced dementia and nutritional/metabolic/endocrine/systemic disorders, such as hypothyroidism, B12 deficiency and systemic infections). Dementia is defined as a syndrome that is characterized by multiple cognitive deficits including

memory impairment and at least one other cognitive disturbance, such as impaired executive function, aphasia, agnosia or apraxia. Activities of daily living (e.g. social and occupational function) are also impaired (Diagnostic and Statistical Manual of Mental Disorders IV – DSM-IV; American Psychiatric Association, 1994). Other causes of dementia include vascular dementia (approximately 20% of cases), hydrocephalus, tumors, and hematoma (Alzheimer's Association, 2012). The National Institute of Neurological and communicative Disorders and Stoke and Alzheimer's Disease and Related Disorders Association (NINCDS-ADRDA) criteria for diagnosis of probable AD includes: 1) Dementia established by objective testing, 2) deficits in two or more cognitive areas, 3) progressive worsening of memory and other cognitive functions, 4) no disturbance in consciousness, 5) onset between ages 40 and 90 and 6) absence of other brain diseases or systemic disorders that could account for the deficits in memory and cognition (McKhann et al., 1984). Cases that involve atypical cognitive symptoms and progression are often referred to specialists for assessment and may result in diagnosis of a more rare neurodegenerative diseases such as frontotemporal lobar dementia, corticobasal degeneration, dementia with Lewy bodies or progressive supranuclear palsy. Importantly, by the time the manifestation of AD is behaviourally observable, significant damage to the brain is already present and is likely irreversible (Ewers, Sperling, Klunk, Weiner, & Hampel, 2011), with a reported hippocampal volume loss of approximately 20% at the mild stages of AD dementia (Karow et al., 2010). Thus, in order to develop

effective treatments that may terminate or slow the neurodegenerative process, early detection prior to the onset of symptoms is essential. Recent structural and functional neuroimaging studies in cognitively healthy older adults at increased genetic risk for AD and in those diagnosed with MCI offer promising evidence for the potential value of brain imaging biomarkers in the early detection of AD pathology.

In recent years, apolipoprotein E epsilon 4 (ApoE4) genotyping (a genetic risk factor for sporadic AD), amyloid-beta (Aβ) imaging and neuropsychological tests of subtle cognitive (generally episodic/working memory) changes have been used to identify individuals at increased risk for AD (Ewers et al., 2011). ApoE is a cholesterol carrying lipoprotein that supports injury repair and lipid transport in the brain. For lipid delivery, ApoE binds to cell-surface receptors, including Aβ peptides. The regulation of Aβ aggregation and clearance in the brain depends on the APOE isoform, specifically, the ApoE4 allele has been associated with late-onset AD, amyloid deposits in the walls of cerebral blood vessels and cognitive decline in normal aging (Liu, Kanekiyo, Xu, & Bu, 2013). Aβ imaging involves measuring the level of amyloid deposition in the brain using C-labeled Pittsburgh Compound-B (PiB), a radiotracer that binds to Aβ, in positron emission tomography (PET) scans. A high level of PiB binding in cognitively healthy individuals is associated with increase AD risk and future declines in episodic and working memory (Storandt, Mintun, Head, & Morris, 2009). MCI involves a clinical diagnosis of subtle cognitive changes (often involving episodic memory impairment).

The clinical criteria for MCI includes a decline in memory (amnestic MCI) or other cognitive domains (non-amnestic MCI), as well as subjective cognitive complaints corroborated by a relative, however social functioning and instrumental activities of daily living remain intact (Petersen et al., 2001a). Individuals who meet the diagnostic criteria for MCI (especially amnestic MCI) are at increased risk of progressing to AD dementia (Mitchell, Arnold, Dawson, Nestor, & Hodges, 2009). By comparing neuroimaging measures in preclinical (i.e. no cognitive symptoms, but at increased risk due to ApoE4 genotype, family history and/or high Aβ deposition) and prodromal (i.e. MCI) groups relative to cognitively healthy low-risk groups, recent studies have provided important insight into early brain changes that may prove useful as biomarkers for the early detection of AD pathology and the prediction of dementia before the onset of clinical symptoms.

1.7 Neural correlates of preclinical and prodromal Alzheimer's disease

Over the past several years many brain-imaging studies have investigated the neural underpinnings of AD. In 2009, a meta-analysis of these studies revealed that, aside from the commonly known structural atrophy in trans-entorhinal and hippocampal regions, hypometabolism and hypoperfusion in the IPL and precuneus (i.e. medial SPL) are also prevalent features of early AD (Schroeter et al., 2009). Furthermore, functional alterations in the left IPL and precuneus (BA 7/31/39/40) distinguished between MCI

converters and non-converters (Schroeter et al., 2009). Disruption to these brain regions, which have been shown to be involved in visuo-spatial processing and spatially guided behaviour (Cavanna & Trimble, 2006), may underlie the early visuomotor impairments observed in AD. It has been suggested that these parietal alterations may be caused by regional amyloid deposits (Braak & Braak, 1991; Chetelat et al., 2008; Jack et al., 2008; Kemppainen et al., 2007), and/or hippocampal-parietal disconnection (diaschisis hypothesis) via disruption of the cingulum bundle (Villain et al., 2008). Villain and colleagues (2008) found support for the diaschisis hypothesis using whole-brain voxel-based correlations to assess the relationships between hippocampal atrophy, white matter integrity, and grey matter metabolism. Their results revealed that hippocampal atrophy is specifically related to cingulum bundle disruption, which is in turn highly correlated with hypometabolism of the posterior cingulate cortex, middle cingulate gyrus, thalamus, mammillary bodies, parahippocampal gyrus, and right temporoparietal association cortex. With regards to visuomotor control, inputs from hippocampus to IPL likely play an important role in the integration of memory into spatial processing and the establishment of maps of extrapersonal space (Clower, West, Lynch, & Strick, 2001).

Many of the more recent neuroimaging studies in MCI and AD have employed DTI to examine the integrity of white matter (WM) tracts connecting various regions of the brain. Using multiple DTI measure, Bosch and colleagues (2012) found that many WM changes in the brains of MCI and AD patients were secondary to grey matter atrophy.

However, radial diffusivity (DR) increases independent of grey matter atrophy were observed in amnestic MCI participants in the posterior parts of the inferior fronto-occipital and longitudinal fasciculi (IFOF and ILF). These results may reflect early WM compromise (i.e. demyelination) in prodromal AD affecting the WM tracts forming parietal- and occipital-frontal connections. Others have reported similar disruption to the integrity of association fibre tracts in early AD, generally including the IFOF, ILF, superior longitudinal fasciculus (SLF), corpus callosum (CC), and cingulum bundle (CG) (Bai et al., 2009; Bartzokis et al., 2004; Stricker et al., 2009). These findings provide support for the "retrogenesis model" of AD, suggesting that WM degeneration occurs in a reverse pattern to myelogenesis. Stricker and colleagues (2009) have specifically demonstrated lower fractional anisotropy (FA), reflecting impaired WM integrity, in late-myelinating but not early-myelinating tracts in AD patients compared to healthy older adults. It has been suggested that, since late-differentiating oligodendrocytes ensheath many more axons and have different lipid properties, late-myelinating regions (e.g. parietal, prefrontal, temporal) may be particularly vulnerable to the myelin breakdown that occurs in aging and AD (Bartzokis et al., 2004).

The observation of WM alterations in prodromal AD (i.e. MCI) in the above studies suggests that disruption to the integrity of association fibre tracts takes place at an early stage of disease progression (Bai et al., 2009; Bosch et al., 2012). These results are consistent with earlier studies in which PET was used to examine glucose metabolism in

the brains of ApoE4 carriers over the age of 50 with AD affected relatives (Reiman et al., 1996; Small et al., 1995). These at-risk participants (i.e. with no cognitive symptoms) showed reduced parietal glucose metabolism, and follow-up assessments showed that cognitive decline after 2 years was greatest in those ApoE4 carriers with the lowest metabolism in parietal and temporal regions at baseline (Small et al., 2000). More recently these studies have been supported, and expanded upon, by PET and magnetic resonance imaging (MRI) studies finding that individuals with a maternal family history of AD are particularly susceptibility to glucose metabolism and grey matter volume alterations (Honea, Swerdlow, Vidoni, Goodwin, & Burns, 2010; Mosconi et al., 2007). Compared with both no family history and paternal family history groups, participants with a maternal family history of AD were found to have reduced cerebral metabolic rate of glucose in the posterior cingulate cortex/precuneus, parieto-temporal cortex, frontal cortex, and medial temporal lobe (Mosconi et al., 2007). Lower grey matter volumes were also observed in AD-vulnerable brain regions, as well as progressive grey matter atrophy overtime in the precuneus and parahippocampal gyrus, in individuals with a maternal family history of AD (Honea et al., 2010). Recent DTI studies have also found microstructural changes in cognitively normal women at increased risk of AD due to family history and carrying one or more ApoE4 allele (Gold, Powell, Andersen, & Smith, 2010; Smith et al., 2010). The brains of these women showed decreased microstructural integrity in WM tracts with direct and secondary connections to the

medial temporal lobe (e.g. the fornix, CG, ILF and IFOF), years before the expected onset of cognitive symptoms.

Several studies using resting-state functional magnetic resonance imaging (rs-fMRI) have also demonstrated reduced functional connectivity across interconnected cortical regions (including the precuneus, lateral parietal, lateral temporal, and medial prefrontal cortices), known as the default mode network (DMN), that are normally active in correlation with each other during rest (Drzezga et al., 2011; Hedden et al., 2009b; Mormino et al., 2011; Petrella et al., 2011; Sheline et al., 2010a; Sheline et al., 2010b). These studies have shown that cognitively normal individuals with high amyloid burden, as well as ApoE4 carriers, exhibit significantly reduced functional connectivity within brain regions of the default network, and that these regions of reduced functional connectivity overlap strongly with regional glucose hypometabolism. Taken together, the above studies indicate that disconnection between the medial temporal lobe and neocortex, as well as between parietal and frontal regions, may occur very early in the course of AD.

1.8 Brief overview of dissertation projects

Project 1) *Visuomotor impairments in older adults at increased Alzheimer's disease risk*. In this first project we asked if a new approach can be used to sensitively detect early AD. In other words, can kinematic measures provide a behavioural means through which

to identify individuals at increased AD risk? We have found, as the current neurological assessments typically find, that reaching and gross motor movements made under direct conditions (congruent gaze and object location, like reaching to pick up a cup of coffee) are *not* generally impaired in early AD and MCI relative to healthy aging. Significantly, however, as soon as an element of dissociation is introduced into a reaching task (e.g. the guiding visual information is dissociated from the required motor act, such as using a computer mouse), the performance of patients with early AD declines precipitously (Ghilardi et al., 1999; Tippett & Sergio, 2006; Tippett et al., 2007; Tippett, Sergio, & Black, 2012; Verheij et al., 2012). Recent results suggest that adults with MCI also show a decline in performance, albeit less dramatically (Salek et al., 2011). Based on these initial findings, we hypothesized that there would be a measurable decline in the brain's ability to integrate visual-spatial and cognitive information with action in going from healthy aging, to increased genetic risk, to MCI. The objectives of this project were 1) to collect normative data from young, low AD risk, and high AD risk populations and perform between group comparisons, and 2) to determine the predictive potential of kinematic outcome measures using a discriminant analysis to separate between high and low AD risk groups. The functional specifications for the cognitive-motor assessment developed for all three projects can be found in Appendix A.

Project 2) *Diffusion tensor imaging correlates of cognitive-motor decline in normal aging and increased Alzheimer's disease risk*, and project 3) *Changes in resting-state*

functional connectivity associated with cognitive-motor impairment in older adults at increased Alzheimer's disease risk. The aim of these projects was to expand upon project #1 by examining the underlying structural and functional connectivity in relation to AD risk and cognitive-motor integration performance. Taken together, recent neuroimaging and motor control studies in early AD suggest that functional alterations in parietal areas associated with hippocampal-parietal and parietal-frontal disconnection may underlie early AD-associated motor control deficits. Thus, in projects 2 and 3 we propose that comparing DTI and resting-state functional connectivity measures between individuals at increased AD risk and both age-matched and young healthy controls may provide insight into the very early structural and functional changes associated with AD pathology, and may correlate with disruptions observed on our cognitive-motor assessment. Specifically, we hypothesized that white matter tracts connecting posterior and anterior brain regions (e.g. SLF, ILF, IFOF), as well as projecting from hippocampal to neocortical regions (e.g. CG), and resting-state functional connectivity within the DMN would be compromised in individuals at increased genetic risk of AD, and would be associated with the cognitive-motor deficits observed in project 1. The objectives of these projects were 1) to compare hippocampal volume, DTI, and resting state functional connectivity measures between healthy aging and increased AD-risk populations, and 2) to correlate DTI and resting state functional connectivity measures with the kinematic measures reflecting poorer cognitive-motor performance in high AD risk relative to healthy control participants in

project 1.

1.9 Summary and knowledge dissemination

The work in this dissertation expands upon previous studies examining cognitive-motor integration deficits in dementia patients, and advances our understanding of the brain mechanisms underlying these deficits. Two manuscripts have been published in the *Journal of Alzheimer's disease* and one has been submitted to *Alzheimer's & Dementia*. Our findings have also been presented at the Society for the Neural Control of Movement, the Canadian Association of Neuroscience, the Canadian Association on Gerontology, and the Society for Neuroscience annual meetings, as well as at invited talks in the community. The findings described are informative for clinicians in the field (through assessment tool development), caregivers and community-based practitioners (through advancing our knowledge of the everyday functional limitations of AD patients), and neuroscientists (through description of the underlying neural correlates of behaviour). The purpose of this research is to understand how the brain's ability to incorporate visual-spatial and cognitive information into a motor act, which is essential to our everyday function, is disrupted by early AD-related brain alterations. The clinical and fundamental projects described in this dissertation also advance our understanding of one of our most basic behaviours - how we interact with objects in the world around us.

Chapter Two

Visuomotor Impairments in Older Adults at Increased Alzheimer's Disease Risk

Kara M. Hawkins and Lauren E. Sergio

Reprinted from the Journal of Alzheimer's Disease: Hawkins KM & Sergio LE (2014). Visuomotor Impairments in Older Adults at Increased Alzheimer's Disease Risk, *Journal of Alzheimer's Disease, 42(2)*, 607-621.

Abstract

Background and objective: Recent evidence suggests that visuomotor behaviours may be disrupted in the very early stages of Alzheimer's disease. Here we propose that using kinematic measures under conditions that place demands on visual-spatial and cognitive-motor processing may provide an effective behavioural means to detect subtle changes associated with Alzheimer's disease risk. **Methods:** To this end, we have tested 22 young adults (mean age = 26.4 +/- 4.1), 22 older adults (mean age = 64.3 +/- 10.1) at low Alzheimer's disease risk, and 22 older adults (mean age = 67.7 +/- 11.3) at high Alzheimer's disease risk (i.e. strong family history or diagnosis of mild cognitive impairment). Kinematic measures were acquired on four visuomotor transformation tasks (standard, feedback reversal, plane dissociated, and plane dissociated + feedback reversal) using a dual-touchscreen tablet. **Results:** Comparing participants at increased Alzheimer's disease risk with both young and old healthy control groups revealed significant performance disruptions in at-risk individuals as task demands increased. Furthermore, we were able to discriminate between individuals at high and low Alzheimer's disease risk with a classification accuracy of 86.4% (sensitivity: 81.8%, specificity: 90.9%). **Conclusion:** We suggest that the impairments observed in individuals at increased Alzheimer's disease risk may reflect inherent brain alteration and/or early neuropathology disrupting the reciprocal communication between hippocampal, parietal, and frontal brain regions required to successfully prepare and

update complex reaching movements. Such impairment has the potential to affect activities of daily living, and may serve as a sensitive measure of functional ability in at-risk adults.

Introduction

Alzheimer's disease (AD) is the most common form of dementia, affecting approximately 13% of individuals aged 65 years and older, and 40-50% of individuals aged 80 years and older (Alzheimer's Association, 2012). Typically, the initial clinical manifestation of AD involves short-term memory deficits, which eventually progress and are accompanied by more global and pronounced cognitive impairments. By the time this behaviourally noticeable manifestation of the disease occurs, significant damage to the brain is already present and may be irreversible (Ewers, Sperling, Klunk, Weiner, & Hampel, 2011). Thus, in order to develop effective treatments that may terminate or slow the neurodegenerative process, recent reports have emphasized the importance of developing better tools for the assessment of impairments in the early stages of AD before substantial neurodegeneration has occurred (Silverberg et al., 2011).

While AD is typically associated with hippocampal atrophy and memory deficits, research has also demonstrated that functional and structural alterations involving posterior parietal association areas are present in the very early stages of the disease (Jacobs et al., 2011; Schroeter, Stein, Maslowski, & Neumann, 2009). Posterior parietal

cortex (PPC) plays an important role in transforming visual-spatial information into goal-directed actions (Galati et al., 2011). In particular, reciprocal parietal-frontal networks involving interconnected neuronal populations are required to transform extrinsic spatial representations into intrinsic joint and muscle representations necessary for the generation of an accurate motor output (Battaglia-Mayer et al., 2000; Crawford, Henriques, & Medendorp, 2011; Galati et al., 2011; Johnson, Ferraina, Bianchi, & Caminiti, 1996; Shen & Alexander, 1997). Disruption to these parietal-frontal networks in the early stages of AD may result in impaired visuomotor control.

In a typical or "standard" reach, the eyes are directed towards an object of interest then the hand moves to that same location in space. Many of the movements that we learn to perform however, require more complex sensorimotor transformations in which the motor system must integrate some form of cognitive information (e.g. visual-spatial, memorized, rule-based, semantic) into the motor program. In these learned "non-standard" sensorimotor transformations the end effector must move to a spatial location that is not directly aligned with the location of the visual target. These indirect visuomotor behaviours rely on the brain's ability to either recalibrate the sensory-motor relationship or use a cognitive strategy to realign the required limb movement relative to the spatial location of the target (Wise, di Pellegrino, & Boussaoud, 1996). For example, guiding a computer mouse relies on the ability to incorporate visual and proprioceptive signals into the remapping of the visual location of the target and representation of the

hand (i.e. cursor) in one plane, onto the true location of the target and hand in the other plane (Say et al., 2011). Furthermore, in order to sustain the motor plan throughout the course of the movement, the current position of the actual hand relative to the actual reach target (both of which the eyes are not looking at) must be continuously updated. On the other hand, when asked to integrate a specific rule into a movement, such as moving in the opposite direction of a visual target, the brain develops a cognitive strategy to generate the desired motor output (Redding & Wallace, 1996).

While the neurological computations underlying the integration of cognition into action remain to be fully elucidated, it is likely that this behaviour relies on the recruitment of additional neural networks (Gorbet, Staines, & Sergio, 2004), which may be more vulnerable to AD pathology than the primary sensorimotor networks known to be preserved until the later stages of the disease (Frisoni, Prestia, Rasser, Bonetti, & Thompson, 2009). Stereotyped motor actions, such as interacting directly with an object, do not appear to be impaired in early AD relative to healthy aging however performance decrements have been observed under conditions in which direct visual feedback is not provided (Buchman & Bennett, 2011; Ghilardi et al., 1999; Ghilardi et al., 2000; Tippett & Sergio, 2006; Tippett, Krajewski, & Sergio, 2007; Tippett, Sergio, & Black, 2012; Verheij et al., 2012). Similar impairments under indirect visuomotor conditions have also been observed in premanifest Huntington's disease (Say et al., 2011). These visuomotor deficits may reflect posterior parietal damage and/or white matter compromise in

parietal-frontal networks.

Traditionally, motor control deficits (e.g. apraxia) have mainly been identified later on in the course of AD (Parakh, Roy, Koo, & Black, 2004). However, recent observations of visuomotor deficits under cognitively demanding task conditions in early AD suggest that deterioration of the neural networks involved in praxic function may occur early in the disease process, and could serve as an early identifying feature of the disease (Buchman & Bennett, 2011; Crutch, Rossor, & Warrington, 2007a; Crutch, Rossor, & Warrington, 2007b; Kluger et al., 1997; Salek, Anderson, & Sergio, 2011; Verheij et al., 2012; Vidoni, Thomas, Honea, Loskutova, & Burns, 2012; Vidoni et al., 2012; Willis, Behrens, Mack, & Chui, 1998; Yamaguchi et al., 2011). Thus, we hypothesized that using kinematic measures to quantify visuomotor performance under cognitively demanding conditions may successfully identify individuals at increased AD risk due to family history or a diagnosis of mild cognitive impairment (MCI). Both MCI and AD family history are known risk factors for the development of AD (Alzheimer's Association, 2012). Diagnosis of MCI typically includes the presence of memory complaints corroborated by a family member when possible, performance of at least 1.5 standard deviations below the normal age-standardized mean on standardized memory tests such as the Montreal Cognitive Assessment (MoCA), absence of dementia based on clinical evaluation, and absence of significant impairment in functional independence based on clinical judgement (Petersen et al., 2001). Increased risk due to family history

includes the rare familial form of the disease resulting in early-onset AD (Alzheimer's Association, 2012), as well as late-onset AD in immediate family members (Fratiglioni, Ahlbom, Viitanen, & Winblad, 1993; Green et al., 2002; Mayeux, Sano, Chen, Tatemichi, & Stern, 1991), especially if multiple family members are affected (Lautenschlager et al., 1996). Our Specific predictions, based on pilot data, were that movement accuracy and precision would be disproportionately compromised as task demands increased in participants at high AD risk. Furthermore, we predicted that psychomotor slowing would be observed with normal aging, but would be exacerbated by AD risk. We also predicted that increasing the cognitive load by combining visual-spatial recalibration and strategic control demands would provide a more sensitive measure for separation between groups.

Materials and Methods

Participants

This study included 66 participants: 22 older adults at high AD risk, 22 older adults at low AD risk, and 22 young adults (see Table 1 for demographic statistics). Older adults were recruited in collaboration with the Canadian Association of Retired People, Southlake Regional Health Centre, and Mackenzie Richmond Hill Hospital (MRHH). Individuals were classified as high AD risk based on AD family history (n=14) or diagnosis of MCI (n=8) using the Petersen criteria (Petersen et al., 2001) at the MRHH

geriatric outpatient clinic. Individuals classified as family history positive scored at or above age- and education-adjusted norms on the MoCA and reported either a maternal (n = 6), multiple (n = 6) or early-onset (n = 2) family history of AD. Paternal family history alone was not included in the high AD risk classification based on recent evidence that paternal history may not carry the same increased risk as maternal history (Honea, Swerdlow, Vidoni, & Burns, 2011; Mosconi et al., 2007; Mosconi et al., 2010). Individuals classified as low AD risk reported no dementia of any type within their known family history, scored at or above age- and education-adjusted norms on the MoCA, and expressed no memory complaints beyond normal expectations for their age. Exclusion criteria included vision or upper-limb impairments, any medical condition that would hinder task performance (e.g. severe arthritis), any neurological or psychiatric illnesses (e.g. schizophrenia, depression, alcoholism, epilepsy, Parkinson's disease), and any history of stroke or severe head injury. For comparison between low and high AD risk older adults, cognitive (MoCA – version 7.1), computer experience, and touchscreen experience data are recorded in Table 2.1. Computer and touchscreen experience were assessed with a frequency of use rating scale (i.e. how frequently do you use a computer or touchscreen? 0 = never, 1 = rarely, 2 = occasionally, 3 = often). The study protocol was approved by the Human Participants Review Sub-Committee, York University's Ethics Review Board, and conforms to the standards of the Canadian Tri-Council Research Ethics guidelines.

Table 2.1

Summary of participant information

	Young	Low AD Risk	High AD Risk
n	22	22	22
Age (SD)	26.4 (4.1)*	64.3 (10.1)	67.7 (11.3)
Range	21-34	54-84	54-91
High AD risk subgroups	-	-	FH+: 60.8 (5.4), MCI: 79.8 (8.2)*
Sex (% female)	50%	50%	77.3%*
High AD risk subgroups	-	-	FH+: 86%*, MCI: 62.5%
Handedness (% right)	90.9%	90.9%	90.9%
Years of education (SD)	NA	15.8 (3.5)	14.6 (5.2)
High AD risk subgroups	-	-	FH+: 17.4 (0.9), MCI: 9.8 (1.4)*
MoCA score (SD)	NA	27.6 (1.6)	25.8 (4.3)
Range	-	25-30	12-30
High AD risk subgroups	-	-	FH+: 27.3 (2.3), MCI: 22.9 (5.5)*
Computer experience (SD)	NA	2.3 (0.8)	2.1 (1.2)
High AD risk subgroups	-	-	FH+: 2.9 (0.1), MCI: 0.9 (0.4)*
Touchscreen experience (SD)	NA	1.0 (0.8)	1.3 (1.2)
High AD risk subgroups	-	-	FH+: 1.7 (0.3), MCI: 0.5 (0.4)*

NA: not applicable; AD: Alzheimer's disease; FH+: family history positive; MCI: mild cognitive impairment; SD: standard deviation. Asterisks denote significant difference from the other groups or, in the case of the sex variable, a significantly greater proportion of female participants at $p < .05$.

Experimental task

All participants were tested on four visuomotor transformation tasks, similar to those used previously by Tippett et al. (2006, 2007, 2012) and Salek et al. (2011). These tasks were presented on an Acer Iconia 6120 dual-touchcreen tablet: One standard (direct) task in which the spatial location of the viewed target and the required movement were the same, and three non-standard (indirect) tasks (feedback reversal, plane dissociated, and plane dissociated + feedback reversal) in which the location of the viewed target was dissociated from the required movement (Figure 2.1A). Task conditions were presented in randomized blocks consisting of five pseudo-randomly presented trials to each of four peripheral targets (from a common central 'home' target), for a total of 20 trials per condition and 80 trials per participant. To ensure task comprehension each participant was given two practice trials per target prior to each condition. Throughout the experiment a webcam was used to monitor eye movements. If incorrect eye movements were made, participants were reminded to always look towards the target and not at their hand.

The peripheral targets were coloured red and presented either directly to the left, right, above, or below the home target. Each peripheral target was centred on a point 75 mm from the middle of the home target (i.e. the centre of the monitor). The size (20 mm diameter), position, and colour of the targets were consistent across all conditions. In order to maintain a consistent visual border around the peripheral targets, the task was

displayed on a 170 x 170 mm black square with the surrounding background coloured grey. The trial timing and participant responses consisted of the following: 1) a green coloured home target was presented on the vertical tablet, 2) participants touched the home target (either directly or with the cursor using the horizontal tablet depending on the condition), which changed its colour to yellow indicating that they had acquired the home target, 3) after holding the home target for a centre hold time (CHT) of 4000 ms a red peripheral target was presented and the home target disappeared, serving as a 'go-signal' for participants to look towards the visual target and slide their finger along the touchscreen in order to direct the cursor to the target, 4) once the peripheral target was acquired and held for a target hold time (THT) of 500 ms it disappeared and the trial ended, 5) the next trial began with the presentation of the home target after an inter trial interval of 2000 ms (Figure 2.1B).

In all conditions, participants were instructed to move as quickly and accurately as possible. In the standard (S) condition, participants were asked to slide their finger directly to the targets on the vertical tablet (i.e. the cursor was under their finger). In the feedback reversal (FR) condition, the cursor moved in the opposite direction of the participant's finger movements, requiring them to slide their finger away from the visual target in order to direct the cursor towards it. In the plane dissociated (PD) condition, participants slid their finger along the horizontal tablet in order to direct the cursor towards visual targets in the vertical plane. And finally, when feedback reversal (PD+FR)

was added, movements in the opposite direction of the visual targets, as well as in a different spatial plane, were required. In all conditions participants were instructed to look at the location of the presented target, regardless of whether their finger was sliding to that target or in a different direction/spatial plane. Thus, in all but the standard condition the final spatial locations of gaze and hand were decoupled.

Data processing

Timing, finger position (x, y coordinates; 60 Hz sampling rate), and error data were recorded for each trial and converted into MATLAB readable format using a custom written C++ application. Unsuccessful trials were coded by the software and resulted in trial termination if the finger left the home target too early (< 4000 ms), reaction time was too short (<150 ms), reaction time was too long (> 8000 ms), or movement time was too long (> 10000 ms). Velocity profiles were computed for each successful trial and displayed alongside a Cartesian plot illustrating finger position data and target locations using a custom-written analysis program (MATLAB). Movement onsets and offsets for the first ballistic movement (i.e. the initial muscular impulse) were scored as 10% peak velocity then verified visually to ensure that computed offsets appropriately reflected the first point at which movements stopped or slowed significantly (i.e. the end of the first ballistic movement before any corrective movements). Total movement offsets were identified visually as the point at which velocity reached a final zero-crossing and position data plateaued (i.e. stopping the cursor inside the peripheral target). In the

feedback reversal conditions, trials in which the first ballistic movement exited the boundaries of the home target in the wrong direction (i.e. moving the finger towards as oppose to away from the visual target) were coded as direction reversal errors and eliminated from further trajectory endpoint analyses. These processed data were then loaded into a custom written analysis program to compute accuracy, precision and timing outcome measures, as well as generate velocity and trajectory plots.

Dependent measures

The dependent measures of interest in this study were on- and off-axis constant errors, variable error, corrective path length, reaction time, total movement time, and direction reversal errors. Accuracy of the first ballistic movement was determined by computing the absolute on-axis (i.e. distance) and off-axis (i.e. direction) constant errors (CE) which reflect components of reaching accuracy that have been shown to be controlled independently by the motor system (Messier & Kalaska, 1997). CEs were calculated as the average distance between the actual target position (defined as the coordinates at the centre of the target) and the on- or off-axis ballistic movement offset for that target (t) [$\Sigma(x_i-t)/n$ or $\Sigma(y_i-t/n)$]. Absolute on- and off-axis CEs were then averaged across targets, resulting in single measures that reflected the magnitude of distance and direction errors for each condition. Precision was determined by computing the variable error (VE), which is the standard deviation (i.e. variation from the mean) of the ballistic movement offsets [$\sqrt{\Sigma}(x_i-\mu)^2/n$, $\sqrt{\Sigma}(y_i-\mu)^2/n$]. The pythagorean resultant VE

(i.e. $\sqrt{VEx^2 + VEy^2}$) was then averaged across targets to generate a single measure for each condition. Corrective movements were quantified by subtracting the ballistic path length from the total path length, resulting in a measure of corrective path length (CPL). Reaction time (RT) was calculated as the time between disappearance of the home target (i.e. the 'go signal') and movement onset. Total movement time (TMT) was calculated as the time between movement onset and the total movement offset upon positioning the cursor inside the peripheral target. Direction reversals (only applicable in the feedback reversal conditions) were recorded as a percentage of completed trials.

Statistical analysis

Partial correlations were used to examine the relationship between our task outcome measures and MoCA scores, while controlling for age, in the older adult groups. To determine significant differences in demographic variables between groups, one-way analysis of variance (ANOVA) tests were used to compare means (i.e. age, years of education, MoCA scores, computer experience, touchscreen experience) and Chi-squared tests were used to compare proportions (i.e. sex; Table 2.1). While most of the potentially confounding demographic characteristics were not significantly different between the young, low AD risk and high AD risk groups, a significantly larger proportion of the high AD risk group was female, thus sex was included as a covariate in the mixed-design analysis of covariance (ANCOVA) tests that were used to compare our dependent measures across the four task conditions (repeated), and between the three experimental

groups (young, low AD risk and high AD risk). Percent direction reversals in the FR and PD+FR conditions were compared between groups using a one-way ANOVA. To overcome violations of the sphericity assumption, Greenhouse-Geisser correction was applied, altering the degrees of freedom and producing an F-ratio where the Type I error rate was reduced. When there were significant main or interaction effects, post hoc analyses were adjusted for multiple comparisons using Bonferroni correction. Dependent measures from the most cognitively demanding task, which demonstrated the strongest predictive potential based on the ANCOVA results, were entered as predictor variables in a stepwise discriminant analysis comparing low and high AD risk groups. MoCA scores were also included as a potential predictor in this stepwise discriminant analysis in order to compare discriminability between high and low AD risk groups based on visuomotor versus cognitive measures. Applying this discriminant analysis to our data allowed us to identify the weighted linear combination of task outcome variables that contributed maximally to the separation between low and high AD risk groups, and provided estimates of sensitivity, specificity, and overall classification accuracy. In order to demonstrate that this separation between low and high AD risk participants based on cognitive-motor performance exists for both family history positive (FH+) and MCI subgroups, we also conducted separate stepwise discriminant analyses comparing the low AD risk group to each subgroup. Statistical significance levels were set to 0.05. All statistical analyses were carried out using SPSS statistical software.

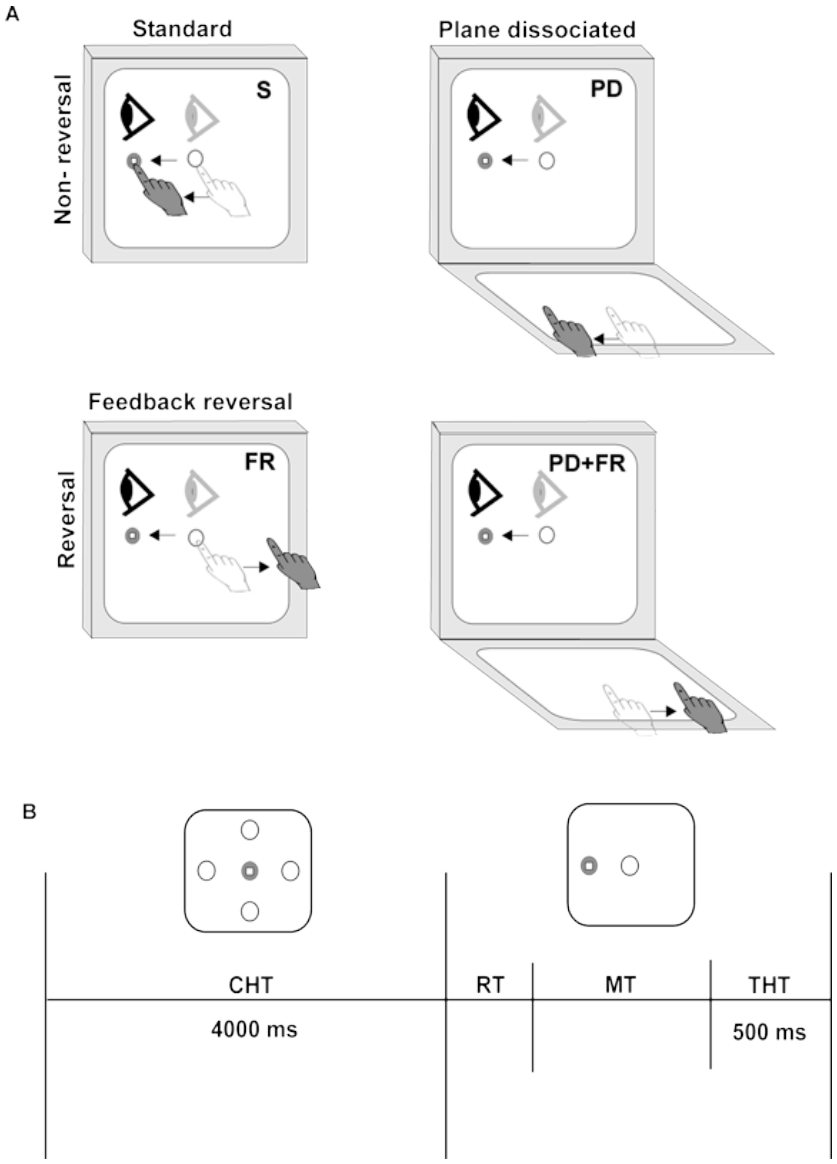

Figure 2.1. A. Schematic drawing of the four experimental conditions. Light grey circle, eye, and hand symbols denote the starting position for each trial (i.e. the home target). Dark grey eye and hand symbols denote the instructed eye and hand movements for each task. Dark grey circle denotes the peripheral target, presented randomly in one of four locations. White square denotes the cursor feedback provided during each condition. **B.** Trial timing. Open circles denote non- illuminated target locations. Disappearance of the home target (which occurred at the same time as presentation of the peripheral target) served as the "go-signal" to initiate movement. CHT: centre hold time, RT: reaction time, MT: movement time, THT: target hold time.

Results

Significant negative correlations between MoCA scores and visuomotor performance in older adults were mainly found in the plane dissociated condition (Table 2.2). These correlations indicate that older adult participants with lower cognitive scores (i.e. those diagnosed with MCI) exhibit greater impairments in visuomotor control under spatially dissociated conditions. The lack of significant correlations between MoCA scores and all but one performance measure in the most cognitively-demanding condition, suggests that the performance decrements observed on this task in the high AD risk group may be independent of more global impairments in cognition detected by standardized cognitive tests.

As predicted, a marked deterioration in movement control was observed in high AD risk participants as the cognitive demands of the task increased. The mean ballistic trajectories plotted in Figure 2.2 illustrate a pronounced disruption in the performance (i.e. larger variability and endpoint errors) of high AD risk participants, including both FH+ and MCI subgroups, during the most cognitively demanding PD+FR condition. Example full trajectories from the PD+FR condition are also displayed in Figure 2.2 in order to demonstrate the typical trajectory deviations observed in the high AD risk group. Figure 3 illustrates mean velocity profiles across task conditions for young, low AD risk, FH+ and MCI participants. Again, performance disruptions in high AD risk participants, including both FH+ and MCI subgroups, were most pronounced in the PD+FR condition.

Figure 2.3 also demonstrates that the performance of MCI patients was affected at lower levels of cognitive demand (i.e. in the FR and PD conditions) than FH+ participants. Our ANCOVA tests resulted in significant condition by group interactions for all dependent measures (on-axis CE: $F_{(3.9,122)} = 14.78$, $p < .001$, $\eta_p^2 = .323$; off-axis CE: $F_{(4.5,141)} = 10.06$, $p < .001$, $\eta_p^2 = .245$; VE: $F_{(3.8,116)} = 8.02$, $p < .001$, $\eta_p^2 = .206$; CPL: $F_{(2.8,85.6)} = 24.79$, $p < .001$, $\eta_p^2 = .444$; RT: $F_{(3.5,110)} = 8.59$, $p < .001$, $\eta_p^2 = .217$; TMT: $F_{(2.9,91)} = 11.61$, $p < .001$, $\eta_p^2 = .272$), indicating impairments in performance with increasing task difficulty that were influenced primarily by the high AD risk group. Figure 2.4 illustrates these interaction effects with the high AD risk group subdivided into FH+ and MCI subgroups. Displaying these subgroups separately demonstrates that the impairment in performance observed in the conditions with only one level of dissociation (i.e. FR and PD) were mainly influenced by MCI participants, while the pronounced performance disruptions observed when combining spatial dissociation and feedback reversal (i.e. in the PD+FR condition) were influenced by both FH+ and MCI participants within the high AD risk group.

Group means in each condition for all dependent variables and effect sizes reflecting the effect of group within each condition are listed in Table 2.3. Post-hoc analyses revealed significantly larger on-axis constant errors in the high AD risk group relative to both the young and low AD risk groups during the PD and PD+FR conditions. On-axis constant errors were also significantly larger in both older adult groups relative to the

young group in the standard condition (Figure 2.4A). Significantly larger off-axis constant errors were observed in the high AD risk group relative to both the young and low AD risk groups in the PD+FR condition, and relative to the young group only in the PD condition (Figure 2.4B). Performance variability (i.e. variable error) and corrective path length were significantly increased in the high AD risk group relative to the low AD risk group for the FR condition and relative to both the young and low AD risk groups for the PD and PD+FR conditions (Figure 2.4C-D). Post-hoc analyses of the timing outcome variables also revealed effects of AD risk, however effects of normal aging were also clearly present. Reaction time was significantly longer in high AD risk participants relative to young participants in all task conditions. However, reaction time was also significantly longer in low AD risk participants relative to young participants in the FR and PD+FR conditions. Reaction time was only significantly different between high and low AD risk groups in the FR condition (Figure 2.4E). Lastly, movement time was significantly longer in high AD risk relative to young participants in all task conditions, as well as in low AD risk relative to young participants in the non-standard conditions. Movement time was only significantly different between high and low AD risk groups in the PD+FR condition (Figure 2.4F).

The one-way ANOVA tests for differences in the percentage of direction reversals between groups for the FR and PD+FR conditions were not significant. Notably, however, we did observe that within the high AD risk group, individuals diagnosed with

MCI tended to commit more direction reversal errors. In order to test this observation, we separated the high AD risk group into FH+ and MCI subgroups and compared percent DR between MCI, FH+, low AD risk, and young groups in the FR and PD+FR conditions using non-parametric Kruskal-Wallis tests. The omnibus Kruskal-Wallis test revealed no significant differences in direction reversal errors between groups in the FR condition (young: M = 1.39 +/- 0.6; low AD risk: M = 2.73 +/- 0.91; FH+: M = 1.79 +/- 1; MCI: M = 11.25 +/- 9.29), however in the PD+FR condition, the percentage of direction reversal errors was significantly different between groups (p = .042). Specifically, post-hoc analyses revealed that in the PD+FR condition, percentage of direction reversals was significantly higher in the MCI group relative to the young group (p = .006), as well as relative to the low AD risk group with marginal significance (p = .056; young: M = 3.91 +/- 1.86; low AD risk: M = 6.31 +/- 2.28; FH+: M = 7.62 +/- 2.45; MCI: M = 19.04 +/- 7.35).

Table 2.2

Significant correlations between MoCA scores and kinematic measures

Kinematic Measures	***r***	***r*²**	***p*-value**
On-axis constant error (PD condition)	- 0.399	0.159	0.008
On-axis constant error (PD+FR condition)	- 0.345	0.119	0.024
Variable error (PD condition)	- 0.336	0.113	0.028
Corrective path length (PD condition)	- 0.379	0.144	0.012
Reaction time (PD condition)	- 0.429	0.184	0.004
Total movement time (PD condition)	- 0.393	0.154	0.009

PD: plane dissociated; PD+FR: plane dissociated + feedback reversal.

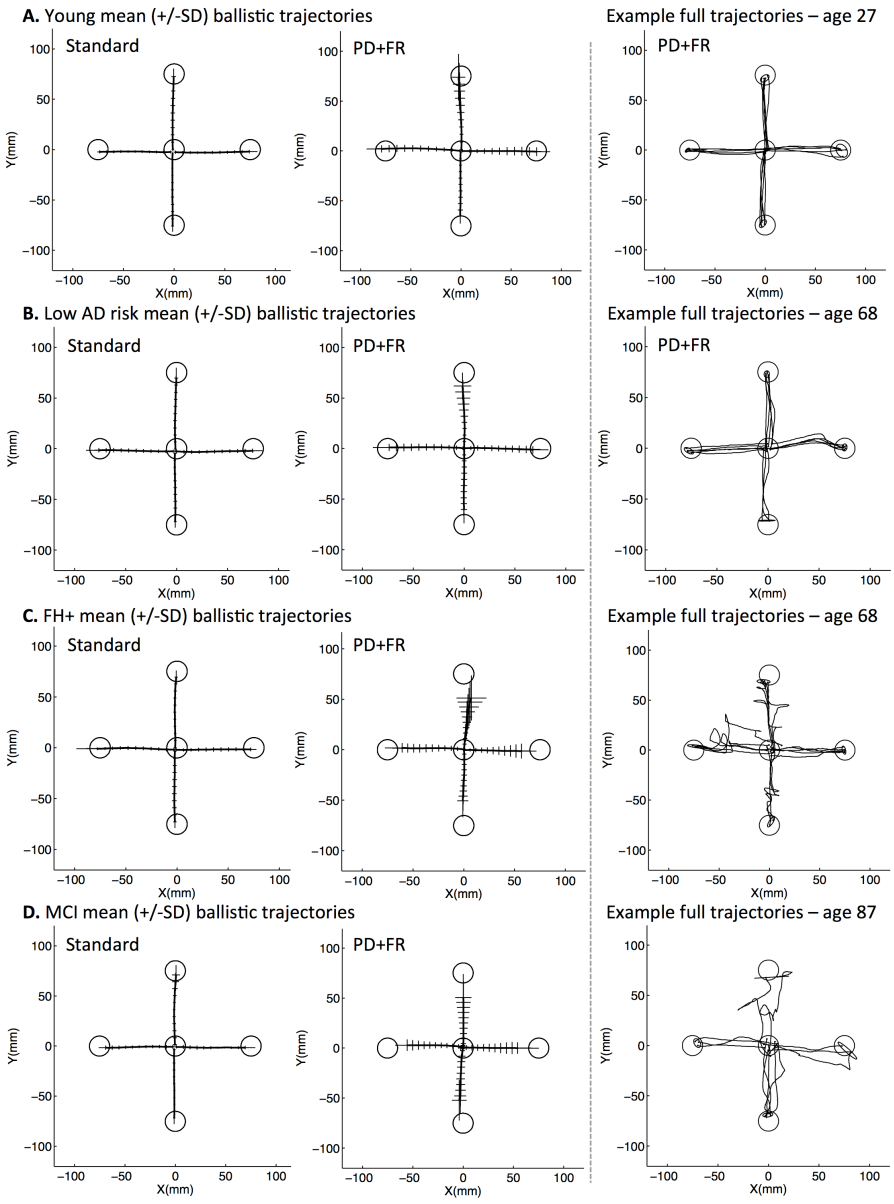

Figure 2.2. Left panel: mean ballistic trajectories (+/- SD) in the standard and plane dissociated + feedback reversal (PD+FR) conditions across groups: **A.** Young, **B.** Low Alzheimer's disease (AD) risk, **C.** Family history positive (FH+) and **D.** Mild cognitive impairment (MCI). Crosshairs reflect variability in reach performance, calculated as the standard deviation (SD) at ten equal points along the reach trajectory. Right panel: examples of the typical full reach trajectories observed during the plane dissociated + feedback reversal (PD+FR) condition in each group (note the pronounce trajectory deviations in the high AD risk participants).

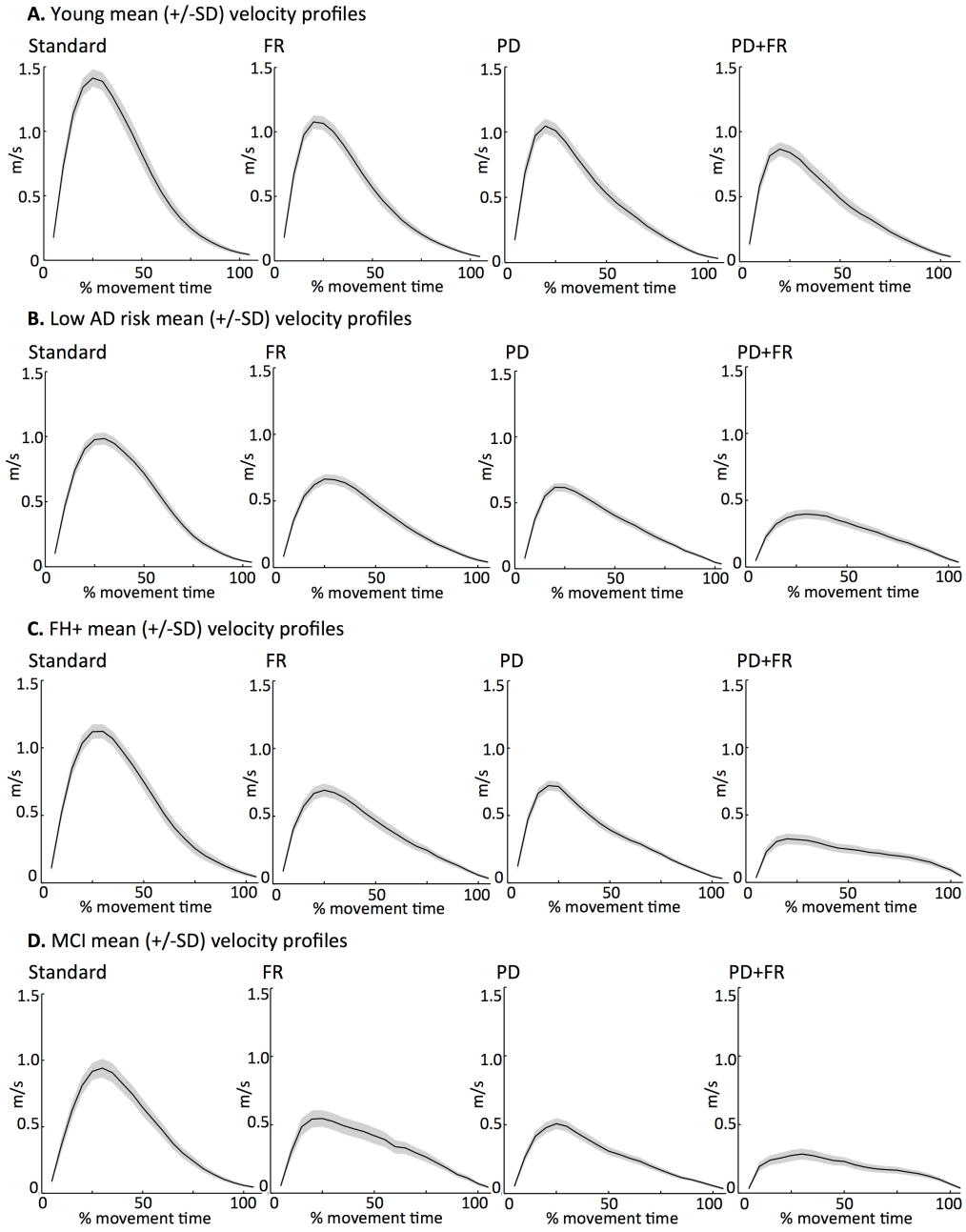

Figure 2.3. Mean velocity profiles (filtered using a 10 Hz low pass Butterworth filter) across task conditions for each group: **A.** Young, **B.** Low Alzheimer's disease (AD) risk, **C.** Family history positive (FH+) and **D.** Mild cognitive impairment (MCI). Shading represents standard deviation. FR: feedback reversal, PD: plane dissociated, PD+FR: plane dissociated + feedback reversal, m/s: metres per second.

Table 2.3

Group means and effect sizes for kinematic measures in each condition

		Group Means (SE)			
Kinematic Measures	**Condition**	**Young**	**Low AD Risk**	**High AD Risk**	η_p^2
On-axis constant error	**Standard**	3.85 (.39)	5.57 (.39)	5.66 (.40)	.176
	FR	7.13 (.69)	6.36 (.69)	8.33 (.71)	.059
	PD	7.19 (.96)	7.18 (.96)	11.06 (.98)	.142
	PD+FR	7.69 (1.46)	11.45 (1.46)	22.23 (1.49)	.450
Off-axis constant error	**Standard**	1.97 (.15)	1.76 (.15)	1.77 (.15)	.021
	FR	2.15 (.19)	1.99 (.19)	2.41 (.19)	.038
	PD	1.48 (.19)	1.74 (.19)	2.15 (.19)	.090
	PD+FR	2.81 (.33)	2.43 (.33)	5.16 (.34)	.376
Variable error	**Standard**	3.73 (.27)	3.26 (.27)	4.03 (.28)	.060
	FR	6.01 (.47)	4.92 (.47)	7.09 (.48)	.141
	PD	5.92 (.50)	5.66 (.50)	7.69 (.50)	.131
	PD+FR	7.41 (.79)	8.63 (.79)	14.02 (.81)	.376
Corrective path length	**Standard**	2.92 (.29)	2.99 (.29)	3.67 (.29)	.059
	FR	6.49 (.70)	5.14 (.70)	8.46 (.72)	.148
	PD	6.72 (.90)	6.10 (.90)	10.03 (.92)	.143
	PD+FR	7.97 (2.16)	10.65 (2.16)	31.49 (2.20)	.519
Reaction time	**Standard**	460 (28)	549 (28)	613 (28)	.191
	FR	587 (42)	823 (42)	982 (43)	.411
	PD	493 (37)	563 (37)	670 (38)	.152
	PD+FR	636 (79)	1044 (79)	1239 (80)	.325
Total movement time	**Standard**	509 (43)	609 (43)	676 (43)	.109
	FR	718 (65)	996 (65)	1093 (67)	.218
	PD	728 (102)	1089 (102)	1196 (104)	.154
	PD+FR	929 (212)	1666 (212)	2665 (216)	.342

Partial eta-squared (η_p^2) effect sizes reflect the effect of group within each condition and are based on the linearly independent pairwise comparisons among the estimated marginal means. AD: Alzheimer's disease; SE: standard error; FR: feedback reversal; PD: plane dissociated.

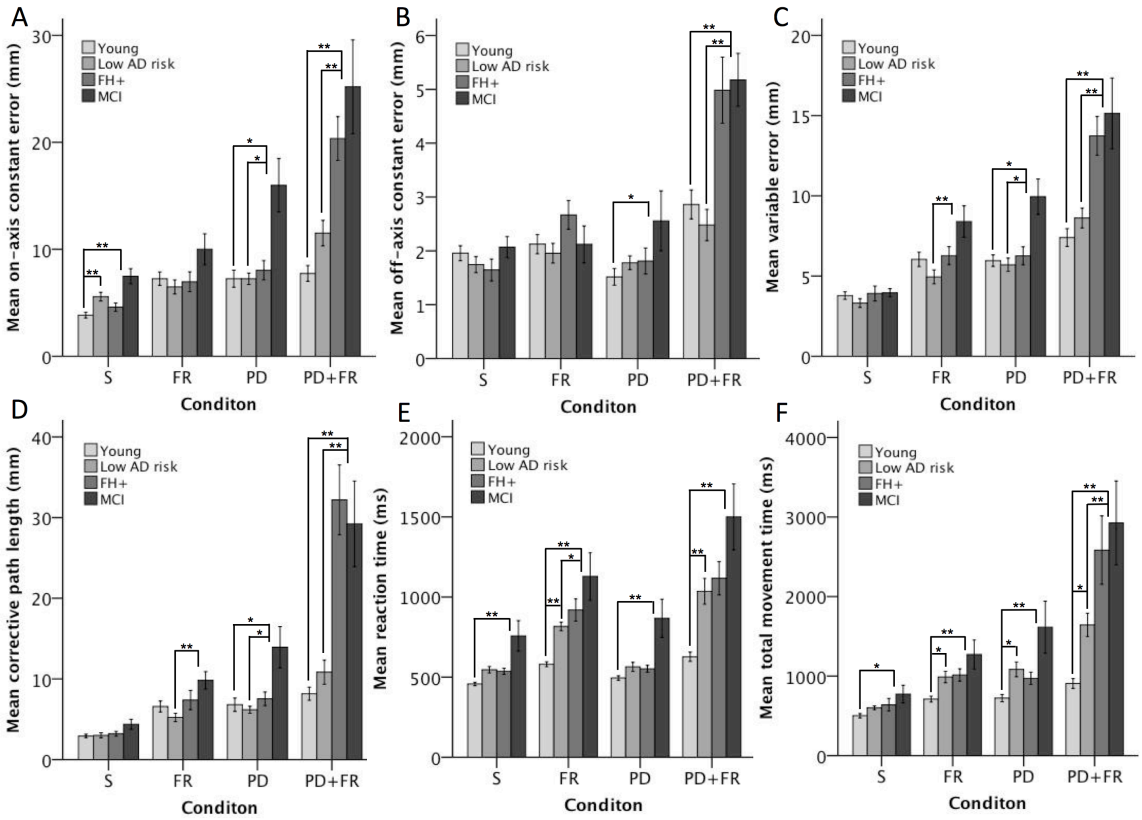

Figure 2.4. A-F. Results of group (young: light grey bars, low AD risk: medium grey bars, FH+: dark grey bars, MCI: black bars) by condition (S: standard, FR: feedback reversal, PD: plane dissociated, PD+FR: plane dissociated + feedback reversal) mixed ANCOVAs on task dependent measures. Means +/- 1 standard error of the mean, * = < .05, ** = < .001. AD: Alzheimer's disease; FH+: family history positive; MCI: mild cognitive impairment.

In order to determine the predictive potential of kinematic measures from a cognitively demanding visuomotor task in discriminating between high and low AD risk participants, the dependent measures from the PD+FR condition, along with MoCA scores, were entered into a stepwise discriminant analysis. The minimum partial F for entrance into the discriminant analysis was 3.84 and the maximum partial F for removal was 2.71. The most correlated, and thus first predictor variable entered into the analysis by the stepwise program, was corrective path length, next was variable error, and the last variable adding significant predictive power to the canonical R squared was off-axis constant error. In a forth and final step, corrective path length was removed from the analysis with an F to remove value of 2.51. The resulting discriminant function was significant (Wilks' Lambda = .468, $p < .001$), with a canonical correlation of .73. The structure matrix indicated that off-axis constant error was the strongest predictor (r = .73), next was variable error (r = .64), followed by corrective path length (r = .53) and on-axis constant error (r = .34). The correlation between MoCA scores and the standardized canonical discriminant function (r = .06) indicated that cognitive scores were not useful in predicting group membership. The resulting canonical discriminant function was: D = (.453 x off-axis constant error) + (.168 x variable error) - 3.614. The grouping of cases resulted in an overall classification accuracy of 86.4%, with a sensitivity of 81.8% and specificity of 90.9%.

The discriminant analyses conducted separately on the high AD risk subgroups also

demonstrated good separation from the low AD risk group (FH+: Wilks' Lambda = .474, $p < .001$, canonical correlation = .73; MCI: Wilks' Lambda = .344, $p < .001$, canonical correlation = .81). The predictors included in the discriminant function classifying FH+ versus low AD risk participants were corrective path length ($r = .89$) and variable error ($r = .68$) [D = (.131 x variable error) + (.067 x corrective path length) – 2.67]. Again, MoCA scores were not useful in predicting group membership in this analysis ($r = .16$). However, in the discriminant function classifying MCI versus low AD risk participants, MoCA scores did add significant predictive power, as would be expected since impaired MoCA performance was one of the diagnostic criteria for MCI classification. Importantly, several kinematic measures were also significant predictors and were better or as good as MoCA scores at predicting group membership, including off-axis constant error ($r = .65$), corrective path length ($r = .62$), on-axis constant error ($r = .57$), and variable error ($r = .51$). MoCA scores were negatively correlated with the discriminant function ($r = -.52$), reflecting lower scores in the MCI group. The predictors included in the discriminant function were off-axis constant error, variable error, and MoCA score [D = (.534 x off-axis constant error) + (.145 x variable error) – (.149 x MoCA score) - .745]. These discriminant analysis classification results are summarized in table 2.4.

Table 2.4

Classification results of stepwise discriminant analyses

			Predicted Group Membership		
		Group	**Low AD Risk**	**High AD Risk**	**Total**
Classification[a]	**Count**	**Low AD Risk**	20	2	22
		High AD Risk	4	18	22
	%	**Low AD Risk**	90.9	9.1	100.0
		High AD Risk	18.2	81.8	100.0
			Low AD Risk	**FH+**	**Total**
Classification[b]	**Count**	**Low AD Risk**	20	2	22
		FH+	3	11	14
	%	**Low AD Risk**	90.9	9.1	100.0
		FH+	21.4	78.6	100.0
			Low AD Risk	**MCI**	**Total**
Classification[c]	**Count**	**Low AD Risk**	21	1	22
		MCI	2	6	8
	%	**Low AD Risk**	95.5	4.5	100.0
		MCI	25	75	100.0

Each case in the analysis is classified by the functions derived from all cases other than that case. *a.* 86.4% of cases correctly classified. *b.* 86.1% of cases correctly classified. *c.* 90% of cases correctly classified. AD: Alzheimer's disease; FH+: family history positive; MCI: mild cognitive impairment.

Discussion

The results of the present study demonstrate a striking impairment of visuomotor integration under cognitively demanding task conditions in high AD risk older adults relative to both low AD risk and young participants. Specifically, we found that when performing the PD+FR task, participants at increased AD risk, due to both family history and MCI, demonstrated significant impairments on measures of accuracy, consistency and timing. Furthermore, we demonstrated that these kinematic measures are useful in discriminating between older adults who are and are not at increased AD risk.

Visuomotor impairment in MCI and AD populations has received little study to date, thus the present state of knowledge in this area is low. Most research involving the assessment of AD in its early stages is cognitive based, and only recently has it been recognized that complex movements may also be affected (Crutch et al., 2007a; Crutch et al., 2007b; Salek et al., 2011; Verheij et al., 2012). The results of the current study indicate that measurable impairments in visuomotor control are already present in individuals at increased risk of developing AD. We suggest that these impairments may reflect inherent brain alterations and/or early neuropathology disrupting the connectivity between hippocampal, parietal and frontal brain regions required to successfully control complex reaching behaviours. In support of this prediction, recent diffusion tensor imaging (DTI) studies in MCI and early AD have revealed disruption to the integrity of prominent association fibre tracts, including parietal-frontal connections (Bai et al., 2009;

Bosch et al., 2012) and projections from the hippocampus to inferior parietal regions (Villain et al., 2008). Furthermore, DTI studies in cognitively normal participants at increased AD risk due to family history and carrying one or more apolipoprotein E epsilon 4 allele have shown decreased microstructural integrity in WM tracts with direct and secondary connections to the medial temporal lobes, years before the expected onset of cognitive symptoms (Gold, Powell, Andersen, & Smith, 2010; Smith et al., 2010).

Taken together the above findings indicate that disconnection between the medial temporal lobes and neocortex, as well as between parietal and frontal cortex, may occur very early in the course of AD. In order to investigate whether or not these brain alterations are responsible for the visuomotor impairments observed in this study, our lab is currently using MRI techniques to correlate anatomical and functional connectivity with visuomotor performance in individuals at increased AD risk.

Interpretation of visuomotor deficits associated with Alzheimer's disease risk

Our results suggest that visuomotor networks involved in both visual-spatial recalibration and strategic control may be compromised in individuals at increased AD risk. Specifically, we found that the performance of MCI patients was impacted at lower levels of cognitive demand when either strategic control (FR condition) or visual-spatial recalibration (PD condition) were required, whereas performance impairments in FH+ participants only became apparent at higher levels of cognitive demand when both strategic control and visual-spatial recalibration were required at the same time (i.e.

PD+FR condition). Furthermore, MCI patients showed direction reversal errors in the feedback reversal conditions reflecting impaired inhibition of prepotent responses, as well as overall slowing in reaction and movement times across task conditions that were not present in FH+ participants. These findings suggest that visuomotor tasks with increasing levels of cognitive demand may be useful not only in detecting AD risk before cognitive declines on standardized tests are present, but also in monitoring disease progression from preclinical to MCI stages.

We propose three putative mechanisms (which are not mutually exclusive) to account for the visuomotor deficits observed in high AD risk participants in the current study. First, increased ballistic endpoint errors may reflect disruption to motor programming, and thus more reliance on online sensory feedback. In turn, these corrective mechanisms may also be disrupted or delayed, resulting in trajectory deviations and extended corrective path lengths. In other words, the internal feedback loop required to update the current location of the hand relative to the position of the target, which relies on intact parietal-frontal connections (Vesia, Yan, Henriques, Sergio, & Crawford, 2008), may be disrupted. Studies examining the control of arm movements in older adults have demonstrated that increased reliance on visual feedback is present in normal healthy aging, which is often interpreted as compensation for deficiencies in central motor planning (Haaland, Harrington, & Grice, 1993; Ketcham, Seidler, Van Gemmert, & Stelmach, 2002; Pratt, Chasteen, & Abrams, 1994; Seidler-Dobrin &

Stelmach, 1998). Furthermore, online corrective mechanisms have been shown to be less efficient in older individuals (Chaput & Proteau, 1996; Sarlegna, 2006). Our results suggest that these changes associated with normal aging may be exacerbated in individuals at increased AD risk.

Second, disruption to attentional control networks (Baddeley, Baddeley, Bucks, & Wilcock, 2001; Gillain et al., 2009) may also play a role in the errors and slowed performance observed under indirect task conditions. Such disruption would impair the ability to inhibit stereotyped eye-hand coupling and divide attention (i.e. neural resources) between incongruent eye and hand movements. Baddeley and colleagues (Baddeley et al., 2001; Gillain et al., 2009) have demonstrated that individuals in the early stages of AD exhibit substantial impairment in the ability to combine performance on two simultaneous tasks, indicating that an attentional processing deficit exists in early AD. Lastly, poorer accuracy and precision under conditions of spatial dissociation may also be explained by disruption to hippocampal-parietal processing, which is required for the integration of visual-spatial information into a motor program (Clower, West, Lynch, & Strick, 2001).

Study limitations

Considering the relatively small sample size used in the present study, future research is required in order to determine the generalizability of our results and to apply appropriate cross-validation to the discriminant analyses. Furthermore, longitudinal

studies are required in order to fully elucidate the predictive potential of kinematic measures in identifying individuals who will later go on to develop Alzheimer's disease. Lastly, while there were similarities between the FH+ and MCI participants combined to form the high AD risk group in the present study, there were also important differences that could not be fully examined statistically due to the small number of MCI participants included. These MCI patients were also older, less educated, and had less computer/touchscreen experience than the other study participants, adding potential confounds that may have exacerbated their impaired performance. Again, future studies with larger sample sizes and better separation between different levels of risk would clarify this issue.

Conclusions and clinical implications

Based on the findings of the current and previous research from our lab, clinical assessment tools incorporating cognition and action together would be useful not only in providing information about the functional abilities of a patient, but also in alerting clinicians to increased dementia risk before cognitive symptoms are consistently present. Furthermore, we speculate that the early detection of visuomotor deficits may serve to identify individuals at increased risk for subsequent clinical decline in areas such as balance and gait (Gillain et al., 2009; Sheridan & Hausdorff, 2007), driving, and activities of daily living. Several studies have demonstrated an association between motor symptoms and adverse health effects in old age (Buchman & Bennett, 2011), thus

assessments that employ motor measures may provide more accurate identification of individuals at increased disease risk. Importantly, our results provide strong evidence that the integration of cognition and movement control can provide valuable, clinically-relevant information that may be more useful than measuring performance in either of these domains in isolation.

Chapter Three

Diffusion tensor imaging correlates of cognitive-motor decline in normal aging and increased Alzheimer's disease risk

Kara M. Hawkins, Aman I. Goyal, and Lauren E. Sergio

Reprinted from the Journal of Alzheimer's Disease: Hawkins KM, Goyal AI & Sergio LE (2015). Diffusion tensor imaging correlates of cognitive-motor decline in normal aging and Increased Alzheimer's Disease Risk, *Journal of Alzheimer's Disease, 44(3)*, 867-878.

Abstract

Alzheimer's disease (AD) is typically associated with impairments in memory and other aspects of cognition, while deficits in complex movements are commonly observed later in the course of the disease. Recent studies, however, have indicated that subtle deteriorations in visuomotor control under cognitively demanding conditions may in fact be an early identifying feature of AD. Our previous work has shown that the ability to perform visuomotor tasks that rely on visual-spatial and rule-based transformations is disrupted in prodromal and preclinical AD. Here, in a sample of 30 female participants (10 young: mean age = 26.6 +/- 2.7, 10 low AD risk: mean age = 58.7 +/- 5.6, and 10 high AD risk: mean age = 58.5 +/- 6.9), we test the hypothesis that these cognitive-motor impairments are associated with early AD-related brain alterations. Using diffusion-weighted magnetic resonance imaging, we assessed the relationship between normal aging, increased AD risk, cognitive-motor performance, and the underlying white matter (WM) integrity of the brain. Our whole-brain analysis revealed significant age-related declines in WM integrity, which were more widespread in high relative to low AD risk participants. Furthermore, analysis of mean diffusivity measures within isolated WM clusters revealed a stepwise decline in WM integrity across young, low AD risk, and high AD risk groups. In support of our hypothesis, we also observed that lower WM integrity was associated with poorer cognitive-motor performance. These results are the first to demonstrate a relationship between AD-related WM alterations and impaired cognitive-

motor control. The application of these findings may provide a novel clinical strategy for the early detection of individuals at increased AD risk.

Introduction

Over the past several years many brain-imaging studies have investigated the neural underpinnings of Alzheimer's disease (AD). In 2009, a meta-analysis of these studies revealed that, aside from the commonly known structural atrophy in trans-entorhinal and hippocampal regions, hypometabolism and hypoperfusion in the inferior parietal lobule (IPL) and precuneus are also prevalent features of early AD (Schroeter et al., 2009). Furthermore, recent neuroimaging studies employing diffusion tensor imaging (DTI) in mild cognitive impairment (MCI) and AD have reported white matter (WM) compromise affecting several major fiber tracts forming parietal-frontal, interhemispheric, and hippocampal-cortical connections, including the inferior fronto-occipital fasciculus (IFOF), inferior longitudinal fasciculus (ILF), superior longitudinal fasciculus (SLF), corpus callosum (CC), and cingulum (CG) bundle (Bai et al., 2009; Bartzokis et al., 2004; Bosch et al., 2012; Stricker et al., 2009). Microstructural declines in the CG, ILF, and IFOF have also been found in cognitively normal women at increased risk of AD due to family history and apolipoprotein E4 (ApoE4) genotype, years before the expected onset of cognitive symptoms (Gold et al., 2010; Smith et al., 2010).

While AD dementia is typically associated with declines in cognition and short-term

memory resulting from hippocampal atrophy (Karow et al., 2010), these clinical symptoms only present themselves after significant damage to the brain has already occurred (Ewers et al., 2011). Thus, neuroimaging studies including individuals in the preclinical (i.e. increased genetic risk) and prodromal (i.e. MCI) stages of AD are essential for the development of early detection strategies. Notably, the alterations in parietal areas and declines in WM integrity that have been observed in these preclinical/prodromal studies provide insight into other behaviors that may be affected even earlier in the disease process. Specifically, parietal cortex plays an important role in transforming visual-spatial information into goal-directed actions (Battaglia-Mayer et al., 2000; Galati et al., 2011; Hawkins, Sayegh, Yan, Crawford, & Sergio, 2013; Sayegh et al., 2014). Further, WM tracts forming hippocampal-parietal and parietal-frontal connections are required to successfully transform spatial representations and contextual information into accurate motor outputs (Clower et al., 2001; Crawford et al., 2011; Johnson et al., 1996). These observations suggest that early neurodegeneration may have an impact on rule-based motor control. Accordingly, impairments in visuomotor control under non-standard conditions, in which the correspondence between vision and action is not direct (Wise et al., 1996), have been observed in early and preclinical AD (de Boer, Mattace-Raso, van der Steen, & Pel, 2013; Ghilardi et al., 1999; Ghilardi et al., 2000; Hawkins & Sergio, 2014; Salek et al., 2011; Tippett & Sergio, 2006; Tippett et al., 2007; Tippett et al., 2012; Verheij et al., 2012). Given the potential impact of AD-related brain

alteration on motor control and the close relationship between cognition and action (Georgopoulos, 2000), the aim of the present study is to examine the underlying structural connectivity associated with impaired cognitive-motor performance observed in individuals at increased AD risk. Using DTI and high-resolution magnetic resonance imaging (MRI), we test the hypothesis that kinematic measures from a cognitively demanding visuomotor task are associated with identifiable brain alterations similar to those observed in early AD, and thus may be useful in identifying individuals at increased AD risk.

Materials and Methods

Subjects

Thirty right-handed female participants were included in this study: 10 healthy young adults (mean age = 26.6 +/- 2.7), 10 low AD risk older adults (mean age = 58.7 +/- 5.6), and 10 high AD risk older adults (mean age = 58.5 +/- 6.9). Individuals classified as high AD risk scored at or above age- and education-adjusted norms on the Montreal Cognitive Assessment (MoCA) and reported either a maternal, multiple, or early-onset family history of AD. While early-onset AD is known to be associated with the rare familial form of the disease (Alzheimer's Association, 2012), individuals with late-onset AD in their immediate family have also been shown to be at increased risk (Fratiglioni et al., 1993; Green et al., 2002; Mayeux et al., 1991), especially if multiple family members

are affected (Lautenschlager et al., 1996). Paternal family history alone was not included in the high AD risk classification based on recent evidence that paternal history may not carry the same increased risk as maternal history (Honea et al. 2011; Mosconi et al., 2007; Mosconi et al., 2010). Individuals classified as low AD risk were aged-matched with high AD risk participants, reported no dementia of any type within their known family history, scored at or above age- and education-adjusted norms on the MoCA, and expressed no memory complaints beyond normal expectations for their age. Exclusion criteria included vision or upper-limb impairments, any medical condition that would hinder task performance (e.g. severe arthritis), any neurological or psychiatric illnesses (e.g. schizophrenia, depression, alcoholism, epilepsy, Parkinson's disease), and any history of stroke or severe head injury. High and low AD risk participants also underwent ApoE genotyping, which supported the notion of increased genetic risk in our family history group (i.e. 80% of this sample were ApoE4 carriers, compared to only 20% of the no family history group). Demographic characteristics for all study participants are summarized in Table 3.1. Our decision to focus on female participants in the current study was based on a few factors: 1) the prevalence of AD is higher in women, emphasizing the importance of studies specifically tailored towards early detection in this population (Carter, Resnick, Mallampalli, & Kalbarczyk, 2012; Schmidt et al., 2008), 2) recent evidence suggesting that sex-differences in the efficacy of ApoE in redistributing myelin cholesterol during nerve repair may increase vulnerability to the degradation of

WM tracts specifically in women who carry the ApoE4 allele (Reilly, Ferrell, & Sing, 1994), and 3) to avoid sex-related confounds inherent in brain imaging studies. The study protocol was approved by the Human Participants Review Sub-Committee, York University's Ethics Review Board, and conformed to the standards of the Canadian Tri-Council Research Ethics guidelines.

Visuomotor assessment

A detailed description of our visuomotor assessment is provided in Hawkins and Sergio (2014). Briefly, in the current study, participants were tested on two visuomotor transformation tasks presented on an Acer Iconia 6120 dual-touchcreen tablet: One standard task in which the spatial location of the viewed target and the required movement were the same, and one cognitively demanding non-standard task (plane dissociated + feedback reversal) in which the location of the viewed target was dissociated from the required movement (Figure 3.1A). Task conditions were presented in randomized blocks consisting of five pseudo-randomly presented trials to each of four peripheral targets (from a common central 'home' target), for a total of 20 trials per condition and 40 trials per participant (Figure 3.1B). Specifically, in the standard condition participants slid their finger directly to targets on the vertical tablet, while in the non-standard condition the same targets were presented on the vertical screen, however now participants had to direct a cursor to these targets by sliding their finger along the horizontal tablet (i.e. in a different spatial plane), as well as in the opposite

direction of the targets (i.e. feedback reversal). To ensure task comprehension each participant was given two practice trials per target prior to each condition, they were then asked to perform the experimental task (i.e. five trials to each target) as quickly and accurately as possible. To ensure dissociation between eye and hand movements in the non-standard task, participants were instructed to always look towards the visual target and not at their hand. To reinforce compliance with these task instructions, the eyes were monitored throughout the experiment using a webcam and a reminder was provided in the event that incorrect eye movements were performed.

Table 3.1

Demographic characteristics of subjects

	Young	Low AD Risk	High AD Risk
Number	10	10	10
Age (SD)	26.6 (2.7)	58.7 (5.6)	58.5 (6.9)
Years of education (SD)	-	17.9 (3.1)	16.8 (3.1)
MoCA score (SD)	-	27.9 (1.7)	28.3 (2.2)
ApoE genotype (% E4 carriers)	-	20%	80%

SD: standard deviation; MoCA: Montreal cognitive assessment; ApoE: apolipoprotein E.

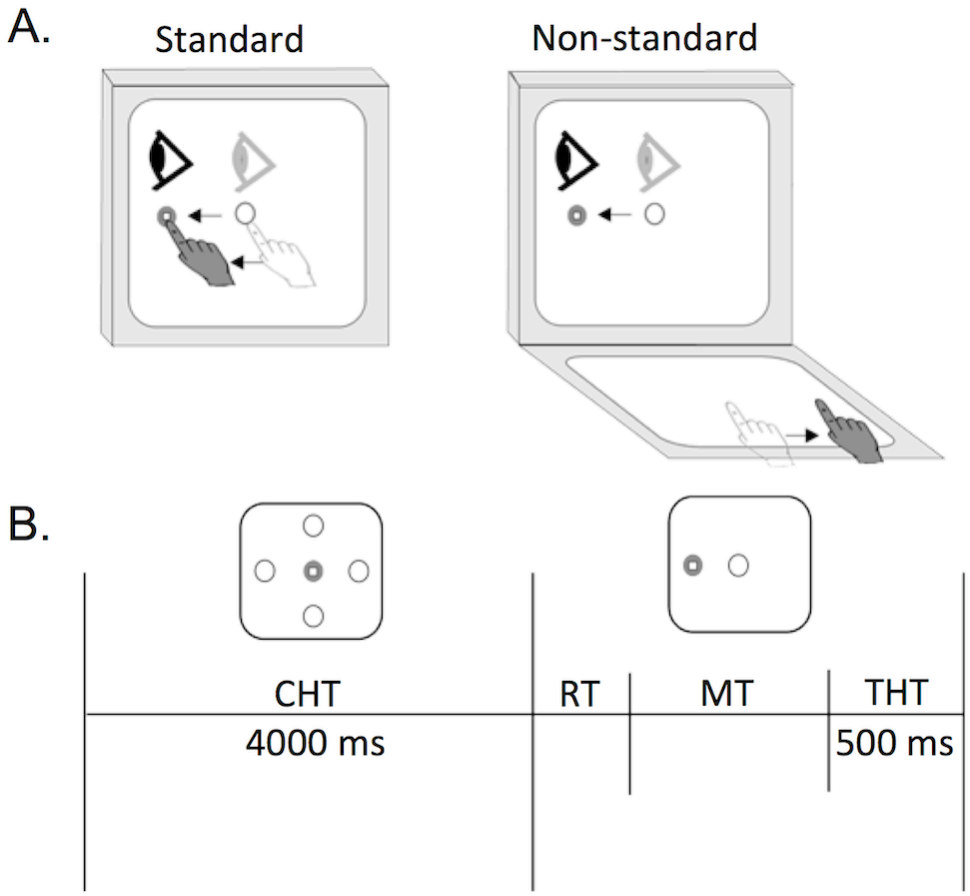

Figure 3.1. A. Schematic drawing of the two experimental conditions. Light grey circle, eye, and hand symbols denote the starting position for each trial (i.e. the home target). Dark grey eye and hand symbols denote the instructed eye and hand movements for each task. Dark grey circle denotes the peripheral target, presented randomly in one of four locations. White square denotes the cursor feedback provided during each condition. **B.** Trial timing. Open circles denote non- illuminated target locations. Disappearance of the home target (which occurred at the same time as presentation of the peripheral target) served as the "go-signal" to initiate movement. CHT: center hold time, RT: reaction time, MT: movement time, THT: target hold time.

Imaging data acquisition

MRI data were acquired using a 3 Tesla Siemens Trio scanner at York University. Sequences included a high-resolution T1-weighted anatomical scan using magnetization prepared rapid gradient echo (MPRAGE) and a whole-brain diffusion-weighted scan with 64 encoding directions. The MPRAGE sequence consisted of 192 sagittal slices with a slice thickness of 1 mm with no gap, field of view (FOV) of 256 x 256 mm, and a matrix size of 240 x 256, resulting in a voxel resolution of 1 x 1 x 1 mm^3 [repetition time (TR) = 2300 ms, echo time (TE) = 2.96 ms, flip angle = 9°]. For the DTI sequence, 56 axial slices were acquired using diffusion weighted spin-echo single-shot echo planar imaging with a b-value of 1000 s/mm^2 (including one volume with no diffusion gradient, $b = 0$ s/mm^2), FOV of 192 x 192 mm, matrix size of 128 x 128, and slice thickness of 2 mm with no gap, resulting in a voxel resolution of 1.5 x 1.5 x 2 mm^3 (TR = 6900 ms, TE = 86 ms).

ApoE genotyping

All older adult participants provided saliva samples for ApoE genotyping conducted at Viaguard Accu-metrics (Toronto ON). DNA samples were extracted from the filter paper blots of saliva and standard polymerase chain reaction (PCR) techniques were applied. The PCR products were then analyzed by electrophoresis and visualized under ultraviolet illumination to determine the presence of specific ApoE haplotypes (i.e. E2, E3, and/or E4).

Kinematic data analysis

The touchscreen data processing and kinematic outcome measures for the visuomotor tasks used in the current study are described in detail in Hawkins and Sergio (2014). Briefly, movement accuracy was determined by calculating the absolute on-axis (distance) and off-axis (direction) constant errors (CE), which involved computing the average distance between the center of the target and the endpoints of each ballistic movement. Movement precision, or consistency (i.e. variable error; VE), was determined by calculating the standard deviation of the ballistic movement endpoints. The extent to which corrective movements were required in order to reach the target was quantified as the difference between the total path length and the ballistic path length, resulting in a measure of corrective path length (CPL). The time between disappearance of the home target (i.e. the movement 'go signal') and movement onset served as the measure of reaction time (RT), and the time between movement onset and the final movement endpoint upon positioning the cursor inside the peripheral target served as the measure of movement time (MT). In order to minimize the number of correlations between the imaging and behavioral data, kinematic measures from the non-standard task were summarized by calculating z-scores and averaging across the CE, VE, and CPL variables to generate a performance error score, and across the RT and MT variables to generate a performance timing score.

Imaging data analysis

Imaging data were analyzed using the Oxford Centre for Functional Magnetic Resonance Imaging of the Brain (FMRIB) Software Library (FSL - http://www.fmrib.ox.ac.uk/fsl). In order to test for any hippocampal atrophy across groups, subcortical segmentation was performed on the brain extracted TI-weighted MPRAGE data using the FSL tool FIRST (Patenaude, Smith, Kennedy, & Jenkinson, 2011) and the FSLUTILS program fslstats was used to determine hippocampal volumes.

DTI data were pre-processed using FMRIB's Diffusion Toolbox (FDT). Eddy current and head motion corrections were applied using the affine image registration tool (FLIRT; Jenkinson, Bannister, Brady, & Smith, 2002) and removal of non-brain structures was applied using the brain extraction tool (Smith, 2002). Maps for fractional anisotropy (FA), mean diffusivity (MD), axial diffusivity (DA), and radial diffusivity (DR) were then extracted using DTIFIT to fit a tensor model to the raw diffusion data and analyzed using whole-brain tract-based spatial statistics (TBSS; Smith et al., 2006). Specifically, FA data for all subjects used in a particular comparison were aligned to a common space using FMRIB's nonlinear image registration tool (FNIRT), then a mean FA image was created and thinned to generate a mean FA skeleton representing the centers of all tracts common to the group. Each subject's aligned FA data was then projected onto the mean skeleton. The nonlinear warps and projection vectors estimated from the FA images were also applied to MD, DR, and DA using the script provided in TBSS for non-FA images. The resulting data were then fed into voxelwise cross-subject

statistics and significant voxels were identified using the Johns Hopkins University (JHU) white matter atlas.

Non-FA diffusion measures were examined in the present study in attempt to understand the underlying alterations driving any observed differences in FA. Specifically, decreased FA with increased MD suggests microstructural declines associated with increased brain water content and macrostructural tissue loss. Whereas, decreased FA without increased MD suggests microstructural changes without gross tissue loss (Sen & Basser, 2005). Reduction in FA accompanied by increased DR may signify loss of myelin integrity, based on experimentally induced myelin degradation in mouse models (Song et al., 2003; Song et al., 2005; Sun et al., 2006). And lastly, decreased FA and DA, without increased DR, may reflect axonal damage (e.g. wallerian degeneration), which has been demonstrated in both rodent and human experiments (Concha, Gross, Wheatley, & Beaulieu, 2006; Sun et al., 2006).

Statistical analysis

Using SPSS statistical software, a mixed-design analysis of variance (ANOVA) was carried out to compare kinematic measures across the two task conditions (standard/non-standard; repeated), and between the three experimental groups (young/low AD risk/high AD risk). One-way ANOVA tests were also used to compare non-standard error and timing scores, and hippocampal volumes between the three experimental groups. When there were significant effects, post hoc analyses were adjusted for multiple comparisons

using Bonferroni correction. ANOVA results were considered statistically significant at $p < .05$.

FSL's Randomise tool was used to run voxelwise statistics on the TBSS data, with threshold-free cluster enhancement (TFCE) applied to correct for multiple comparisons. Between-group contrasts in both directions for each of the diffusivity measures were tested for young versus low AD risk, young versus high AD risk, and low AD risk versus high AD risk groups. Due to the widespread decline in FA between the young and older adult groups, significant FA differences between groups are reported and displayed at $p < .01$, while significant DR and DA differences are reported and displayed at $p < .05$ (no significant differences in MD were observed). FSL's cluster tool was used on the significant Randomise results to form clusters and report their sizes, locations (using the JHU white matter atlas), and significance levels. Lastly, mean diffusivity measures were calculated within the clusters that showed significant age-related WM impairment in the high AD risk group. One-way ANOVA tests were used to compare these mean diffusivity measures (i.e. FA/DR/DA) between groups for each WM cluster and post hoc analyses were adjusted for multiple comparisons using Bonferroni correction (alpha-level: $p < .05$). In order to examine the relationship between WM integrity and cognitive-motor performance, mean FA, DR, and DA in these WM clusters were also correlated with error and timing scores from the non-standard task using two-tailed Pearson's r in SPSS. Correlations were considered statistically significant at $p < .01$.

Results

Kinematic data

Consistent with our previous findings (Hawkins & Sergio, 2014), significant condition by group interactions driven by greater performance declines between the standard and non-standard tasks in the high AD risk group were found for all kinematic measures (On-axis CE: $F_{2,27} = 7.36$, $p = 0.003$; Off-axis CE: $F_{2,27} = 7.13$, $p = 0.003$; VE: $F_{2,27} = 11.35$, $p < 0.0001$; CPL: $F_{2,27} = 25.51$, $p < 0.0001$; RT: $F_{2,27} = 4.52$, $p = 0.02$; MT: $F_{2,27} = 4.97$, $p = 0.015$). Specifically, all three groups performed similarly on the standard visuomotor task, however in the non-standard task on-axis CE, off-axis CE, VE, and CPL were significantly larger in the high AD risk group relative to both the low AD risk and young groups, while RT and MT in the non-standard task were significantly longer in the high AD risk group relative to the young group only (see Table 3.2 for group means and effect sizes; group means are also plotted in Appendix B, along with a discriminant analysis). Average z-scores calculated to summarize the above error (i.e. CE, VE, CPL) and timing (i.e. RT and MT) results are displayed in Figure 3.2. Accordingly, error scores were significantly larger in the high AD risk group relative to both the young and low AD risk groups ($F_{2,27} = 21.39$, $p < 0.0001$; post-hoc: high AD risk - young $= 4.95$, $p < 0.00001$, high AD risk - low AD risk $= 4.04$, $p < 0.0001$), and timing scores were significantly larger in the high AD risk group relative to the young group only ($F_{2,27} = 5.31$, $p = 0.011$; post-hoc: high AD risk - young $= 1.87$, $p = 0.009$).

Table 3.2

Group means and effect sizes for kinematic measures in each condition

		Group Means (SE)			
Kinematic Measures	Condition	Young	Low AD Risk	High AD Risk	η_p^2
On-axis constant error	Standard	4.01 (.4)	4.47 (.3)	3.91 (.2)	.059
	Non-standard	8.50 (1.0)[a]	9.76 (1.8)[a]	18.67 (3.1)[b]	.334
Off-axis constant error	Standard	1.64 (.2)	1.50 (.3)	1.82 (.2)	.039
	Non-standard	2.96 (.5)[a]	2.96 (.5)[a]	5.93 (.6)[b]	.420
Variable error	Standard	3.47 (.2)	3.01 (.3)	3.28 (.2)	.067
	Non-standard	6.41 (.7)[a]	9.56 (1.2)[a]	14.44 (1.7)[b]	.440
Corrective path length	Standard	3.40 (.4)	3.33 (.2)	3.11 (.2)	.026
	Non-standard	8.73 (1.3)[a]	10.45 (1.9)[a]	32.91 (4.0)[b]	.655
Reaction time	Standard	444 (14)[a]	508 (20)[b]	470 (17)	.212
	Non-standard	603 (23)[a]	875 (62)	1013 (142)[b]	.282
Movement time	Standard	556 (28)	661 (35)	586 (35)	.168
	Non-standard	1096 (73)[a]	1577 (169)	2443 (496)[b]	.270

Superscripts denote significant differences between group means ($p < .05$). Partial eta-squared (η_p^2) effect sizes reflect the effect of group within each condition and are based on the linearly independent pairwise comparisons among the estimated marginal means. SE: standard error.

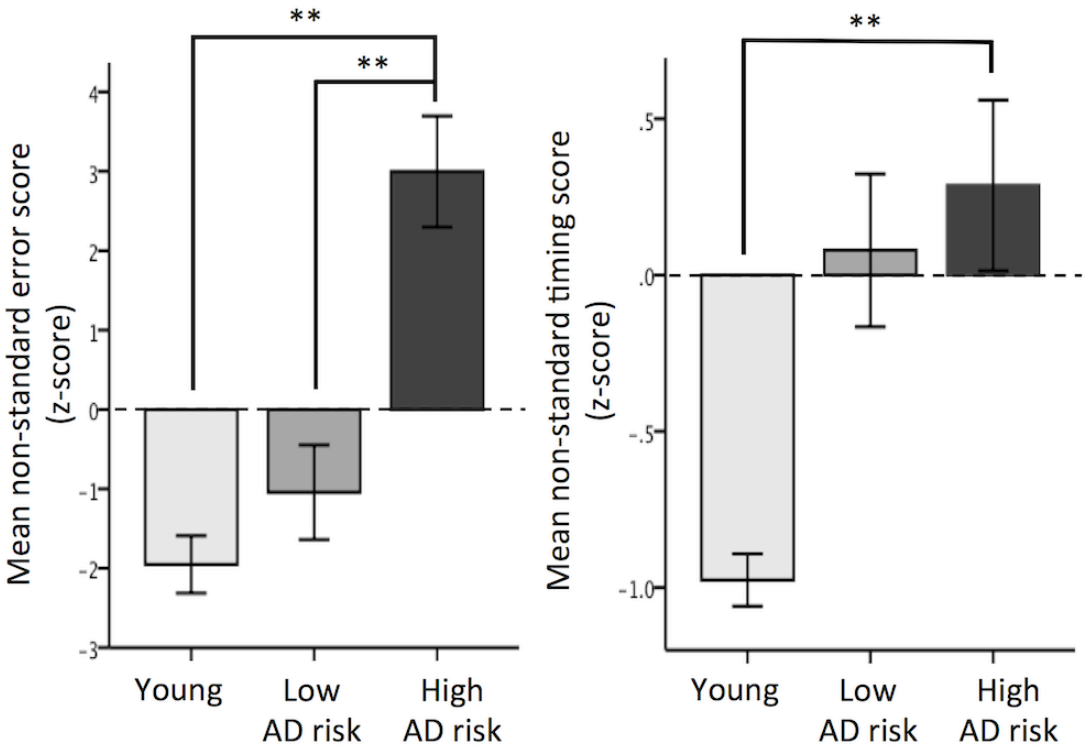

Figure 3.2. Mean z-scores for error and timing kinematic measures in the non-standard task across groups (young: light grey bars, low AD risk: medium grey bars, high AD risk: dark grey bars). Note that higher error scores reflect less accuracy and precision and higher timing scores reflect longer reaction and movement times. Means +/- 1 SEM, ** = < .01.

Imaging data

The whole-brain TBSS analysis revealed regions of significantly lower WM integrity in both low AD risk and high AD risk older adults relative to young adults. These results are displayed in Figures 3.3 using FSL's tbss_fill to thicken the thresholded stats results for better visualization. No significant differences on any of the diffusivity measures were found in the opposite direction (i.e. there were no regions of lower WM integrity in young relative to older adults). Significantly lower FA (Figure 3.3A, *left panel*; Supplementary Table 3.1), higher DR (Figure 3.3B, *left panel*; Supplementary Table 3.2), and lower DA (Figure 3.3C, *left panel*; Supplementary Table 3.3) in the low AD risk group (blue-light blue) were found primarily in anterior regions including the forceps minor (FMi), body of the CC, and corticospinal tract (CST), while in the high AD risk group (red-yellow) these age-related declines in WM integrity were more widespread, extending into posterior regions including the forceps major (FMa), IFOF, ILF, SLF, and hippocampal CG. While the observed age-related declines in WM integrity were more extensive in the high AD risk group relative to the low AD risk group, this whole-brain analysis did not reveal any significant differences between low and high AD risk groups on any of the diffusivity measures. There were also no significant differences in MD and hippocampal volume between groups (group mean hippocampal volumes are plotted in Appendix C).

In support of our hypothesis, a number of significant correlations were found

between mean diffusivity measures in isolated WM clusters and cognitive-motor performance scores. Specifically, larger error and timing scores were significantly correlated with lower mean FA in the right FMi (extending into the IFOF, ILF, SLF, FMa, and hCG), left FMa, left SLF, and left CST (Figure 3.3A, *right panel*). Similarly, we also found significant correlations between larger error and timing scores and higher mean DR in the left FMi (extending into the CC, IFOF, ILF, SLF, and FMa) and right FMi (extending into the CC and IFOF; Figure 3.3B, *right panel*). Finally, significant correlations were also observed between larger error scores and lower mean DA in the right FMi, SLF, ILF, primary motor cortex (M1), and IPL, and between larger timing scores and lower mean DA in the right FMi, SLF, CC, ILF, and IPL (Figure 3.3C, *right panel*). The statistics for these correlations are listed in Tables 3.3. (Additional methodology and correlational results for diffusivity measure within JHU atlas generated WM tracts of interest are reported in Appendix D).

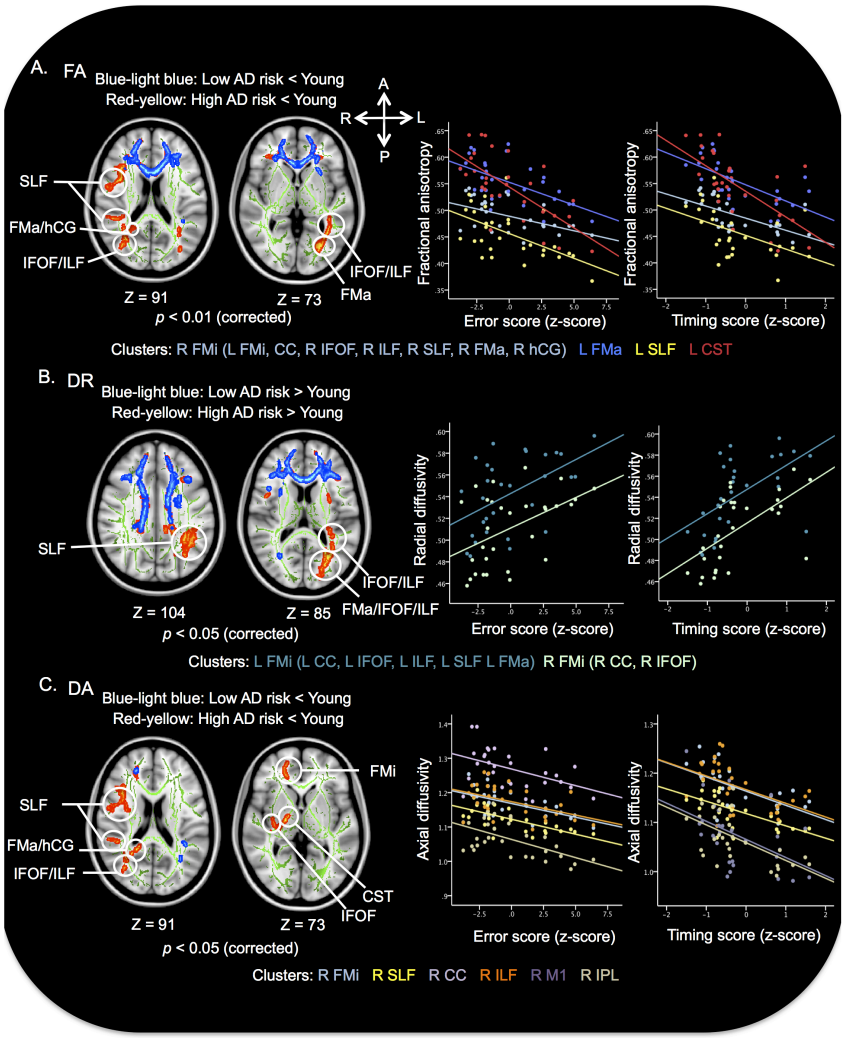

Figure 3.3. *Left panel*: Significant voxelwise between group tract-based spatial statistics (TBSS) results demonstrating **A.** lower fractional anisotropy (FA), **B.** higher radial diffusivity (DR), and **C.** lower axial diffusivity (DA) in both low AD risk (blue-light blue) and high AD risk (red-yellow) older adults relative to young adults. Thickened thresholded p-values (tbss_fill) are overlaid on the group mean FA skeleton and displayed on a standard MNI152 brain. Tracts are labeled using the JHU white matter atlas. *Right panel*: Scatterplots of significant correlations between diffusivity measures (**A.** FA, **B.** DR, **C.** DA) and cognitive-motor performance scores. Correlation statistics are listed in Table 3. R, right; L, left; FMi, forceps minor; CC, corpus callosum; IFOF, inferior fronto-occipital fasciculus; ILF, inferior longitudinal fasciculus; SLF, superior longitudinal fasciculus; FMa, forceps major; hCG, cingulum (hippocampal region); CST, corticospinal tract; M1, primary motor cortex; IPL, inferior parietal lobule.

Table 3.3

Correlations between diffusivity measures and cognitive-motor kinematics

	Error Score			*Timing Score*		
Mean FA TBSS clusters	*r*	r^2	*p* (2-tailed)	*r*	r^2	*p* (2-tailed)
R FMi (L FMi, R/L CC body, R/L SLF, R/L CST)	-0.51	0.26	0.004	-0.64	0.41	0.0002
L FMa	-0.59	0.35	0.001	-0.64	0.41	0.0002
L SLF	-0.56	0.32	0.001	-0.47	0.22	0.01
L CST	-0.70	0.48	0.00002	-0.66	0.44	0.0001
Mean DR TBSS clusters	*r*	r^2	*p* (2-tailed)	*r*	r^2	*p* (2-tailed)
L FMi (L CC body, L IFOF, L ILF, L SLF, L FMa)	0.51	0.26	0.004	0.57	0.32	0.001
R FMi (R CC body, R IFOF)	0.47	0.22	0.009	0.61	0.37	0.001
Mean DA TBSS clusters	*r*	r^2	*p* (2-tailed)	*r*	r^2	*p* (2-tailed)
R FMi	-0.55	0.30	0.002	-0.60	0.37	0.001
R SLF	-0.67	0.45	0.00005	-0.59	0.34	0.001
R CC	-0.47	0.22	0.009	-	-	-
R ILF	-0.47	0.22	0.009	-0.50	0.25	0.006
R IPL	-0.57	0.32	0.001	-0.61	0.37	0.0004
R M1	-	-	-	-0.49	0.24	0.008

R, right; L, left; FMi, forceps minor; CC, corpus callosum; SLF, superior longitudinal fasciculus; CST, corticospinal tract; IFOF, inferior fronto-occipital fasciculus; ILF, inferior longitudinal fasciculus; FMa, forceps major; hCG, cingulum (hippocampal region); IPL, inferior parietal lobule; M1, primary motor cortex.

Importantly, and in accordance with the whole-brain TBSS analysis, the one-way ANOVA tests comparing mean FA, DR, and DA in these isolated WM clusters revealed a stepwise decline in WM integrity across groups (Figure 3.4). Specifically, post-hoc analyses revealed significant age-related declines in WM integrity across all clusters and diffusivity measures, which were greater in the high AD risk group. In particular, decreased FA in the right and left ILF, and decreased DA in the right CC, M1, IFOF, CST, and IPL were only significant between the young and high AD risk groups and not between the young and low AD risk groups (highlighted by light boxes in Figure 3.4). Furthermore, these post-hoc analyses revealed significant differences between the low and high AD risk groups that the whole-brain analysis was not sensitive enough to detect. Specifically, FA was significantly lower in the left SLF and CST clusters, and DA was significantly lower in the right SLF cluster, in high relative to low AD risk participants (highlighted by dark boxes in Figure. 3.4).

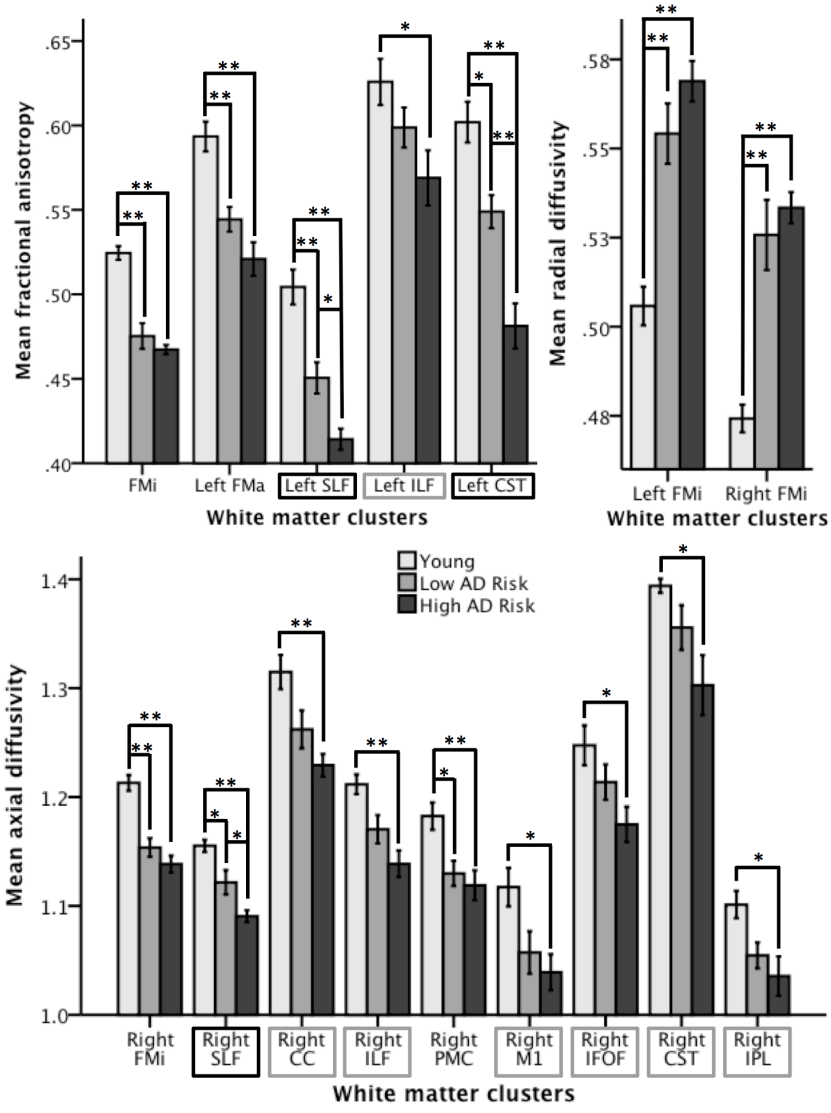

Figure 3.4. Mean fractional anisotropy, radial diffusivity, and axial diffusivity measures in isolated white matter (WM) clusters across groups (young: light grey bars, low AD risk: medium grey bars, high AD risk: dark grey bars). Asterisks denote Bonferroni corrected post-hoc analysis results. Means +/- 1 SEM, * = < .05, ** = < .01. Dark boxes indicate clusters showing significantly lower WM integrity in high relative to low AD risk participants, and light boxes indicate clusters showing significant age-related WM declines in the high AD risk group only. FMi, forceps minor; FMa, forceps major; SLF, superior longitudinal fasciculus; ILF, inferior longitudinal fasciculus; CST, corticospinal tract; CC, corpus callosum; PMC, premotor cortex; M1, primary motor cortex; IFOF, inferior fronto-occipital fasciculus; IPL, inferior parietal lobule.

Discussion

The present study revealed declines in WM integrity associated with aging that were more pronounced in older adults at increased AD risk. Specifically, declines in WM integrity in the low AD risk group mainly involved the FMi, body of the CC, and CST, while declines in the high AD risk group extended into the FMa, IFOF, ILF, SLF, and hippocampal CG. These findings are consistent with the observation that WM changes in early AD and MCI typically occur in more posterior regions, whereas changes associated with normal aging tend to occur in anterior regions (Head et al., 2004; Head, Snyder, Girton, Morris, & Buckner, 2005). Furthermore, the observation that hippocampal volumes did not differ between groups and MD was not increased in regions with decreased FA is consistent with previous evidence suggesting that alterations in WM integrity in individuals at increase AD risk are not secondary to grey matter atrophy, but rather are the result of microstructural changes without macrostructural tissue loss (Gold et al., 2010; Smith et al., 2010).

Our most notable finding, in support of our hypothesis, was the significant relationship between participant performance on a cognitively demanding visuomotor task and the underlying WM integrity of the brain. Consistent with our previous work (Hawkins & Sergio, 2014), we found that measures of timing (reaction and movement time), consistency (variable error), and accuracy (constant error and corrective path length) were significantly impaired in older adults at increased AD risk. While, in

accordance with changes in sensorimotor control typically observed in normal aging (Spirduso, 1975; Spirduso & Clifford, 1978; Yan et al., 2000), older adults at low AD risk only showed slightly increased reaction times, movement times, and variable errors relative to young adults. Correlations between visuomotor performance scores and measures of FA, DR, and DA in several WM clusters (see Tables 3.3) revealed that lower WM integrity was associated with psychomotor slowing, as well as decreased movement accuracy. In combination with the more pronounced declines in WM integrity observed in high AD risk participants in both the whole-brain and isolated WM cluster analyses, these results provide novel evidence for an association between impaired cognitive-motor performance observed in high AD risk participants and underlying WM compromise. While no known previous studies have examined the relationship between WM integrity and cognitive-motor performance in AD, these results are consistent with the finding that lower FA values correspond with worse performance on neuropsychological assessments (Mielke et al., 2009; Rose et al., 2006).

In agreement with previous DTI studies (Gold et al., 2010; Persson et al., 2006; Smith et al., 2010), our observed WM alterations in participants at increased AD risk, without any clinical symptoms of dementia, suggest that disruption to the integrity of WM tracts takes place at an early stage of disease progression. Similar to our results, previous studies in preclinical populations have found declines in FA in the posterior CC, IFOF, and left hippocampus in ApoE4 carriers relative to non-carriers (Persson et al.,

2006), as well as microstructural changes in WM tracts with direct and secondary connections to the medial temporal lobe (i.e. the fornix, CG, ILF and posterior portions of the IFOF) in cognitively normal women at increased AD risk due to family history and carrying one or more ApoE4 allele(s) (Gold et al., 2010; Smith et al., 2010). Earlier studies have also demonstrated reduced glucose metabolism in parietal and temporal areas of ApoE4 carriers over the age of 50 with AD affected relatives (Reiman et al., 1996; Small et al., 1995; Small et al., 2000). Furthermore, individuals with a maternal family history of AD have been shown to exhibit reduced cerebral metabolic rate of glucose in the posterior cingulate cortex/precuneus, parieto-temporal cortex, frontal cortex, and medial temporal lobe (Mosconi et al., 2007). Taken together, the above results suggest that disconnection between the medial temporal lobe and neocortex, as well as between parietal and frontal regions, may occur very early in the course of AD.

Villain and colleagues (2008) have provided direct evidence for this "disconnection hypothesis" using whole-brain voxel-based correlations to assess the relationships between hippocampal atrophy, WM integrity, and grey matter metabolism in early AD. Their results revealed that hippocampal atrophy is specifically related to cingulum bundle disruption, which is in turn highly correlated with hypometabolism of the posterior cingulate cortex, middle cingulate gyrus, parahippocampal gyrus, and right temporoparietal association cortex. Other studies using DTI in AD patients have also revealed reduced WM integrity in large-scale networks involving the cingulum bundle

(Zhang et al., 2007), as well as fibers connecting prefrontal, medial temporal and parietal cortices (Sexton, Kalu, Filippini, Mackay, & Ebmeier, 2011). Based on results such as these, it has been suggested that later myelinating regions with lower oligodendrocyte-to-axon ratios and smaller diameter axons are more vulnerable to myelin degeneration and thus affected earlier in the course of the disease (Bartzokis, 2004; Bartzokis et al., 2004; Reisberg et al., 2002). In accordance with this "retrogenesis model" of AD (i.e. degeneration occurring in a reverse pattern to myelogenesis), Stricker and colleagues (2009) have demonstrated lower FA and higher DR values in late-myelinating (ILF, SLF) but not early-myelinating (internal capsule, cerebral peduncles) tracts in AD patients relative to healthy controls. While direct comparisons between late- and early-myelinating tracts were not made in the present study, the greater age-related declines in WM integrity observed in posterior regions in high AD risk relative to low AD risk participants are consistent with this retrogenesis model. Furthermore, the observation that decreased FA and increased DR occur in similar WM clusters (including those forming the hippocampal-parietal and parietal-frontal connections required for visuomotor transformations), and the observation that these changes are correlated with poorer cognitive-motor performance, suggests that myelin degradation may play a role in the visuomotor impairments reported in early AD. However, declines in DA, particularly in the right hemisphere, and significant correlations with performance were also observed, suggesting the additional involvement of axonal disruption.

The present study represents the first attempt to investigate the neural basis of declines in cognitive-motor control observed in older adults at increased AD risk. In summary, our whole-brain and isolated WM cluster group-level analyses revealed that increased AD risk was associated with greater and more widespread age-related declines in WM integrity, while our correlational analysis demonstrated significant associations between WM compromise and cognitive-motor performance. It should be noted, however, that the findings presented here only apply to a relatively small sample of women at increased AD risk. Future work is needed to determine if these results can be generalized to a larger sample and to include men at increased genetic risk for AD. Furthermore, considering the cross-sectional nature of the present study, our findings are not predictive and will require longitudinal follow-up in order to demonstrate whether or not the brain-behavior alterations observed are associated with increased risk of future decline. That being said, not only do these findings in a preclinical population provide support for the view that disruption to WM tracts may be an early identifying feature of AD (Bartzokis et al., 2004; Bartzokis, 2004; Gold et al., 2010; Persson et al., 2006; Reisberg et al., 2002; Smith et al., 2010), they also provide insight into the impact of AD-related brain alterations on the neural networks underlying complex visuomotor transformations. Importantly, the correlations observed in the present study between kinematic measures on an easily administered visuomotor assessment and microstructural brain alterations suggest that visuomotor performance testing may be applied as a novel

behavioral approach to identify individuals at increased AD risk.

Supplementary materials

Supplementary Table 3.1

White matter regions with significantly lower FA values in low AD risk and high AD risk older adults relative to young adults

Low AD risk

Region (cluster extension)	# of voxels	x	y	z	*t*-value	*p*-value
R FMi (L FMi, R/L CC body, R/L SLF, R/L CST)	14402	17	35	-5	8.23	0.002

High AD risk

Region (cluster extension)	# of voxels	x	y	z	*t*-value	*p*-value
R FMi (L FMi, R/L CC body, R IFOF, R ILF, R SLF, R FMa, R hCG)	13926	20	42	10	6.58	0.002
L FMa	748	-26	-72	1	5.07	0.004
L SLF	263	-34	-44	31	4.39	0.006
L ILF	57	-41	-40	-9	3.49	0.01
L CST	20	-41	-4	35	7.51	0.008

Regions of maximum significant difference between groups with cluster sizes of at least 20 voxels are reported in MNI coordinates. R, right; L, left; FMi, forceps minor; CC, corpus callosum; SLF, superior longitudinal fasciculus; CST, corticospinal tract; IFOF, inferior fronto-occipital fasciculus; ILF, inferior longitudinal fasciculus; FMa, forceps major; hCG, cingulum (hippocampal region).

Supplementary Table 3.2

White matter regions with significantly higher DR values in low AD risk and high AD risk older adults relative to young adults

Low AD risk

Region (cluster extension)	# of voxels	x	y	z	*t*-value	*p*-value
L FMi	14128	-7	49	-21	6.28	0.004
(R FMi, R/L CC body)						
R ILF	493	41	-41	-4	6.73	0.038
R IFOF	121	37	-20	-6	4.35	0.048

High AD risk

Region (cluster extension)	# of voxels	x	y	z	*t*-value	*p*-value
L FMi	8287	-11	43	-17	6.63	0.002
(L CC body, L IFOF, L ILF, L SLF, L FMa)						
R FMi	5697	13	37	-15	5.87	0.002
(R CC body, R IFOF)						

Regions of maximum significant difference between groups with cluster sizes of at least 20 voxels are reported in MNI coordinates. See Supplementary Table 3.1 for abbreviation definitions.

Supplementary Table 3.3

White matter regions with significantly lower DA values in low AD risk and high AD risk older adults relative to young adults

Low AD risk

Region (cluster extension)	# of voxels	x	y	z	*t*-value	*p*-value
L CST (L CC body)	3350	-19	-10	42	5.47	0.01
R FMi	200	22	46	13	4.73	0.034

High AD risk

Region (cluster extension)	# of voxels	x	y	z	*t*-value	*p*-value
R FMi	1291	22	46	10	5.76	0.014
R SLF	981	42	-3	25	5.5	0.022
R CC body	830	13	-6	32	5.09	0.022
R ILF	758	34	-55	19	5.07	0.022
R PMC	369	7	6	63	5.74	0.022
R M1/CST	362	11	-28	66	4.88	0.022
R IFOF	355	37	-17	-8	4.58	0.034
R CST	231	14	-23	-16	3.93	0.034
R IPL	216	52	-35	15	4.23	0.04

Regions of maximum significant difference between groups with cluster sizes of at least 20 voxels are reported in MNI coordinates. PMC, premotor cortex; M1, primary motor cortex; IPL, inferior parietal lobule. See Supplementary Table 1 for other abbreviation definitions.

Chapter Four

Changes in resting-state functional connectivity associated with cognitive-motor impairment in older adults at increased Alzheimer's disease risk

Kara M. Hawkins and Lauren E. Sergio

(Manuscript prepared for submission)

Abstract

Developing novel techniques for the identification of individual at increased Alzheimer's disease (AD) risk is an important component of disease prevention strategies. A large literature exists examining neuroimaging parameters that may serve as useful biomarkers in preclinical AD, including resting-state functional connectivity in the default mode network (DMN). Here we investigate the relationship between alterations in resting-state functional connectivity and kinematic measures of performance on a cognitively demanding visuomotor assessment. We have previously shown that compromise in white matter structural connectivity in female participants at increased AD risk is associated with poorer cognitive-motor performance. In the current study, we sought to expand upon this finding by examining functional connectivity in the same population. To this end, 10 young (mean age = 26.6 +/- 2.7), 10 low AD risk (mean age = 58.7 +/- 5.6), and 10 high AD risk (mean age = 58.5 +/- 6.9) participants underwent blood-oxygen level dependent functional magnetic resonance imaging at rest and performed both standard and cognitively demanding non-standard visuomotor tasks outside of the scanner. In support of previous research examining resting-state functional connectivity in the DMN in preclinical AD, we found that DMN activation was reduced in high relative to low AD risk participants. In line with our previous work, we also found that lower resting-state functional connectivity (using DMN seed-regions) was significantly associated with poorer cognitive-motor performance. These findings provide novel insight into

underlying AD-related brain alterations associated with a potential behavioral assessment that can be easily administered in clinical settings.

Introduction

While the major neuropathological changes associated with Alzheimer's disease (AD) have been identified (i.e. amyloid-beta accumulation and neurofibrillary tangles), the underlying cause is largely unknown. Furthermore, current clinical criteria for the probable diagnosis of AD, largely involving behavioral assessments of short-term and episodic memory, can only identify individuals after significant damage to the brain has already occurred (Ewers et al., 2011). In order to develop and evaluate treatments that may prevent or delay this neurodegenerative process, research investigating early disease detection strategies is essential. In recent years, apolipoprotein E epsilon 4 (ApoE4) genotyping (a genetic risk factor for sporadic AD), family history, amyloid-beta (Aβ) imaging, and neuropsychological tests of subtle cognitive changes (i.e. mild cognitive impairment – MCI) have been used to identify individuals at increased risk for AD (Ewers et al., 2011). Using these methods to compare neuroimaging measures in at-risk groups relative to cognitively healthy low-risk groups can provide important insight into early brain changes, which may prove useful in developing biomarkers for the early detection of AD pathology and the prediction of dementia before the onset of clinical symptoms.

Here we use resting-state functional magnetic resonance imaging (rs-fMRI) to investigate the neural underpinnings of recent behavioral evidence demonstrating impaired visuomotor control under cognitively demanding conditions in early and preclinical AD (Ghilardi et al., 1999; Ghilardi et al., 2000; Hawkins & Sergio, 2014; Salek et al., 2011; Tippett & Sergio, 2006; Tippett et al., 2007; Tippett et al., 2012; Verheij et al., 2012). Specifically, we test the hypothesis posited in Hawkins and Sergio (2014) that the cognitive-motor deficits observed in high AD risk participants may be explained by brain alterations disrupting reciprocal communication in neural networks supporting this behavior. The present functional connectivity study compliments our previous structural neuroimaging work demonstrating an association between diffusion tensor imaging (DTI) measures of white matter (WM) integrity and cognitive-motor performance in preclinical AD (Hawkins et al., 2015). The accumulation of recent evidence from functional connectivity and DTI studies provides support for the view that AD is a disconnection syndrome, with cognitive impairment resulting from disruption to functional activity across interconnected brain regions (Agosta et al., 2012; Liu et al., 2014). Furthermore, evidence in preclinical populations of structural (Bartzokis et al., 2004; Bartzokis, 2004; Gold et al., 2010; Persson et al., 2006; Reisberg et al., 2002; Smith et al., 2010) and functional (Bonni et al. 2013; Hedden et al., 2009; Mormino et al., 2011; Petrella, Sheldon, Prince, Calhoun, & Doraiswamy, 2011; Sheline et al., 2010a; Sheline et al., 2010b; Sorg et al., 2007) disconnection suggests that this may be an early

identifying feature of the disease. Thus, by investigating the relationship between these imaging measures of neural network efficiency and simple kinematic measures of cognitive-motor performance in preclinical AD, we provide novel insight into a potential behavioral assessment for early disease detection.

Materials and Methods

Subjects

Thirty right-handed female participants were included in this study: 10 healthy young controls (mean age = 26.6 +/- 2.7), 10 low AD risk older adults (mean age = 58.7 +/- 5.6), and 10 high AD risk older adults (mean age = 58.5 +/- 6.9). We focused on female participants in the current study due to the greater prevalence of AD in this population (Carter, Resnick, Mallampalli, & Kalbarczyk, 2012; Schmidt et al., 2008), evidence that women who carry the ApoE4 allele may be particularly vulnerable to AD pathology affecting brain connectivity (Reilly et al., 1994), and in order to avoid sex-related confounds inherent in brain imaging studies. Exclusion criteria were the same as in Hawkins et al. (2015), specifically only participants without vision or upper-limb impairments, medical conditions that would hinder task performance (e.g. severe arthritis), neurological or psychiatric illnesses (e.g. schizophrenia, depression, alcoholism, epilepsy, Parkinson's disease), and/or history of stroke or severe head injury were included. Classification as high AD risk was based on reporting either a maternal,

multiple, or early-onset family history of AD (Fratiglioni et al., 1993; Green et al., 2002; Mayeux et al., 1991), but with no cognitive impairment as indicated by the Montreal Cognitive Assessment (MoCA). Since paternal history alone may not carry the same increased risk as maternal history, this was not included as part of the high AD risk classification (Honea et al., 2011; Mosconi et al., 2007; Mosconi et al., 2010). Low AD risk participants were age-matched with high AD risk participants and reported no dementia of any type within their known family history, expressed no memory complaints beyond normal expectations for their age and scored at or above age- and education-adjusted norms on the MoCA. Older adult participants also provided saliva samples for ApoE genotyping at Viaguard Accu-metrics (Toronto ON), which supported the increased genetic risk in our positive family history sample (i.e. 80% ApoE4 carriers). Demographic characteristics for all study participants are summarized in Table 4.1. The study protocol was approved by the Human Participants Review Sub-Committee, York University's Ethics Review Board, and conforms to the standards of the Canadian Tri-Council Research Ethics guidelines.

Table 4.1

Demographic characteristics of subjects

	Young	Low AD Risk	High AD Risk
Number	10	10	10
Age (SD)	26.6 (2.7)	58.7 (5.6)	58.5 (6.9)
Years of education (SD)	-	17.9 (3.1)	16.8 (3.1)
MoCA score (SD)	-	27.9 (1.7)	28.3 (2.2)
ApoE genotype (% E4 carriers)	-	20%	80%

SD: standard deviation; MoCA: Montreal cognitive assessment; ApoE: apolipoprotein E.

Visuomotor assessment

Our visuomotor assessment is described in detail in Hawkins and Sergio (2014). Briefly, as in Hawkins et al. (2015), participants were tested on two visuomotor transformation tasks presented on an Acer Iconia 6120 dual-touchcreen tablet. In one task the spatial location of the viewed target and the required movement were the same (standard task), and in the other, more cognitively demanding non-standard task, the location of the viewed target was dissociated from the required movement (i.e. in both a different spatial plane and in the opposite direction; Figure 4.1A). These two tasks were presented in a random order across participants and consisted of five pseudo-randomly presented trials to each of four peripheral targets (from a common central 'home' target), for a total of 20 trials per condition and 40 trials per participant (Figure 4.1B). Each participant was also given two practice trials per target prior to each condition and their eyes were monitored throughout the experiment using a webcam to ensure compliance with the task instructions (i.e. always look towards the visual target).

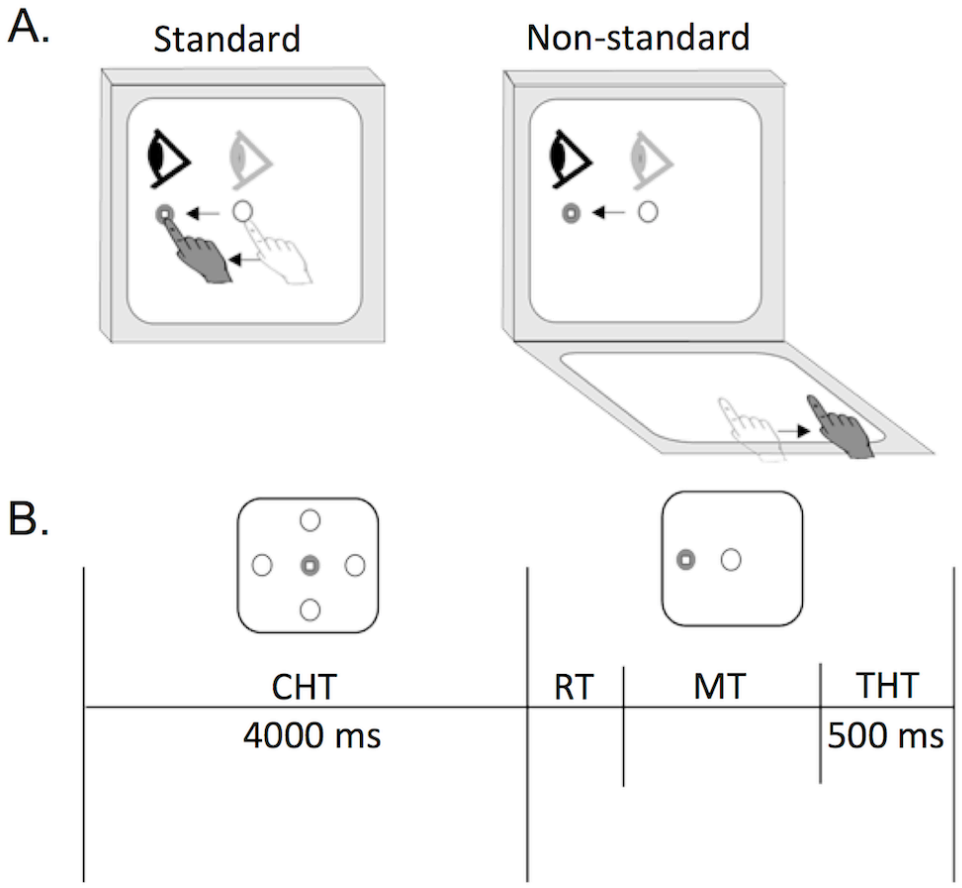

Figure 4.1. A. Schematic drawing of the two experimental conditions. Light grey circle, eye, and hand symbols denote the starting position for each trial (i.e. the home target). Dark grey eye and hand symbols denote the instructed eye and hand movements for each task. Dark grey circle denotes the peripheral target, presented randomly in one of four locations. White square denotes the cursor feedback provided during each condition. **B.** Trial timing. Open circles denote non- illuminated target locations. Disappearance of the home target (which occurred at the same time as presentation of the peripheral target) served as the "go-signal" to initiate movement. CHT: center hold time, RT: reaction time, MT: movement time, THT: target hold time. Reprinted with permission from Hawkins et al. 2015.

Imaging data acquisition

A 3 Tesla Siemens Trio scanner was used to acquire anatomical and functional magnetic resonance imaging (MRI) data. Sequences included a high-resolution T1-weighted anatomical scan using magnetization prepared rapid gradient echo (MPRAGE), and an echo planar imaging (EPI) sequence sensitive to blood-oxygenation-level dependent (BOLD) contrast. The MPRAGE sequence consisted of 192 sagittal slices with a slice thickness of 1 mm with no gap, field of view (FOV) of 256 mm x 256 mm, and a matrix size of 240 x 256, resulting in a voxel resolution of 1 x 1 x 1 mm^3 [repetition time (TR) = 2300 ms, echo time (TE) = 2.96 ms, flip angle = 9°]. For the functional sequence, participants were asked to lie still in the scanner with their eyes closed for six minutes and to let their mind wander. 35 axial slices were acquired with a TR of 2000 ms, TE of 30 ms, flip angle of 90°, slice thickness of 4 mm with no gap, FOV of 210 mm x 210 mm, and matrix size of 56 x 70, resulting in a voxel resolution of 3 x 3 x 4 mm^3.

Kinematic data analysis

A custom written C++ application was used to record and covert the touchscreen data to MATLAB format in order to calculate kinematic outcome measures as described in detail in Hawkins and Sergio (2014). Briefly, on- and off-axis constant errors (CE) were computed as the average distance between the target and the ballistic movement endpoints, serving as a measure of movement accuracy. Variable error (VE) was computed as the standard deviation of the ballistic movement endpoints, serving as a

measure of movement consistency. Corrective movements (CPL: corrective path length) were quantified as the difference between the total path length and the ballistic path length. Reaction time (RT) and movement time (MT) were calculated as the time between disappearance of the home target ('go signal') and movement onset, and the time between movement onset and the final movement endpoint, respectively. All kinematic measures were averaged across the four peripheral targets. For the non-standard condition, these kinematic measures were summarized into error and timing scores by calculating z-scores and averaging across the CE, VE, and CPL variables, and the RT and MT variables, respectively. These performance error and timing scores from the non-standard condition were then used to assess the relationship between cognitive-motor performance and resting-state functional connectivity in our seed-based correlational analyses.

Imaging data analysis

Imaging data were analyzed using the Oxford Centre for Functional Magnetic Resonance Imaging of the Brain (FMRIB) Software Library (FSL - http://www.fmrib.ox.ac.uk/fsl; Jenkinson, Beckmann, Behrens, Woolrich, & Smith, 2012). First, in order to identify regions with coherent spontaneous fluctuations in the BOLD signal, a temporally concatenated independent component analysis (ICA) was applied to the resting state data using FSL's MELODIC. Specifically, for each experimental group, the 2D matrices of each subject's preprocessed (i.e. high-pass

filtered at 0.01 Hz, MCFLIRT motion corrected, slice timing corrected, spatially smoothed by an 8 mm FWHM Gaussian kernel, and registered to standard MNI space) functional data set were stacked on top of each other, and then a single ICA was run on this concatenated data matrix. This approach allowed us to look for common spatial patterns in the resting state data without assuming that the associated temporal response was consistent between subjects. In order to minimize false-positives, a threshold level of 0.66 was used. The spatial maps generated by the MELODIC ICA allowed us to identify the component representing the default mode network (DMN), which was then isolated using the 'fslsplit' command. In order to estimate a "version" of the healthy young group-level DMN functional connectivity for each subject, the FSL 'dual_regression' command was used to regress the young DMN spatial map into each subject's 4D dataset, resulting in a set of time courses. These time courses were then regressed into the same 4D dataset to get subject-specific spatial maps of the DMN (Filippini et al., 2009). The FSL 'cluster' and 'fslmaths' commands were also used on the subject-specific spatial maps in order to determine the peak activations (local maxima) and cluster sizes within each subject's DMN.

In order to conduct seed-based analyses, the DMN cluster coordinates generated in standard Montreal Neurological Institute (MNI) space by FSL MELODIC for each subject were converted to functional space using the FSL command 'std2imgcoord'. Eight seed regions were isolated, including the precuneus (PCUN), medial frontal cortex,

right/left parietal cortex, right/left middle temporal gyrus (MTG), and right/left middle frontal gyrus (MFG). Seed masks (6 mm radius) for each subject were then generated around these coordinates in functional space. Next, the raw functional data were preprocessed by applying a high-pass filter (0.01 Hz), motion correction (MCFLIRT; Jenkinson et al., 2002), slice timing correction (interleaved), removal of non-brain structures, spatial smoothing (6 mm FWHM), and registration to both brain-extracted anatomical (BET; Smith, 2002) and standard space (MNI152) images. A 5^{th} order bandpass Butterworth filter was then applied in MATLAB in order to include only low-frequency fluctuations in the BOLD signal between 0.01 and 0.1 Hz (Biswal, Yetkin, Haughton, & Hyde, 1995). These preprocessed and filtered resting state data were then used to calculate the average time series of all voxels in each seed mask for each volume in every subject. In order to calculate mean white matter, cerebral spinal fluid, and global signals for use, along with the translational and rotational motion correction parameters, as nuisance regressors, the brain-extracted anatomical images were also segmented using FMRIB's Automated Segmentation Tool (FAST; Zhang, Brady, & Smith, 2001). Prior to running group-level statistical analyses, within subject first-level analyses were run for each seed region using FSL's FMRI Expert Analysis Tool (FEAT), with the above nuisance regressors entered as additional confound variables and the seed time course entered as the predictor variable.

Statistical analysis

Statistical analyses of the behavioral data are presented in Hawkins et al. (2015). These analyses were carried out in SPSS and included a mixed-design analysis of variance (ANOVA) to compare all six kinematic measures across the two task conditions and between the three experimental groups, as well as one-way ANOVAs to compare the summarized non-standard error and timing z-scores between the three experimental groups. Post hoc analyses were adjusted for multiple comparisons using Bonferroni correction and were considered statistically significant a $p < .05$.

In order to statistically compare the DMN spatial maps between groups, permutation testing (thresholded at $p < 0.05$ and corrected for multiple comparisons using threshold-free cluster enhancement - TFCE) was applied using the FSL 'randomise' command. Peak activations and cluster sizes for the six classic DMN clusters (precuneus, medial frontal, right/left parietal, and right/left temporal; Agosta et al., 2012; Raichle et al., 2001) were also compared between the high and low AD risk older adult groups using independent samples t-tests in SPSS (alpha-level = 0.05).

Since no significant age-related declines in DMN functional connectivity were observed (based on DMN spatial maps permutation testing between the young and older adult low AD risk groups), we restricted our seed-based correlational analyses examining the relationship between resting-state functional connectivity and cognitive-motor performance to older adult participants. Specifically, group-level analyses comparing low and high AD risk older adults, with error and timing scores entered as covariates of

interest, were run separately in FEAT for each DMN seed region using FMRIB's Local Analysis of Mixed Effects modeling (FLAME 1; cluster-thresholding for multiple comparisons: $z = 2.7$, $p = 0.05$). The purpose of this analysis was to examine the effects of error and timing scores on functional connectivity with DMN seed regions. Specifically, a significant positive effect of error or timing score would suggest an association between greater functional connectivity and poorer performance, whereas a significant negative effect would suggest the expected association between lower functional connectivity and poorer performance (i.e. larger error and timing scores). For seed regions where significant effects of error and/or timing score(s) on functional connectivity were found, mean z-transformed *r*-values across all voxels were calculated for each participant and scatterplots were generated by correlating these values with error or timing scores in SPSS (two-tailed Pearson's *r*; alpha-level = 0.05).

Results

Kinematic data

The ANOVA results on our kinematic data are presented in Hawkins et al. (2015). Briefly, we found that all three groups performed similarly across all outcome measures in the standard visuomotor task, whereas performance in the non-standard task was significantly slower, less accurate and less consistent in the high AD risk group. These cognitive-motor deficits observed in high AD risk participants are summarized in Figure

4.2, illustrating that error scores were significantly larger in high AD risk relative to both young and low AD risk participants ($F_{2,27} = 21.39$, $p < 0.0001$; post-hoc: high AD risk - young = 4.95, $p < 0.00001$, high AD risk - low AD risk = 4.04, $p < 0.0001$), and timing scores were significantly longer in high AD risk relative to young participants ($F_{2,27} = 5.31$, $p = 0.011$; post-hoc: high AD risk - young = 1.87, $p = 0.009$).

Imaging data

Significant mean co-activations with the young group-level DMN component for both the low (red-yellow) and high (blue-light blue) AD risk older adult groups are displayed in figure 4.3A ($p < 0.02$, corrected). Figure 4.3B quantifies the sizes and peak activations of these DMN clusters, revealing a tendency towards smaller cluster sizes and lower peak activations in the high AD risk group. Statistical comparisons between groups revealed that peak activation within the right parietal cluster was significantly lower in the high AD risk group ($t_{18} = 2.59$, $p = 0.019$). Figure 4.3C illustrates the permutation test results, revealing regions of significantly greater DMN functional connectivity in low AD risk relative to high AD risk participants ($p < 0.02$, corrected). These regions include the precuneus/posterior cingulate, anterior cingulate, superior frontal gyrus (SFG), MFG, left post- and pre-central gyri, and the right thalamus. Coordinates in standard space (MNI152), Harvard-Oxford structural labels, and significance values for these clusters are listed in Table 4.2. There were no regions of significantly greater DMN functional connectivity in the high AD risk group relative to the low AD risk group, as well as no

significant age-related declines in DMN functional connectivity in the low AD risk older adult group relative to the young group.

In support of our hypothesis, significant correlations were found between cognitive-motor performance and resting-state functional connectivity in older adult participants. Specifically, we found that larger error scores were associated with lower functional connectivity between the left MFG and right posterior parietal regions (Fig. 4.4A), as well as between the right MTG and the right thalamus/basal ganglia (Fig. 4.4B). We also found that slower timing scores were associated with lower functional connectivity between the right PCUN and left frontal regions (Fig. 4.4C), as well as between the right MFG and left frontal regions (Fig. 4.4D). These significant effects of error and timing scores on seed-based functional connectivity are summarized in Table 4.3.

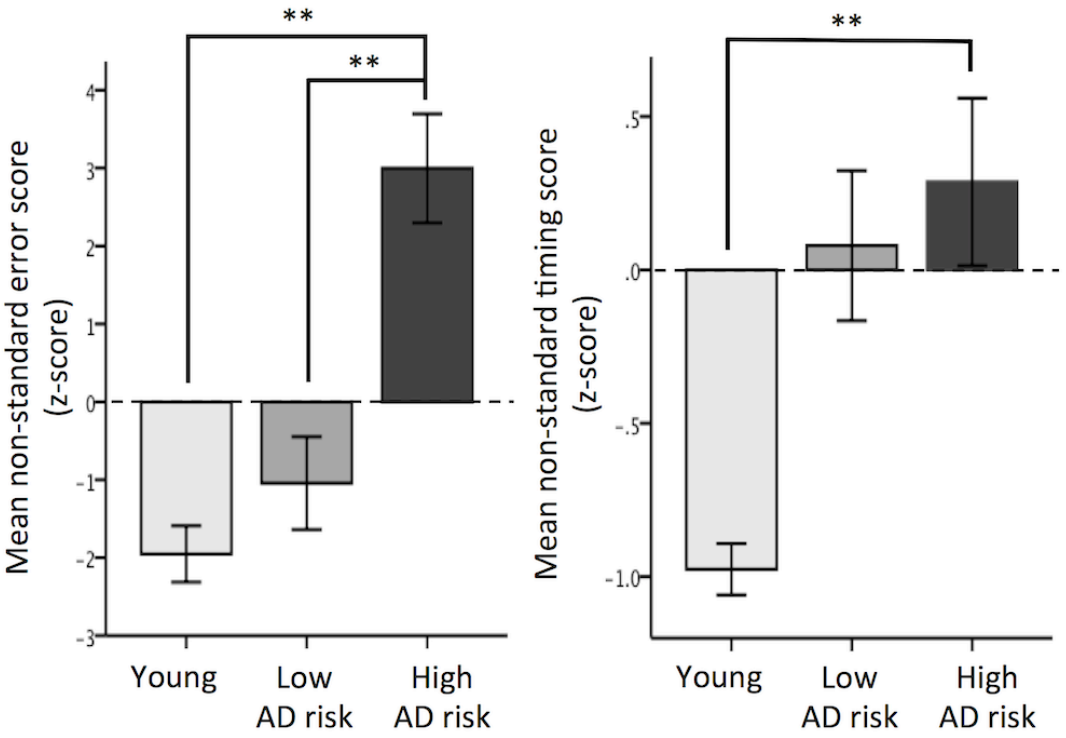

Figure 4.2. Mean z-scores for error and timing kinematic measures in the non-standard task across groups (young: light grey bars, low AD risk: medium grey bars, high AD risk: dark grey bars). Note that higher error scores reflect less accuracy and precision and higher timing scores reflect longer reaction and movement times. Means +/- 1 SEM, ** = < .01. Reprinted with permission from Hawkins et al. 2015.

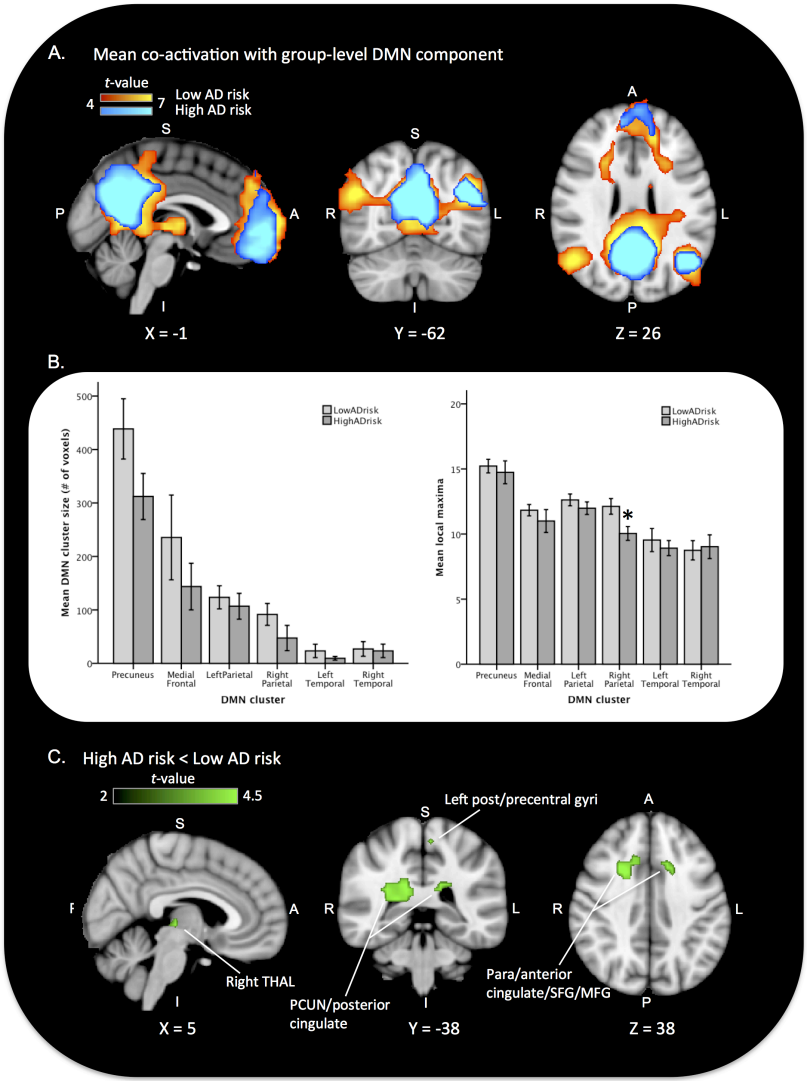

Figure 4.3. A. Mean co-activation with the FSL MELODIC group-level default mode network (DMN) component in the low (red-yellow) and high (blue-light blue) AD risk groups ($p < 0.02$, corrected). **B.** Bar graphs comparing mean (+/- 1 SEM) DMN cluster sizes and peak activations (local maxima) between the low (light grey) and high (dark gray) AD risk groups. Asterisk denotes significantly lower peak activation in the right parietal cluster for the high relative to low AD risk group ($p < 0.05$). **C.** Regions of the DMN spatial map showing significantly lower functional connectivity in high relative to low AD risk older adult participants. Group differences calculated using permutation testing (FSL randomise) and displayed at $p < 0.02$ (corrected). AD: Alzheimer's disease, S: superior, P: posterior, I: inferior, A: anterior, R: right, L: left, THAL: thalamus, PCUN: precuneus, SFG: superior frontal gyrus, MFG: middle frontal gyrus.

Table 4.2

Regions of the DMN spatial map showing significantly lower resting-state functional connectivity in high AD risk relative low AD risk older adults

Brain region	*Local maxima (MNI152)*				
Harvard-Oxford structural label	x	y	z	*t*-value	*p*-value
Left para/anterior cingulate/SFG	-18	18	32	4.96	0.008
Right para/anterior cingulate/MFG/SFG	22	10	36	5.08	0.008
Right PCUN/posterior cingulate	30	-50	20	5.48	0.008
Left PCUN/posterior cingulate	-18	-46	20	4.66	0.008
Right frontal pole	26	43	17	5.11	0.039
Right THAL	6	-22	0	4.33	0.008
Left post/precentral gyri	-6	-38	60	4.44	0.010

DMN: default mode network; AD: Alzheimer's disease; MNI: Montreal Neurological Institute; SFG: superior frontal gyrus; MFG: middle frontal gyrus; PCUN: precuneus; THAL: thalamus.

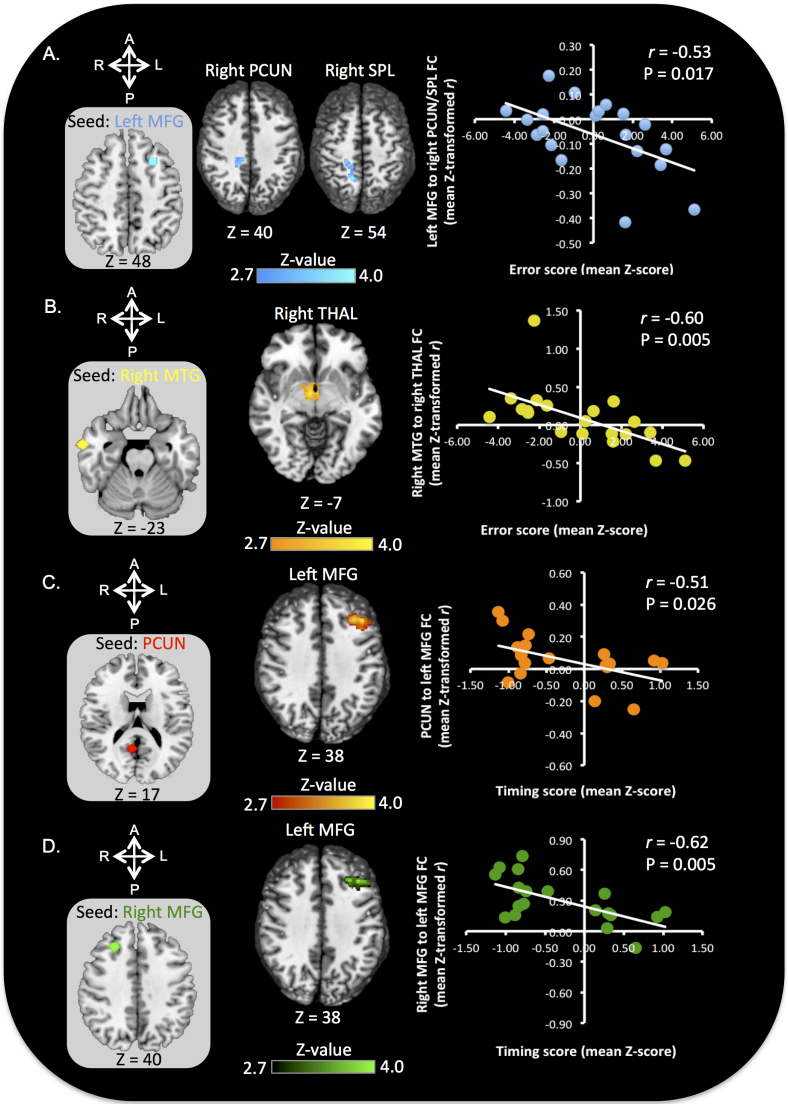

Figure 4.4. *Left panel*: clusters showing significantly lower functional connectivity with **A.** the left middle frontal gyrus (MFG), **B.** the right middle temporal gyrus (MTG), **C.** the precuneus (PCUN), and **D.** the right middle frontal gyrus (MFG) in older adult participants with poorer performance (i.e. either larger error or timing scores) on a cognitively demanding visuomotor task. *Right panel*: scatterplots illustrating the significant negative correlation found between **A.** left MFG to right parietal functional connectivity and performance error scores, **B.** right MTG to thalamus/putamen functional connectivity and performance error scores, **C.** PCUN to left MFG functional connectivity and performance timing scores, and **D.** right MFG to left MFG functional connectivity and performance timing scores. R: right, L: left, A: anterior, P: posterior, SPL: superior parietal lobule, THAL: thalamus, FC: functional connectivity.

Table 4.3

Significant effects of cognitive-motor error and timing scores on functional connectivity with DMN seed regions

Error score

Seed region	Functionally connected cluster (Harvard-Oxford structural atlas)	# of voxels	x	y	z	*z*-value	*p*-value
Left MFG	Right PCUN/LOC/SPL	324	14	-58	54	4.01	0.024
	Right postcentral gyrus/SPL		16	-44	58	3.82	
	Right post/precentral gyri		22	-34	52	3.49	
	Right posterior cingulate/PCUN		12	-32	36	3.44	
Right MTG	Right thalamus	275	6	-6	-6	3.82	0.048
	Right Pallidum/Putamen		14	2	-10	3.26	

Timing score

Seed region	Functionally connected cluster (Harvard-Oxford structural atlas)	# of voxels	x	y	z	*z*-value	*p*-value
PCUN	Left MFG/IFG/frontal pole	556	-42	30	36	3.85	0.0009
	Left SFG/frontal pole/MFG		-22	34	48	3.5	
Right MFG	Left MFG/frontal pole	422	-38	32	36	4.06	0.005
	Left MFG/SFG		-28	28	52	3.02	

LOC: lateral occipital cortex; SPL: superior parietal lobule; MTG: middle temporal gyrus; IFG: inferior frontal gyrus. See Table 4.2 for other abbreviation definitions

Discussion

In the current study, we demonstrate that female participants at increased genetic risk of developing AD exhibit significantly reduced resting-state functional connectivity within the DMN in the absence of cognitive impairment on standardized tests. When using kinematic measures of cognitive-motor performance however, significant correlations were observed between DMN functional connectivity and behavior. We have previously found that individuals at increased AD risk (either due to family history or MCI) perform significantly worse on visuomotor tasks under cognitively demanding conditions (Hawkins & Sergio, 2014), and that poorer cognitive-motor performance is associated with lower WM integrity in the brain (Hawkins et al., 2015). Here we extend these findings by demonstrating that poorer cognitive-motor performance in high AD risk participants is also associated with reduced resting-state functional connectivity, including parietal-frontal, interhemispheric, and temporal-subcortical connections.

These findings are consistent with several studies demonstrating reduced functional connectivity in the DMN (Drzezga et al., 2011; Hedden et al., 2009b; Mormino et al., 2011; Petrella et al., 2011; Sheline et al., 2010a; Sheline et al., 2010b), as well as studies demonstrating decreased glucose metabolism in parietal brain regions (Mosconi et al., 2007; Reiman et al., 1996; Reiman et al., 2004; Small et al., 1995; Small et al., 2000) in preclinical AD. For example, Hedden et al. (2009) used Aβ imaging in combination with measures of resting-state functional connectivity in the DMN to compare participants

with and without high amyloid burden. After controlling for age, cognitively normal participants with high amyloid burden were shown to exhibit significantly reduced functional connectivity within brain regions of the default network, including the posterior cingulate, lateral parietal, and medial prefrontal regions, relative to individuals with low amyloid burden. Furthermore, functional correlations between the hippocampus and posterior cingulate were diminished in participants harboring high amyloid burden. These results suggest that disruptions in functional connectivity within the DMN, as observed in the present study, may predict the presence of Aβ in AD affected brain regions before clinical symptoms emerge.

More recently, Sheline et al. (2010b) and Mormino et al. (2011) have also demonstrated significant differences in functional connectivity between participants with high versus low Aβ deposition in the brain. Specifically, they found similar decreases in connectivity between the precuneus and the left hippocampus, parahippocampus, anterior cingulate, gyrus rectus, dorsal cingulate, and superior precuneus in both AD patients and participants with high Aβ deposition. Although these studies demonstrate some degree of association between elevated Aβ and altered activation of the DMN, Sheline et al. (2010b) actually found no significant correlation between precuneus functional connectivity and Aβ deposition in this region. Thus, as a follow-up to this finding, the same group (Sheline et al., 2010a) conducted a study comparing resting-state functional connectivity in Aβ negative participants either with or without an ApoE4 allele.

Interestingly, they found that these Aβ negative ApoE4 carriers showed similar decreased functional connectivity between the precuneus and various DMN brain regions as that observed in Aβ positive and AD participants in their previous study. These results indicate that alterations in functional connectivity in genetically predisposed participants may reflect early manifestation of a genetic effect that actually precedes pathological Aβ neurotoxicity.

The disruptions in resting-state functional connectivity in preclinical AD observed in the present and previous studies, particularly in parietal regions, have also been shown to overlap strongly with regional glucose hypometabolism (Drzezga et al., 2011). For example, studies examining glucose metabolism in the brains of ApoE4 carriers over the age of 50 with AD affected relatives have demonstrated reduced glucose metabolism in parietal regions relative to non-carriers (Reiman et al., 1996; Small et al., 1995). Furthermore, follow-up assessments have shown that cognitive decline after 2 years is greatest in those ApoE4 carriers with the lowest metabolism in parietal and temporal regions at baseline (Small et al., 2000). Glucose metabolism studies in young (ages 20-39) ApoE4 carriers have also revealed hypometabolism, specifically in the posterior cingulate, parietal, temporal and prefrontal cortices, suggesting fundamental metabolic abnormalities decades before any deposition of Aβ protein and the onset of dementia symptoms (Reiman et al., 2004). A recent study has also found susceptibility to glucose metabolism changes in individuals with a maternal family history of AD (Mosconi et al.,

2007). Specifically, compared to both no family history and paternal family history groups, participants with a maternal family history of AD were found to have reduced cerebral metabolic rate of glucose in the posterior cingulate cortex/precuneus, parietotemporal cortex, frontal cortex, and medial temporal lobe.

Hypometabolism in the precuneus and temporo-parietal cortex has also been observed in MCI patients (Mosconi, Pupi, & De Leon, 2008). Furthermore, several studies have demonstrated accurate prediction (accuracy rates of 80-90%) of progression from MCI to AD within 1-1.5 years based on glucose hypometabolism in inferior parietal, temporoparietal, and posterior cingulate regions, especially in ApoE4 carriers (Anchisi et al., 2005; Drzezga et al., 2005; Mosconi et al., 2004). Fundamentally deficient or altered energy metabolism may be a predisposing factor in AD, which is consistent with evidence that metabolic dysfunction precedes the onset of hallmark AD pathology (such as Aβ accumulation and hippocampal atrophy). Disrupted energy metabolism may change the overall oxidative microenvironment for neurons, resulting in increased susceptibility to synaptic pathology from oxidative stress (Mosconi et al., 2008). Interestingly, regions of the DMN correspond almost exactly with regions of high aerobic glycolysis in the brain (i.e. the process responsible for most of the energy produced for glutamate cycling in the brain at rest), suggesting a relationship between resting-state functional connectivity and energy metabolism (Buckner et al., 2005; Sheline & Raichle, 2013). Furthermore, strong correlations between Aβ depositions and aerobic glycolysis

have been found in both AD and Aβ positive participants (Vlassenko et al., 2010), suggesting increased susceptibility to Aβ-induced neurotoxicity in regions of high metabolic demand and a possible link with the later development of Alzheimer's pathology (Sheline & Raichle, 2013). These links between resting-state functional connectivity, energy metabolism, and hallmark AD pathology provide strong support for the use of rs-fMRI in early disease detection.

Importantly, the current study expands upon the large literature of purely neuroimaging studies in preclinical AD discussed above by considering the impact of early AD-related brain alterations on behavior. While the preclinical definition implies no decline on standardized tests of cognitive function, novel clinical assessments that can detect subtle behavioral alterations (e.g. in the kinematics of eye and limb movements) may be useful in identifying individuals at increased AD risk (Hawkins & Sergio, 2014; Salek et al., 2011; Verheij et al., 2012). The findings presented here, and in Hawkins et al. (2015), suggest that a relationship exists between deficits in cognitive-motor performance and alterations in structural and functional connectivity in preclinical AD. The correlations observed between parietal-frontal functional connectivity and cognitive-motor performance are consistent with the important role of reciprocal cortical networks involving parietal, temporal, and frontal regions in transforming visual-spatial and contextual information into the intrinsic joint and muscle representation required to successfully generate a goal-directed action (Battaglia-Mayer et al., 2000; Galati et al.,

2011; Hawkins et al., 2013). Furthermore, the reduced temporal-subcortical functional connectivity observed in correlation with poorer cognitive-motor performance is consistent with the role of temporal-thalamic connections in arousal and information integration (Shao et al., 2013), as well as the role of the basal ganglia in the anticipation and selection of body movements (Purves et al., 2001), cognitive-motor interactions (Middleton & Strick, 2000; Leisman et al., 2014), and multisensory integration (Reig & Silberberg, 2014).

Through investigation of the neural basis of deficits in cognitive-motor performance observed in preclinical AD, our current and previous (Hawkins et al., 2015) work provides a link between a potential clinical assessment tool and underlying AD-related neuroimaging biomarkers. In summary, the findings presented here support previous evidence for reduced functional connectivity in the DMN in individuals at increased genetic risk of developing AD. They also provided novel evidence that a relationship exists between reduced resting-state functional connectivity and poorer cognitive-motor performance in individuals at increased AD risk. The generalizability of this evidence is limited however by the inclusion of a relatively small sample of female participants in this preliminary study. Larger-scale longitudinal studies will provide important information about the time course of any alterations in cognitive-motor performance and both structural and functional connectivity in at-risk populations, which is required in order to determine the optimal timing of intervention studies. The potential use of

kinematic measures reflecting cognitive-motor integration in distinguishing between healthy versus pathological aging is a promising area of investigation that remains to be fully elucidated.

Chapter Five

General Discussion

5.1. General discussion and conclusions

Although the more stereotyped ability to interact directly with objects (i.e. standard reaching) is not typically impaired in early AD and MCI relative to health aging, performance decrements observed in this population under more cognitively-demanding conditions suggest that disruption to parietal-frontal cognitive-motor integration networks occurs early in the disease process. Such impairment has the potential to affect activities of daily living, and may serve as a sensitive measure for the detection of older adults at increased AD risk before cognitive symptoms are consistently present. Furthermore, clinical assessment tools that incorporate cognition and action together may be useful in identifying individuals at increased risk for future decline in areas such as balance and gait, and driving ability. Importantly, we know of no other lab currently using this type of paradigm to develop a clinical assessment tool, thus working towards the development of a sensitive, clinically accessible tablet-based tool that can measure functional changes over time is of great value. The three studies presented here provide novel insight into subtle, but measurable deficits in complex visuomotor control associated with underlying structural and functional brain alterations in older adults at increase AD risk.

In our first study in chapter two, not only do we provide further support for previous findings in MCI and early AD populations (Ghilardi et al., 1999; Ghilardi et al., 2000; Salek, Anderson, & Sergio, 2011; Tippett & Sergio, 2006; Tippett, Krajewski, & Sergio, 2007; Tippett, Sergio, & Black, 2012; Verheij et al., 2012), we also demonstrate for the

first time that visuomotor impairments can be observed in otherwise cognitively healthy individuals at increased genetic risk of developing AD. These impairments occurred under task conditions with two levels of dissociation between vision and action, that is, when both visual-spatial and explicit rule-based information had to be integrated into the motor plan. Fundamentally, this work offers insight into the mechanisms underlying age- and disease-related changes in cognitive-motor control. Specifically, we suggest that larger endpoint errors and corrective path lengths may result from disruption to motor programming leading to increased reliance on online sensory feedback (Haaland et al., 1993; Ketcham et al., 2002; Pratt et al., 1994; Seidler-Dobrin & Stelmach, 1998), and that online corrective mechanisms may also be disrupted or delayed (Chaput & Proteau, 1996; Sarlegna, 2006), resulting in trajectory deviations and longer path lengths. Furthermore, increased variability and direction reversal errors may reflect disruption to attentional control networks, affecting the ability to inhibit "automatic" eye-hand coupling and divide attention (i.e. neural resources) between incongruent eye and hand movements (Baddeley, Baddeley, Bucks, & Wilcock, 2001; Sheridan & Hausdorff, 2007). The behavioural findings from this study lead to the hypothesis that early AD-related brain alterations may disrupt the reciprocal communication between hippocampal, parietal, and frontal cortical regions required to successfully prepare, update and execute complex reaching behaviours.

In our second and third studies described in chapters three and four, the hypothesis

put forth in our first study is tested using both diffusion-weighted and resting-state functional MRI to examine structural and functional connectivity in the brain. Specifically, in these studies we investigated the underlying neural correlates associated with impaired cognitive-motor integration in female participants at increased genetic risk of developing AD. Our results demonstrated declines in both structural and functional connectivity within the brains of older adults at increased AD risk relative to both young and older adult participants at low AD risk, and supported our hypothesis by demonstrating significant correlation between these MRI measures and cognitive-motor performance. We also conducted a follow-up analysis in order to assess whether or not a relationship exists between the structural connectivity results presented in our second study and the resting-state functional connectivity results presented in our third study. Specifically, we correlated measures of WM integrity (i.e. FA, DR, and DA) in the clusters identified in our second study with mean z-transformed *r*-values reflecting the strength of functional connectivity with DMN seed regions identified in our third study. Interestingly, we found significant correlations indicating an association between lower FA in the splenium of the corpus callosum and lower right precuneus to left frontal functional connectivity ($r = 0.46$, $p = 0.043$), as well as between lower DA in the right inferior parietal lobule and both lower right MTG to thalamus ($r = 0.58$, $p = 0.007$) and right to left MFG ($r = 0.70$, $p = 0.001$) functional connectivity. These relationships between parietal/splenium WM disruption and reduced resting-state functional

connectivity suggest that WM compromise involving parietal and posterior interhemispheric connectivity may play a role in the declines in functional connectivity across interconnected neural networks observed in early AD.

The neuroimaging findings presented in chapters three and four are the first to show a relationship between AD-related brain alterations and declines in cognitive-motor control. In these studies, not only have we provided support for the view that disruption to brain connectivity may be an early identifying feature of AD, we have also provided insight into the impact of AD-related brain alterations on the neural networks underlying complex visuomotor transformations. Furthermore, these neuroimaging results provide support for the notion that kinematic measures on an easily administered visuomotor assessment are associated with underlying brain alterations, and thus may offer a novel behavioral approach for the identification of individuals at increased AD risk.

Taken together, this series of studies provides a link between our previous fundamental work examining cognitive-motor networks in non-human primates and applied behavioural work demonstrating alterations in visuomotor control in early AD. Importantly, our results have the potential to translate into a functional biomarker for early AD detection and support the hypothesis the structural and functional disconnection occur early in the disease process. Interestingly, the human brain has disproportionately more white matter than the brains of other animals. During brain evolution, glial cell (e.g. oligodendrocyte) numbers have increased disproportionately compared to neurons,

reflecting an evolutionary trend of increasing cognitive abilities. Evidence for disconnection in preclinical AD supports the view that oligodendrocytes and the myelin they produce are particularly vulnerable to genetic and environmental insults, underlying our brain's unique susceptibility to highly prevalent and often unique human disorders in older age, such as AD (Bartzokis & Lu, 2009). During development, such vulnerability may also underlie disorders such as autism, developmental dyspraxia, and schizophrenia (Bartzokis & Lu, 2009). A commonality between these disorders early and late in life may be the enhanced susceptibility of late-myelinating regions, which are regions that have undergone substantial evolutionary expansion (Bartzokis et al., 2004; Stricker et al., 2009).

5.2. Limitations and future directions

Considering the preliminary and cross-sectional nature of the studies outlined in this dissertation, further research is required in order to fully elucidate the use of kinematic measures in predicting future cognitive and functional decline. Specifically, longitudinal studies monitoring large samples of both male and female participants over time are required. Furthermore, future studies may also consider the potential use of cognitive-motor integration measures in distinguishing between different types of dementia. For example, the predominant disinhibition deficits in patients with frontal-temporal dementia may result in a different kinematic profile from that observed in AD patients.

Assessment tools incorporating measures of cognition and action together may also be useful in the evaluation of functional deficits resulting from mild traumatic brain injuries (TBI), such as accident- and sport-related concussions (Brown, Hughes, & Sergio, 2011). The diffuse axonal injury underlying mild TBIs, including disruption to interhemispheric and parietal-frontal connections (Niogi et al., 2008), may result is similar cognitive-motor deficits as those observed in early AD. Lastly, future work in the Sergio lab will investigate the potential use of cognitive-motor training in building "cognitive reserve" and delaying or preventing age- and disease-related decline.

References

Agosta, F., Pievani, M., Geroldi, C., Copetti, M., Frisoni, G. B., & Filippi, M. (2012). Resting state fMRI in alzheimer's disease: Beyond the default mode network. *Neurobiology of Aging, 33*(8), 1564-1578.

Alexander, N. B., Shepard, N., Gu, M. J., & Schultz, A. (1992). Postural control in young and elderly adults when stance is perturbed: Kinematics. *Journal of Gerontology, 47*(3), M79-87.

Alzheimer's Association. (2012). 2012 alzheimer's disease facts and figures. *Alzheimer's & Dementia, 8*(2), 131-168.

American Psychiatric Association. *Diagnostic and Statistical Manual of Mental Disorders, 4th edition.* Washington, D.C.: American Psychiatric Press, 1994.

Anchisi, D., Borroni, B., Franceschi, M., Kerrouche, N., Kalbe, E., Beuthien-Beumann, B., et al. (2005). Heterogeneity of brain glucose metabolism in mild cognitive impairment and clinical progression to alzheimer disease. *Archives of Neurology, 62*(11), 1728-1733.

Ashe, J., & Georgopoulos, A. P. (1994). Movement parameters and neural activity in motor cortex and area 5. *Cerebral Cortex, 4*(6), 590-600.

Baddeley, A. D., Baddeley, H. A., Bucks, R. S., & Wilcock, G. K. (2001). Attentional control in alzheimer's disease. *Brain, 124*(Pt 8), 1492-1508.

Bai, F., Zhang, Z., Watson, D. R., Yu, H., Shi, Y., Yuan, Y., et al. (2009). Abnormal integrity of association fiber tracts in amnestic mild cognitive impairment. *Journal of the Neurological Sciences, 278*(1-2), 102-106.

Bartzokis, G. (2004). Age-related myelin breakdown: A developmental model of cognitive decline and alzheimer's disease. *Neurobiology of Aging, 25*(1), 5-18; author reply 49-62.

Bartzokis, G. & Lu, P. H. (2009). Brain Volume: Age-Related Changes. In P. R. Hof & C. V. Mobbs (Eds.), *Handbook of the Neuroscience of Aging* (pp. 27-37). London: Elsevier/Academic Press

Bartzokis, G., Sultzer, D., Lu, P. H., Nuechterlein, K. H., Mintz, J., & Cummings, J. L. (2004). Heterogeneous age-related breakdown of white matter structural integrity: Implications for cortical "disconnection" in aging and alzheimer's disease. *Neurobiology of Aging, 25*(7), 843-851.

Batista, A. P., Buneo, C. A., Snyder, L. H., & Andersen, R. A. (1999). Reach plans in eye-centered coordinates. *Science, 285*(5425), 257-260.

Battaglia-Mayer, A., Ferraina, S., Genovesio, A., Marconi, B., Squatrito, S., Molinari, M., et al. (2001). Eye-hand coordination during reaching. II. an analysis of the relationships between visuomanual signals in parietal cortex and parieto-frontal association projections. *Cerebral Cortex, 11*(6), 528-544.

Battaglia-Mayer, A., Ferraina, S., Mitsuda, T., Marconi, B., Genovesio, A., Onorati, P., et al. (2000). Early coding of reaching in the parietooccipital cortex. *Journal of Neurophysiology, 83*(4), 2374-2391.

Bedford, F. L. (1993). Perceptual and cognitive spatial learning. *Journal of Experimental Psychology: Human Perception and Performance, 19*(3), 517-530.

Biswal, B., Yetkin, F. Z., Haughton, V. M., & Hyde, J. S. (1995). Functional connectivity in the motor cortex of resting human brain using echo-planar MRI. *Magnetic Resonance in Medicine, 34*(4), 537-541.

Blangero, A., Menz, M. M., McNamara, A., & Binkofski, F. (2009). Parietal modules for reaching. *Neuropsychologia, 47*(6), 1500-1507.

Bonni, S., Lupo, F., Lo Gerfo, E., Martorana, A., Perri, R., Caltagirone, C., et al. (2013). Altered parietal-motor connections in alzheimer's disease patients. *Journal of Alzheimer's Disease : JAD, 33*(2), 525-533.

Bosch, B., Arenaza-Urquijo, E. M., Rami, L., Sala-Llonch, R., Junque, C., Sole-Padulles, C., et al. (2012). Multiple DTI index analysis in normal aging, amnestic MCI and AD. relationship with neuropsychological performance. *Neurobiology of Aging, 33*(1), 61-74.

Braak, H., & Braak, E. (1991). Neuropathological stageing of alzheimer-related changes. *Acta Neuropathologica, 82*(4), 239-259.

Brown, J. A., Hughes, C., & Sergio, L. E. (2011). The detrimental effects of concussion on cognitive-motor integration. [Abstract]. *Society for Neuroscience Abstract,* November*,* 698.19.

Buchman, A. S., & Bennett, D. A. (2011). Loss of motor function in preclinical alzheimer's disease. *Expert Review of Neurotherapeutics, 11*(5), 665-676.

Buckner, R. L., Snyder, A. Z., Shannon, B. J., LaRossa, G., Sachs, R., Fotenos, A. F., et al. (2005). Molecular, structural, and functional characterization of alzheimer's disease: Evidence for a relationship between default activity, amyloid, and memory. *The Journal of Neuroscience, 25*(34), 7709-7717.

Buneo, C. A., Jarvis, M. R., Batista, A. P., & Andersen, R. A. (2003). Properties of spike train spectra in two parietal reach areas. *Experimental Brain Research, 153*(2), 134-139.

Bunge, S. A., Wallis, J. D., Parker, A., Brass, M., Crone, E. A., Hoshi, E., et al. (2005). Neural circuitry underlying rule use in humans and nonhuman primates. *The Journal of Neuroscience, 25*(45), 10347-10350.

Buxbaum, L. J., Johnson-Frey, S. H., & Bartlett-Williams, M. (2005). Deficient internal models for planning hand-object interactions in apraxia. *Neuropsychologia, 43*(6), 917-929.

Buxbaum, L. J., Kyle, K., Grossman, M., & Coslett, H. B. (2007). Left inferior parietal

representations for skilled hand-object interactions: Evidence from stroke and corticobasal degeneration. *Cortex, 43*(3), 411-423.

Buxbaum, L. J., Sirigu, A., Schwartz, M. F., & Klatzky, R. (2003). Cognitive representations of hand posture in ideomotor apraxia. *Neuropsychologia, 41*(8), 1091-1113.

Carter, C. L., Resnick, E. M., Mallampalli, M., & Kalbarczyk, A. (2012). Sex and gender differences in alzheimer's disease: Recommendations for future research. *Journal of Women's Health (2002), 21*(10), 1018-1023.

Cavanna, A. E., & Trimble, M. R. (2006). The precuneus: A review of its functional anatomy and behavioural correlates. *Brain, 129*(Pt 3), 564-583.

Chapman, G. J., & Hollands, M. A. (2006a). Age-related differences in stepping performance during step cycle-related removal of vision. *Experimental Brain Research, 174*(4), 613-621.

Chapman, G. J., & Hollands, M. A. (2006b). Evidence for a link between changes to gaze behaviour and risk of falling in older adults during adaptive locomotion. *Gait & Posture, 24*(3), 288-294.

Chapman, G. J., & Hollands, M. A. (2007). Evidence that older adult fallers prioritise the planning of future stepping actions over the accurate execution of ongoing steps during complex locomotor tasks. *Gait & Posture, 26*(1), 59-67.

Chaput, S., & Proteau, L. (1996). Aging and motor control. *The Journals of Gerontology Series B, Psychological Sciences and Social Sciences, 51*(6), P346-55.

Chetelat, G., Desgranges, B., Landeau, B., Mezenge, F., Poline, J. B., de la Sayette, V., et al. (2008). Direct voxel-based comparison between grey matter hypometabolism and atrophy in alzheimer's disease. *Brain, 131*(Pt 1), 60-71.

Clower, D. M., & Boussaoud, D. (2000). Selective use of perceptual recalibration versus visuomotor skill acquisition. *Journal of Neurophysiology, 84*(5), 2703-2708.

Clower, D. M., West, R. A., Lynch, J. C., & Strick, P. L. (2001). The inferior parietal lobule is the target of output from the superior colliculus, hippocampus, and cerebellum. *The Journal of Neuroscience, 21*(16), 6283-6291.

Colby, C. L., & Goldberg, M. E. (1999). Space and attention in parietal cortex. *Annual Review of Neuroscience, 22*, 319-349.

Concha, L., Gross, D. W., Wheatley, B. M., & Beaulieu, C. (2006). Diffusion tensor imaging of time-dependent axonal and myelin degradation after corpus callosotomy in epilepsy patients. *NeuroImage, 32*(3), 1090-1099.

Crawford, J. D., Henriques, D. Y., & Medendorp, W. P. (2011). Three-dimensional transformations for goal-directed action. *Annual Review of Neuroscience, 34*, 309-331.

Crutch, S. J., Rossor, M. N., & Warrington, E. K. (2007a). A novel technique for the

quantitative assessment of apraxic deficits: Application to individuals with mild cognitive impairment. *Journal of Neuropsychology, 1*(Pt 2), 237-257.

Crutch, S. J., Rossor, M. N., & Warrington, E. K. (2007b). The quantitative assessment of apraxic deficits in alzheimer's disease. *Cortex, 43*(7), 976-986.

Crutcher, M. D., & Alexander, G. E. (1990). Movement-related neuronal activity selectively coding either direction or muscle pattern in three motor areas of the monkey. *Journal of Neurophysiology, 64*(1), 151-163.

Culham, J. C., & Kanwisher, N. G. (2001). Neuroimaging of cognitive functions in human parietal cortex. *Current Opinion in Neurobiology, 11*(2), 157-163.

Darling, W. G., Cooke, J. D., & Brown, S. H. (1989). Control of simple arm movements in elderly humans. *Neurobiology of Aging, 10*(2), 149-157.

de Boer, C., Mattace-Raso, F., van der Steen, J., & Pel, J. J. (2013). Mini-mental state examination subscores indicate visuomotor deficits in alzheimer's disease patients: A cross-sectional study in a dutch population. *Geriatrics & Gerontology International,* DOI: 10.1111/ggi.12183.

Desmurget, M., Grea, H., Grethe, J. S., Prablanc, C., Alexander, G. E., & Grafton, S. T. (2001). Functional anatomy of nonvisual feedback loops during reaching: A positron emission tomography study. *The Journal of Neuroscience, 21*(8), 2919-2928.

Dong, W. K., Chudler, E. H., Sugiyama, K., Roberts, V. J., & Hayashi, T. (1994).

Somatosensory, multisensory, and task-related neurons in cortical area 7b (PF) of unanesthetized monkeys. *Journal of Neurophysiology, 72*(2), 542-564.

Drzezga, A., Becker, J. A., Van Dijk, K. R., Sreenivasan, A., Talukdar, T., Sullivan, C., et al. (2011). Neuronal dysfunction and disconnection of cortical hubs in non-demented subjects with elevated amyloid burden. *Brain, 134*(Pt 6), 1635-1646.

Drzezga, A., Grimmer, T., Riemenschneider, M., Lautenschlager, N., Siebner, H., Alexopoulus, P., et al. (2005). Prediction of individual clinical outcome in MCI by means of genetic assessment and (18)F-FDG PET. *Journal of Nuclear Medicine, 46*(10), 1625-1632.

Ewers, M., Sperling, R. A., Klunk, W. E., Weiner, M. W., & Hampel, H. (2011). Neuroimaging markers for the prediction and early diagnosis of alzheimer's disease dementia. *Trends in Neurosciences, 34*(8), 430-442.

Ferraina, S., Battaglia-Mayer, A., Genovesio, A., Marconi, B., Onorati, P., & Caminiti, R. (2001). Early coding of visuomanual coordination during reaching in parietal area PEc. *Journal of Neurophysiology, 85*(1), 462-467.

Ferraina, S., & Bianchi, L. (1994). Posterior parietal cortex: Functional properties of neurons in area 5 during an instructed-delay reaching task within different parts of space. *Experimental Brain Research, 99*(1), 175-178.

Filippini, N., MacIntosh, B. J., Hough, M. G., Goodwin, G. M., Frisoni, G. B., Smith, S.

M., et al. (2009). Distinct patterns of brain activity in young carriers of the APOE-epsilon4 allele. *Proceedings of the National Academy of Sciences of the United States of America, 106*(17), 7209-7214.

Flash, T., & Mussa-Ivaldi, F. (1990). Human arm stiffness characteristics during the maintenance of posture. *Experimental Brain Research, 82*(2), 315-326.

Foster, N. L., Chase, T. N., Mansi, L., Brooks, R., Fedio, P., Patronas, N. J., et al. (1984). Cortical abnormalities in alzheimer's disease. *Annals of Neurology, 16*(6), 649-654.

Fratiglioni, L., Ahlbom, A., Viitanen, M., & Winblad, B. (1993). Risk factors for late-onset alzheimer's disease: A population-based, case-control study. *Annals of Neurology, 33*(3), 258-266.

Frisoni, G. B., Prestia, A., Rasser, P. E., Bonetti, M., & Thompson, P. M. (2009). In vivo mapping of incremental cortical atrophy from incipient to overt alzheimer's disease. *Journal of Neurology, 256*(6), 916-924.

Galati, G., Committeri, G., Pitzalis, S., Pelle, G., Patria, F., Fattori, P., et al. (2011). Intentional signals during saccadic and reaching delays in the human posterior parietal cortex. *The European Journal of Neuroscience, 34*(11), 1871-1885.

Georgopoulos, A. P. (2000). Neural aspects of cognitive motor control. *Current Opinion in Neurobiology, 10*(2), 238-241.

Ghilardi, M. F., Alberoni, M., Marelli, S., Rossi, M., Franceschi, M., Ghez, C., et al.

(1999). Impaired movement control in alzheimer's disease. *Neuroscience Letters, 260*(1), 45-48.

Ghilardi, M. F., Alberoni, M., Rossi, M., Franceschi, M., Mariani, C., & Fazio, F. (2000). Visual feedback has differential effects on reaching movements in parkinson's and alzheimer's disease. *Brain Research, 876*(1-2), 112-123.

Gillain, S., Warzee, E., Lekeu, F., Wojtasik, V., Maquet, D., Croisier, J. L., et al. (2009). The value of instrumental gait analysis in elderly healthy, MCI or alzheimer's disease subjects and a comparison with other clinical tests used in single and dual-task conditions. *Annals of Physical and Rehabilitation Medicine, 52*(6), 453-474.

Gold, B. T., Powell, D. K., Andersen, A. H., & Smith, C. D. (2010). Alterations in multiple measures of white matter integrity in normal women at high risk for alzheimer's disease. *NeuroImage, 52*(4), 1487-1494.

Goodale, M. A. (1993). Visual pathways supporting perception and action in the primate cerebral cortex. *Current Opinion in Neurobiology, 3*(4), 578-585.

Gorbet, D. J., Staines, W. R., & Sergio, L. E. (2004). Brain mechanisms for preparing increasingly complex sensory to motor transformations. *NeuroImage, 23*(3), 1100-1111.

Green, R. C., Cupples, L. A., Go, R., Benke, K. S., Edeki, T., Griffith, P. A., et al. (2002). Risk of dementia among white and african american relatives of patients with

alzheimer disease. *The Journal of the American Medical Association, 287*(3), 329-336.

Haaland, K. Y., Harrington, D. L., & Grice, J. W. (1993). Effects of aging on planning and implementing arm movements. *Psychology and Aging, 8*(4), 617-632.

Hawkins, K.M., Goyal, A.I., & Sergio, L.E. (2015). Diffusion tensor imaging correlates of cognitive-motor decline in normal aging and increased Alzheimer's disease risk. *Journal of Alzhiemer's Disease, 44(3)*, 867-878.

Hawkins, K. M., Sayegh, P., Yan, X., Crawford, J. D., & Sergio, L. E. (2013). Neural activity in superior parietal cortex during rule-based visual-motor transformations. *Journal of Cognitive Neuroscience, 25*(3), 436-454.

Hawkins, K. M., & Sergio, L. E. (2014). Visuomotor impairments in older adults at increased alzheimer's disease risk. *Journal of Alzheimer's Disease, 42(2)*, 607-621.

Head, D., Buckner, R. L., Shimony, J. S., Williams, L. E., Akbudak, E., Conturo, T. E., et al. (2004). Differential vulnerability of anterior white matter in nondemented aging with minimal acceleration in dementia of the alzheimer type: Evidence from diffusion tensor imaging. *Cerebral Cortex, 14*(4), 410-423.

Head, D., Snyder, A. Z., Girton, L. E., Morris, J. C., & Buckner, R. L. (2005). Frontal-hippocampal double dissociation between normal aging and alzheimer's disease. *Cerebral Cortex, 15*(6), 732-739.

Hedden, T., Van Dijk, K. R., Becker, J. A., Mehta, A., Sperling, R. A., Johnson, K. A., et al. (2009a). Disruption of functional connectivity in clinically normal older adults harboring amyloid burden. *The Journal of Neuroscience, 29*(40), 12686-12694.

Hedden, T., Van Dijk, K. R., Becker, J. A., Mehta, A., Sperling, R. A., Johnson, K. A., et al. (2009b). Disruption of functional connectivity in clinically normal older adults harboring amyloid burden. *The Journal of Neuroscience, 29*(40), 12686-12694.

Heuninckx, S., Wenderoth, N., Debaere, F., Peeters, R., & Swinnen, S. P. (2005). Neural basis of aging: The penetration of cognition into action control. *The Journal of Neuroscience, 25*(29), 6787-6796.

Heuninckx, S., Wenderoth, N., & Swinnen, S. P. (2008). Systems neuroplasticity in the aging brain: Recruiting additional neural resources for successful motor performance in elderly persons. *The Journal of Neuroscience, 28*(1), 91-99.

Honea, R. A., Swerdlow, R. H., Vidoni, E. D., & Burns, J. M. (2011). Progressive regional atrophy in normal adults with a maternal history of alzheimer disease. *Neurology, 76*(9), 822-829.

Honea, R. A., Swerdlow, R. H., Vidoni, E. D., Goodwin, J., & Burns, J. M. (2010). Reduced gray matter volume in normal adults with a maternal family history of alzheimer disease. *Neurology, 74*(2), 113-120.

Inoue, K., Kawashima, R., Sugiura, M., Ogawa, A., Schormann, T., Zilles, K., et al.

(2001). Activation in the ipsilateral posterior parietal cortex during tool use: A PET study. *NeuroImage, 14*(6), 1469-1475.

Iriki, A., Tanaka, M., Obayashi, S., & Iwamura, Y. (2001). Self-images in the video monitor coded by monkey intraparietal neurons. *Neuroscience Research, 40*(2), 163-173.

Jack, C. R.,Jr, Lowe, V. J., Senjem, M. L., Weigand, S. D., Kemp, B. J., Shiung, M. M., et al. (2008). 11C PiB and structural MRI provide complementary information in imaging of alzheimer's disease and amnestic mild cognitive impairment. *Brain, 131*(Pt 3), 665-680.

Jacobs, H. I., Van Boxtel, M. P., Uylings, H. B., Gronenschild, E. H., Verhey, F. R., & Jolles, J. (2011). Atrophy of the parietal lobe in preclinical dementia. *Brain and Cognition, 75*(2), 154-163.

Jenkinson, M., Bannister, P., Brady, M., & Smith, S. (2002). Improved optimization for the robust and accurate linear registration and motion correction of brain images. *NeuroImage, 17*(2), 825-841.

Jenkinson, M., Beckmann, C. F., Behrens, T. E., Woolrich, M. W., & Smith, S. M. (2012). Fsl. *NeuroImage, 62*(2), 782-790.

Johnson, P. B., Ferraina, S., Bianchi, L., & Caminiti, R. (1996). Cortical networks for visual reaching: Physiological and anatomical organization of frontal and parietal

lobe arm regions. *Cerebral Cortex, 6*(2), 102-119.

Kalaska, J. F. (1996). Parietal cortex area 5 and visuomotor behavior. *Canadian Journal of Physiology and Pharmacology, 74*(4), 483-498.

Kalaska, J. F., Cohen, D. A., Prud'homme, M., & Hyde, M. L. (1990). Parietal area 5 neuronal activity encodes movement kinematics, not movement dynamics. *Experimental Brain Research, 80*(2), 351-364.

Kalaska, J. F., Scott, S. H., Cisek, P., & Sergio, L. E. (1997). Cortical control of reaching movements. *Current Opinion in Neurobiology, 7*(6), 849-859.

Kalaska, J. F., Sergio, L. E., & Cisek, P. (1998). Cortical control of whole-arm motor tasks. *Novartis Foundation Symposium, 218*, 176-90; discussion 190-201.

Karnath, H. O., & Perenin, M. T. (2005). Cortical control of visually guided reaching: Evidence from patients with optic ataxia. *Cerebral Cortex, 15*(10), 1561-1569.

Karow, D. S., McEvoy, L. K., Fennema-Notestine, C., Hagler, D. J.,Jr, Jennings, R. G., Brewer, J. B., et al. (2010). Relative capability of MR imaging and FDG PET to depict changes associated with prodromal and early alzheimer disease. *Radiology, 256*(3), 932-942.

Kemppainen, N. M., Aalto, S., Wilson, I. A., Nagren, K., Helin, S., Bruck, A., et al. (2007). PET amyloid ligand [11C]PIB uptake is increased in mild cognitive impairment. *Neurology, 68*(19), 1603-1606.

Ketcham, C. J., Seidler, R. D., Van Gemmert, A. W., & Stelmach, G. E. (2002). Age-related kinematic differences as influenced by task difficulty, target size, and movement amplitude. *The Journals of Gerontology Series B, Psychological Sciences and Social Sciences, 57*(1), P54-64.

Kluger, A., Gianutsos, J. G., Golomb, J., Ferris, S. H., George, A. E., Franssen, E., et al. (1997). Patterns of motor impairement in normal aging, mild cognitive decline, and early alzheimer's disease. *The Journals of Gerontology Series B, Psychological Sciences and Social Sciences, 52*(1), P28-39.

Lackner, J. R., & Dizio, P. (1994). Rapid adaptation to coriolis force perturbations of arm trajectory. *Journal of Neurophysiology, 72*(1), 299-313.

Lamar, M., & Resnick, S. M. (2004). Aging and prefrontal functions: Dissociating orbitofrontal and dorsolateral abilities. *Neurobiology of Aging, 25*(4), 553-558.

Lautenschlager, N. T., Cupples, L. A., Rao, V. S., Auerbach, S. A., Becker, R., Burke, J., et al. (1996). Risk of dementia among relatives of alzheimer's disease patients in the MIRAGE study: What is in store for the oldest old? *Neurology, 46*(3), 641-650.

Leisman, G., Braun-Benjamin, O., & Melillo, R. (2014). Cognitive-motor interactions of the basal ganglia in development. *Frontiers in Systems Neuroscience 8:16*. DOI 10.3389/fnsys.2014.00016.

Liu, C. C., Kanekiyo, T., Xu, H., & Bu, G. (2013). Apolipoprotein E and alzheimer

disease: Risk, mechanisms and therapy. *Nature Reviews.Neurology, 9*(2), 106-118.

Liu, Y., Yu, C., Zhang, X., Liu, J., Duan, Y., Alexander-Bloch, A. F., et al. (2014). Impaired long distance functional connectivity and weighted network architecture in alzheimer's disease. *Cerebral Cortex, 24*(6), 1422-1435.

Lu, M. T., Preston, J. B., & Strick, P. L. (1994). Interconnections between the prefrontal cortex and the premotor areas in the frontal lobe. *The Journal of Comparative Neurology, 341*(3), 375-392.

Marzocchi, N., Breveglieri, R., Galletti, C., & Fattori, P. (2008). Reaching activity in parietal area V6A of macaque: Eye influence on arm activity or retinocentric coding of reaching movements? *The European Journal of Neuroscience, 27*(3), 775-789.

Mayeux, R., Sano, M., Chen, J., Tatemichi, T., & Stern, Y. (1991). Risk of dementia in first-degree relatives of patients with alzheimer's disease and related disorders. *Archives of Neurology, 48*(3), 269-273.

Mazzoni, P., & Krakauer, J. W. (2006). An implicit plan overrides an explicit strategy during visuomotor adaptation. *The Journal of Neuroscience, 26*(14), 3642-3645.

McKhann, G., Drachman, D., Folstein, M., Katzman, R., Price, D., & Stadlan, E. M. (1984). Clinical diagnosis of alzheimer's disease: Report of the NINCDS-ADRDA work group under the auspices of department of health and human services task force on alzheimer's disease. *Neurology, 34*(7), 939-944.

Messier, J., & Kalaska, J. F. (1997). Differential effect of task conditions on errors of direction and extent of reaching movements. *Experimental Brain Research, 115*(3), 469-478.

Mesulam, M. M. (1990). Large-scale neurocognitive networks and distributed processing for attention, language, and memory. *Annals of Neurology, 28*(5), 597-613.

Mesulam, M. M., Nobre, A. C., Kim, Y. H., Parrish, T. B., & Gitelman, D. R. (2001). Heterogeneity of cingulate contributions to spatial attention. *NeuroImage, 13*(6 Pt 1), 1065-1072.

Middleton, F.A., & Strick, P.L. (2000). Basal ganglia and cerebellar loops: motor an cognitive circuits. *Brain Research Reviews 31*, 236-250.

Mielke, M. M., Kozauer, N. A., Chan, K. C., George, M., Toroney, J., Zerrate, M., et al. (2009). Regionally-specific diffusion tensor imaging in mild cognitive impairment and alzheimer's disease. *NeuroImage, 46*(1), 47-55.

Mitchell, J., Arnold, R., Dawson, K., Nestor, P. J., & Hodges, J. R. (2009). Outcome in subgroups of mild cognitive impairment (MCI) is highly predictable using a simple algorithm. *Journal of Neurology, 256*(9), 1500-1509.

Mormino, E. C., Smiljic, A., Hayenga, A. O., Onami, S. H., Greicius, M. D., Rabinovici, G. D., et al. (2011). Relationships between beta-amyloid and functional connectivity in different components of the default mode network in aging. *Cerebral Cortex,*

21(10), 2399-2407.

Mosconi, L., Brys, M., Switalski, R., Mistur, R., Glodzik, L., Pirraglia, E., et al. (2007). Maternal family history of alzheimer's disease predisposes to reduced brain glucose metabolism. *Proceedings of the National Academy of Sciences of the United States of America, 104*(48), 19067-19072.

Mosconi, L., Glodzik, L., Mistur, R., McHugh, P., Rich, K. E., Javier, E., et al. (2010). Oxidative stress and amyloid-beta pathology in normal individuals with a maternal history of alzheimer's. *Biological Psychiatry, 68*(10), 913-921.

Mosconi, L., Perani, D., Sorbi, S., Herholz, K., Nacmias, B., Holthoff, V., et al. (2004). MCI conversion to dementia and the APOE genotype: A prediction study with FDG-PET. *Neurology, 63*(12), 2332-2340.

Mosconi, L., Pupi, A., & De Leon, M. J. (2008). Brain glucose hypometabolism and oxidative stress in preclinical alzheimer's disease. *Annals of the New York Academy of Sciences, 1147*, 180-195.

Moscovitch, C., Kapur, S., Kohler, S., & Houle, S. (1995). Distinct neural correlates of visual long-term memory for spatial location and object identity: A positron emission tomography study in humans. *Proceedings of the National Academy of Sciences of the United States of America, 92*(9), 3721-3725.

Neggers, S. F., & Bekkering, H. (2001). Gaze anchoring to a pointing target is present

during the entire pointing movement and is driven by a non-visual signal. *Journal of Neurophysiology, 86*(2), 961-970.

Niogi, S. N., Mukherjee, P., Ghajar, J., Johnson, C., Kolster, R. A., Sarkar, R., et al. (2008). Extent of microstructural white matter injury in postconcussive syndrome correlates with impaired cognitive reaction time: A 3T diffusion tensor imaging study of mild traumatic brain injury. *American Journal of Neuroradiology, 29*(5), 967-973.

Parakh, R., Roy, E., Koo, E., & Black, S. (2004). Pantomime and imitation of limb gestures in relation to the severity of alzheimer's disease. *Brain and Cognition, 55*(2), 272-274.

Patenaude, B., Smith, S. M., Kennedy, D. N., & Jenkinson, M. (2011). A bayesian model of shape and appearance for subcortical brain segmentation. *NeuroImage, 56*(3), 907-922.

Pazzaglia, M., Smania, N., Corato, E., & Aglioti, S. M. (2008). Neural underpinnings of gesture discrimination in patients with limb apraxia. *The Journal of Neuroscience, 28*(12), 3030-3041.

Persson, J., Lind, J., Larsson, A., Ingvar, M., Cruts, M., Van Broeckhoven, C., et al. (2006). Altered brain white matter integrity in healthy carriers of the APOE epsilon4 allele: A risk for AD? *Neurology, 66*(7), 1029-1033.

Petersen, R. C., Doody, R., Kurz, A., Mohs, R. C., Morris, J. C., Rabins, P. V., et al. (2001a). Current concepts in mild cognitive impairment. *Archives of Neurology, 58*(12), 1985-1992.

Petersen, R. C., Doody, R., Kurz, A., Mohs, R. C., Morris, J. C., Rabins, P. V., et al. (2001b). Current concepts in mild cognitive impairment. *Archives of Neurology, 58*(12), 1985-1992.

Petrella, J. R., Sheldon, F. C., Prince, S. E., Calhoun, V. D., & Doraiswamy, P. M. (2011). Default mode network connectivity in stable vs progressive mild cognitive impairment. *Neurology, 76*(6), 511-517.

Petrides, M. (1997). Visuo-motor conditional associative learning after frontal and temporal lesions in the human brain. *Neuropsychologia, 35*(7), 989-997.

Pisella, L., Grea, H., Tilikete, C., Vighetto, A., Desmurget, M., Rode, G., et al. (2000). An 'automatic pilot' for the hand in human posterior parietal cortex: Toward reinterpreting optic ataxia. *Nature Neuroscience, 3*(7), 729-736.

Prado, J., Clavagnier, S., Otzenberger, H., Scheiber, C., Kennedy, H., & Perenin, M. T. (2005). Two cortical systems for reaching in central and peripheral vision. *Neuron, 48*(5), 849-858.

Pratt, J., Chasteen, A. L., & Abrams, R. A. (1994). Rapid aimed limb movements: Age differences and practice effects in component submovements. *Psychology and*

Aging, 9(2), 325-334.

Purves, D., Augustine, G.J., Fitzpatrick, D., Katz, L.C., LaMantia, A., McNamara, J.O., & Williams, S.M., editors (2001). Neuroscience. 2nd edition. Sunderland (MA): Sinauer Associates.

Raichle, M. E., MacLeod, A. M., Snyder, A. Z., Powers, W. J., Gusnard, D. A., & Shulman, G. L. (2001). A default mode of brain function. *Proceedings of the National Academy of Sciences of the United States of America, 98*(2), 676-682.

Redding, G. M., Rossetti, Y., & Wallace, B. (2005). Applications of prism adaptation: A tutorial in theory and method. *Neuroscience and Biobehavioral Reviews, 29*(3), 431-444.

Redding, G. M., & Wallace, B. (1996). Adaptive spatial alignment and strategic perceptual-motor control. *Journal of Experimental Psychology: Human Perception and Performance, 22*(2), 379-394.

Reig, R., & Silberberg, G. (2014). Multisensory integration in the mouse striatum. *Neuron* [Epud ahead of print] DOI: 10.1016/j.neuron.2014.07.003

Reilly, S. L., Ferrell, R. E., & Sing, C. F. (1994). The gender-specific apolipoprotein E genotype influence on the distribution of plasma lipids and apolipoproteins in the population of rochester, MN. III. correlations and covariances. *American Journal of Human Genetics, 55*(5), 1001-1018.

Reiman, E. M., Caselli, R. J., Yun, L. S., Chen, K., Bandy, D., Minoshima, S., et al. (1996). Preclinical evidence of alzheimer's disease in persons homozygous for the epsilon 4 allele for apolipoprotein E. *The New England Journal of Medicine, 334*(12), 752-758.

Reiman, E. M., Chen, K., Alexander, G. E., Caselli, R. J., Bandy, D., Osborne, D., et al. (2004). Functional brain abnormalities in young adults at genetic risk for late-onset alzheimer's dementia. *Proceedings of the National Academy of Sciences of the United States of America, 101*(1), 284-289.

Reisberg, B., Franssen, E. H., Souren, L. E., Auer, S. R., Akram, I., & Kenowsky, S. (2002). Evidence and mechanisms of retrogenesis in alzheimer's and other dementias: Management and treatment import. *American Journal of Alzheimer's Disease and Other Dementias, 17*(4), 202-212.

Rizzolatti, G., Luppino, G., & Matelli, M. (1998). The organization of the cortical motor system: New concepts. *Electroencephalography and Clinical Neurophysiology, 106*(4), 283-296.

Rizzolatti, G., & Matelli, M. (2003). Two different streams form the dorsal visual system: Anatomy and functions. *Experimental Brain Research, 153*(2), 146-157.

Rose, S. E., McMahon, K. L., Janke, A. L., O'Dowd, B., de Zubicaray, G., Strudwick, M. W., et al. (2006). Diffusion indices on magnetic resonance imaging and

neuropsychological performance in amnestic mild cognitive impairment. *Journal of Neurology, Neurosurgery, and Psychiatry, 77*(10), 1122-1128.

Rossetti, Y., Revol, P., McIntosh, R., Pisella, L., Rode, G., Danckert, J., et al. (2005). Visually guided reaching: Bilateral posterior parietal lesions cause a switch from fast visuomotor to slow cognitive control. *Neuropsychologia, 43*(2), 162-177.

Salek, Y., Anderson, N. D., & Sergio, L. (2011). Mild cognitive impairment is associated with impaired visual-motor planning when visual stimuli and actions are incongruent. *European Neurology, 66*(5), 283-293.

Sarlegna, F. R. (2006). Impairment of online control of reaching movements with aging: A double-step study. *Neuroscience Letters, 403*(3), 309-314.

Say, M. J., Jones, R., Scahill, R. I., Dumas, E. M., Coleman, A., Santos, R. C., et al. (2011). Visuomotor integration deficits precede clinical onset in huntington's disease. *Neuropsychologia, 49*(2), 264-270.

Sayegh, P. F., Hawkins, K. M., Hoffman, K. L., & Sergio, L. E. (2013). Differences in spectral profiles between rostral and caudal premotor cortex when eye-hand actions are decoupled. *Journal of Neurophysiology,*

Sayegh, P. F., Hawkins, K. M., Neagu, B., Crawford, J. D., Hoffman, K. L., & Sergio, L. E. (2014). Decoupling the actions of the eyes from the hand alters beta and gamma synchrony within SPL. *Journal of Neurophysiology, 111*(11), 2210-2221.

Schmidt, R., Kienbacher, E., Benke, T., Dal-Bianco, P., Delazer, M., Ladurner, G., et al. (2008). Sex differences in alzheimer's disease. [Geschlechtsspezifische Unterschiede der Alzheimer Demenz] *Neuropsychiatrie : Klinik, Diagnostik, Therapie Und Rehabilitation : Organ Der Gesellschaft Osterreichischer Nervenarzte Und Psychiater, 22*(1), 1-15.

Schroeter, M. L., Stein, T., Maslowski, N., & Neumann, J. (2009). Neural correlates of alzheimer's disease and mild cognitive impairment: A systematic and quantitative meta-analysis involving 1351 patients. *NeuroImage, 47*(4), 1196-1206.

Seidler-Dobrin, R. D., & Stelmach, G. E. (1998). Persistence in visual feedback control by the elderly. *Experimental Brain Research, 119*(4), 467-474.

Sen, P. N., & Basser, P. J. (2005). A model for diffusion in white matter in the brain. *Biophysical Journal, 89*(5), 2927-2938.

Sergio, L. E., & Kalaska, J. F. (2003). Systematic changes in motor cortex cell activity with arm posture during directional isometric force generation. *Journal of Neurophysiology, 89*(1), 212-228.

Sexton, C. E., Kalu, U. G., Filippini, N., Mackay, C. E., & Ebmeier, K. P. (2011). A meta-analysis of diffusion tensor imaging in mild cognitive impairment and alzheimer's disease. *Neurobiology of Aging, 32*(12), 2322.e5-2322.18.

Shao, Y., Wang, L., Ye, E., Jin, X., Ni, W., Yang, Y., et al. (2013). Decreased

thalamocortical functional connectivity after 36 hours of total sleep deprivation: Evidence from resting state FMRI. *PloS One, 8*(10), e78830.

Sheline, Y. I., Morris, J. C., Snyder, A. Z., Price, J. L., Yan, Z., D'Angelo, G., et al. (2010a). APOE4 allele disrupts resting state fMRI connectivity in the absence of amyloid plaques or decreased CSF Abeta42. *The Journal of Neuroscience, 30*(50), 17035-17040.

Sheline, Y. I., & Raichle, M. E. (2013). Resting state functional connectivity in preclinical alzheimer's disease. *Biological Psychiatry, 74*(5), 340-347.

Sheline, Y. I., Raichle, M. E., Snyder, A. Z., Morris, J. C., Head, D., Wang, S., et al. (2010b). Amyloid plaques disrupt resting state default mode network connectivity in cognitively normal elderly. *Biological Psychiatry, 67*(6), 584-587.

Shen, L., & Alexander, G. E. (1997). Neural correlates of a spatial sensory-to-motor transformation in primary motor cortex. *Journal of Neurophysiology, 77*(3), 1171-1194.

Sheridan, P. L., & Hausdorff, J. M. (2007). The role of higher-level cognitive function in gait: Executive dysfunction contributes to fall risk in alzheimer's disease. *Dementia and Geriatric Cognitive Disorders, 24*(2), 125-137.

Silverberg, N. B., Ryan, L. M., Carrillo, M. C., Sperling, R., Petersen, R. C., Posner, H. B., et al. (2011). Assessment of cognition in early dementia. *Alzheimer's &*

Dementia, 7(3), e60-e76.

Small, G. W., Ercoli, L. M., Silverman, D. H., Huang, S. C., Komo, S., Bookheimer, S. Y., et al. (2000). Cerebral metabolic and cognitive decline in persons at genetic risk for alzheimer's disease. *Proceedings of the National Academy of Sciences of the United States of America, 97*(11), 6037-6042.

Small, G. W., Mazziotta, J. C., Collins, M. T., Baxter, L. R., Phelps, M. E., Mandelkern, M. A., et al. (1995). Apolipoprotein E type 4 allele and cerebral glucose metabolism in relatives at risk for familial alzheimer disease. *The Journal of the American Medical Association, 273*(12), 942-947.

Smith, C. D., Chebrolu, H., Andersen, A. H., Powell, D. A., Lovell, M. A., Xiong, S., et al. (2010). White matter diffusion alterations in normal women at risk of alzheimer's disease. *Neurobiology of Aging, 31*(7), 1122-1131.

Smith, S. M. (2002). Fast robust automated brain extraction. *Human Brain Mapping, 17*(3), 143-155.

Smith, S. M., Jenkinson, M., Johansen-Berg, H., Rueckert, D., Nichols, T. E., Mackay, C. E., et al. (2006). Tract-based spatial statistics: Voxelwise analysis of multi-subject diffusion data. *NeuroImage, 31*(4), 1487-1505.

Snyder, L. H., Batista, A. P., & Andersen, R. A. (2000). Saccade-related activity in the parietal reach region. *Journal of Neurophysiology, 83*(2), 1099-1102.

Snyder, L. H., Calton, J. L., Dickinson, A. R., & Lawrence, B. M. (2002). Eye-hand coordination: Saccades are faster when accompanied by a coordinated arm movement. *Journal of Neurophysiology, 87*(5), 2279-2286.

Soechting, J. F., & Flanders, M. (1992). Moving in three-dimensional space: Frames of reference, vectors, and coordinate systems. *Annual Review of Neuroscience, 15*, 167-191.

Song, S. K., Sun, S. W., Ju, W. K., Lin, S. J., Cross, A. H., & Neufeld, A. H. (2003). Diffusion tensor imaging detects and differentiates axon and myelin degeneration in mouse optic nerve after retinal ischemia. *NeuroImage, 20*(3), 1714-1722.

Song, S. K., Yoshino, J., Le, T. Q., Lin, S. J., Sun, S. W., Cross, A. H., et al. (2005). Demyelination increases radial diffusivity in corpus callosum of mouse brain. *NeuroImage, 26*(1), 132-140.

Sorg, C., Riedl, V., Muhlau, M., Calhoun, V. D., Eichele, T., Laer, L., et al. (2007). Selective changes of resting-state networks in individuals at risk for alzheimer's disease. *Proceedings of the National Academy of Sciences of the United States of America, 104*(47), 18760-18765.

Spirduso, W. W. (1975). Reaction and movement time as a function of age and physical activity level. *Journal of Gerontology, 30*(4), 435-440.

Spirduso, W. W., & Clifford, P. (1978). Replication of age and physical activity effects

on reaction and movement time. *Journal of Gerontology, 33*(1), 26-30.

Storandt, M., Mintun, M. A., Head, D., & Morris, J. C. (2009). Cognitive decline and brain volume loss as signatures of cerebral amyloid-beta peptide deposition identified with pittsburgh compound B: Cognitive decline associated with abeta deposition. *Archives of Neurology, 66*(12), 1476-1481.

Stricker, N. H., Schweinsburg, B. C., Delano-Wood, L., Wierenga, C. E., Bangen, K. J., Haaland, K. Y., et al. (2009). Decreased white matter integrity in late-myelinating fiber pathways in alzheimer's disease supports retrogenesis. *NeuroImage, 45*(1), 10-16.

Sun, S. W., Liang, H. F., Trinkaus, K., Cross, A. H., Armstrong, R. C., & Song, S. K. (2006). Noninvasive detection of cuprizone induced axonal damage and demyelination in the mouse corpus callosum. *Magnetic Resonance in Medicine, 55*(2), 302-308.

Tippett, W. J., Krajewski, A., & Sergio, L. E. (2007). Visuomotor integration is compromised in alzheimer's disease patients reaching for remembered targets. *European Neurology, 58*(1), 1-11.

Tippett, W. J., & Sergio, L. E. (2006). Visuomotor integration is impaired in early stage alzheimer's disease. *Brain Research, 1102*(1), 92-102.

Tippett, W. J., Sergio, L. E., & Black, S. E. (2012). Compromised visually guided motor

control in individuals with alzheimer's disease: Can reliable distinctions be observed? *Journal of Clinical Neuroscience, 19*(5), 655-660.

Verheij, S., Muilwijk, D., Pel, J. J., van der Cammen, T. J., Mattace-Raso, F. U., & van der Steen, J. (2012). Visuomotor impairment in early-stage alzheimer's disease: Changes in relative timing of eye and hand movements. *Journal of Alzheimer's Disease, 30*(1), 131-143.

Vesia, M., Yan, X., Henriques, D. Y., Sergio, L. E., & Crawford, J. D. (2008). Transcranial magnetic stimulation over human dorsal-lateral posterior parietal cortex disrupts integration of hand position signals into the reach plan. *Journal of Neurophysiology, 100*(4), 2005-2014.

Vidoni, E. D., Thomas, G. P., Honea, R. A., Loskutova, N., & Burns, J. M. (2012). Evidence of altered corticomotor system connectivity in early-stage alzheimer's disease. *Journal of Neurologic Physical Therapy, 36*(1), 8-16.

Villain, N., Desgranges, B., Viader, F., de la Sayette, V., Mezenge, F., Landeau, B., et al. (2008). Relationships between hippocampal atrophy, white matter disruption, and gray matter hypometabolism in alzheimer's disease. *The Journal of Neuroscience, 28*(24), 6174-6181.

Vlassenko, A. G., Vaishnavi, S. N., Couture, L., Sacco, D., Shannon, B. J., Mach, R. H., et al. (2010). Spatial correlation between brain aerobic glycolysis and amyloid-beta

(abeta) deposition. *Proceedings of the National Academy of Sciences of the United States of America, 107*(41), 17763-17767.

White, I. M., & Wise, S. P. (1999). Rule-dependent neuronal activity in the prefrontal cortex. *Experimental Brain Research, 126*(3), 315-335.

Willis, L., Behrens, M., Mack, W., & Chui, H. (1998). Ideomotor apraxia in early alzheimer's disease: Time and accuracy measures. *Brain and Cognition, 38*(2), 220-233.

Wise, S. P., di Pellegrino, G., & Boussaoud, D. (1996). The premotor cortex and nonstandard sensorimotor mapping. *Canadian Journal of Physiology and Pharmacology, 74*(4), 469-482.

Woollacott, M. H., Shumway-Cook, A., & Nashner, L. M. (1986). Aging and posture control: Changes in sensory organization and muscular coordination. *International Journal of Aging & Human Development, 23*(2), 97-114.

Wu, T., & Hallett, M. (2005). The influence of normal human ageing on automatic movements. *The Journal of Physiology, 562*(Pt 2), 605-615.

Yamaguchi, H., Takahashi, S., Kosaka, K., Okamoto, K., Yamazaki, T., Ikeda, M., et al. (2011). Yamaguchi fox-pigeon imitation test (YFPIT) for dementia in clinical practice. *Psychogeriatrics, 11*(4), 221-226.

Yan, J. H., Thomas, J. R., Stelmach, G. E., & Thomas, K. T. (2000). Developmental

features of rapid aiming arm movements across the lifespan. *Journal of Motor Behavior, 32*(2), 121-140.

Zhang, J., Riehle, A., Requin, J., & Kornblum, S. (1997). Dynamics of single neuron activity in monkey primary motor cortex related to sensorimotor transformation. *The Journal of Neuroscience, 17*(6), 2227-2246.

Zhang, Y., Brady, M., & Smith, S. (2001). Segmentation of brain MR images through a hidden markov random field model and the expectation-maximization algorithm. *IEEE Transactions on Medical Imaging, 20*(1), 45-57.

Zhang, Y., Schuff, N., Jahng, G. H., Bayne, W., Mori, S., Schad, L., et al. (2007). Diffusion tensor imaging of cingulum fibers in mild cognitive impairment and alzheimer disease. *Neurology, 68*(1), 13-19.

Appendix A - Functional specifications for the cognitive-motor assessment application

For: Mike Williams

Prepared by: Kara Hawkins June 10, 2011

1. Introduction

1.1 Purpose

The purpose of this application is to run, and save the data acquired from, eight separate "centre-out reaching" visuomotor control tasks. These tasks require the user to respond to visual stimuli presented on a vertical tablet through touch input either on the same vertical tablet as the presentation or a separate tablet oriented horizontally on a tabletop, with visual feedback provided by a cursor on the vertical tablet. This application will be used by researchers to collect visuomotor control data from various populations (e.g. varsity athletes with and without concussions, healthy young and old adults, dementia patients etc.). Thus, the application must save all experimental configurations, time and position of touch input, and time at which specific user dependent events occur.

2. General description

2.1 User interfaces

a) For the experimenter – The home screen on the vertical tablet will display an "Experimental Configurations" button (which, when selected, provides the experimenter

with a dialog box in which the position, size, and colour of items can be changed, as well as the number of trials and timing parameters; described in detail in section 3.3), along with buttons for each cognitive-motor assessment task (listed in section 3.2) allowing the experimenter to select the desired conditions. Once the conditions have been selected by the experimenter, a randomized condition order is generated using only the condition numbers that have been selected (e.g. if the experimenter wants to run the vertical, vertical memory, vertical rotated, horizontal, horizontal memory, and horizontal rotated conditions, the numbers 1, 2, 3, 6, 7, and 8 are randomly organized). Next, a dialog box opens allowing the experimenter to enter a new subject by typing their initials. For data saving, the application must generate separate file names for each condition by adding _condition# to the subjects initials (e.g. kh_1). The task screen will then appear displaying two buttons, one labelled "Practice" the other labelled with the name of the appropriate condition based on the random condition order sequence (e.g. "Vertical Rotated"). Selecting the Practice button runs a short version of the task (two trials in each target direction) without saving, then returns to previous screen. Selecting the condition button runs the appropriate task according to the parameter set in the experimental configurations dialog box, finishing with a screen displaying practice and condition buttons for the next task in the condition order sequence.

Webcam software will also be required allowing the experimenter to observe and save

video of the subjects' eye movements throughout all tasks by displaying the video window on a separate monitor.

b) For the subject – items displayed on the vertical tablet will respond to touch input from the subject's finger, which they will be instructed to slide along either the vertical or the horizontal tablet depending on the task. A cross-hair cursor will provide visual feedback of the subject's movements throughout all tasks.

2.2 Proposed future alterations

Currently we are using offline means (MATLAB) to analyze the data acquired from the cognitive-motor assessment application in order to identify the most useful measures for differentiating healthy controls from individuals with neurological impairments such as Alzheimer's disease or concussion. In the future, the cognitive-motor assessment application will be required to handle these computations online in order to provide the clinician or researcher with immediate scores and percentile rankings on relevant measures upon completion of each task, as well as a summary graphic upon completion of the entire cognitive-motor assessment.

3. Specific requirements

3.1 General description of the centre-out reaching paradigm

All of the tasks included in the cognitive-motor assessment application fall within a paradigm referred to as centre-out reaching, which consists of a home target at the centre of the display and the presentation of peripheral targets towards which the subject must initiate a motor response upon instruction. In the current application, there will be four peripheral targets: left, up, right, and down, each centred on a point 75 mm from the centre of the home target (i.e. the centre of the monitor; this 75 mm distance is based on the maximum distance for a target 20 mm in diameter that can fit within the height of the Acer Iconia monitor). The size, position, and colour of these targets is consistent across all tasks, and the target sizes and distances from centre must be kept consistent across all monitor sizes and resolutions (i.e. the application must convert pixels to mm in order to adjust the target sizes and positions in response to user input specifying the monitor

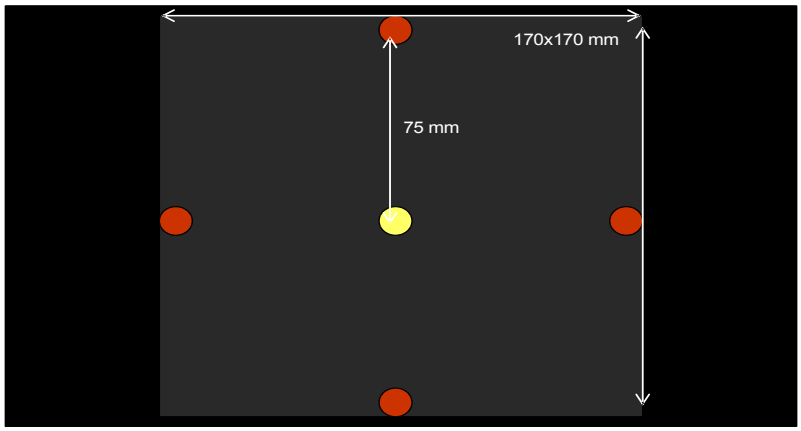

dimensions and resolution). In order to maintain a consistent visual border around the peripheral targets, the task will be displayed on a 170 x 170 mm dark grey background with the surrounding background coloured black.

In general, the trial timing and subject responses (user input) consist of the following: 1) presentation of the home target on the vertical tablet, 2) subject touches the home target (either directly or with the cursor using the horizontal monitor), which changes its colour, 3) after holding the home target for a set amount of time (experimental configurations: centre hold time) a peripheral target is presented (locations pseudo-randomized such that all four directions appear for the set trial number) and the home target disappears, instructing the subject to slide their finger directing the cursor to the target, 4) once the peripheral target is held for a set amount of time (experimental configurations: target hold time) it disappears and the trial ends, 5) the next trial begins with the presentation of the home target after a set amount of time (experimental configurations: inter trial interval)... this sequence continues for a set number of trials per target (experimental configurations: Nb_Trials per target). The specific requirements for each condition are described below.

3.2 Specific condition requirements

- Vertical (V – condition #1) – 1) presentation of home target on the vertical tablet, 2) subject touches home target on the vertical tablet which changes its colour, 3) after holding the home target for the set centre hold time a peripheral target is presented and the home target disappears instructing the subject to slide their finger directly towards the target on the vertical tablet, 4) once the peripheral target is held for the

set target hold time it disappears and the trial ends, 5) the next trial begins with the presentation of the home target after the set inter trial interval... this sequence continues for the set number of trials per target.

- Vertical memory (VM – condition #2) – 1) presentation of home target on the vertical tablet, 2) subject touches home target on the vertical tablet which changes its colour and initiates the presentation of a peripheral target, 3) after the set cue period the peripheral target disappears, 4) the subject holds the home target for the set centre hold time (i.e. until it disappears), which will be longer than the cue period, 5) the disappearance of the home target instructs the subject to slide their finger directly towards the remembered target location on the vertical tablet, 6) once the appropriate location of the peripheral target is reached, the target is displayed to provide the subject with feedback and must be held for the set target hold time before disappearing again and ending the trial, 7) the next trial begins with the presentation of the home target after the set inter trial interval... this sequence continues for the set number of trials per target.
- Vertical rotated (VR – condition #3) – 1) presentation of home target on the vertical tablet, 2) subject touches home target on the vertical tablet which changes its colour, 3) after holding the home target for the set centre hold time a peripheral target is presented and the home target disappears instructing the subject to slide their finger on the vertical tablet in the direction opposite that of the target in order to guide the

cursor towards the target (i.e. cursor feedback is rotated 180°), 4) once the cursor reaches the peripheral target it is held there for the set target hold time, after which the target disappears and the trial ends, 5) the next trial begins with the presentation of the home target after the set inter trial interval... this sequence continues for the set number of trials per target.

- Vertical rotated memory (VRM – condition #4) – 1) presentation of home target on the vertical tablet, 2) subject touches home target on the vertical tablet which changes its colour and initiates the presentation of a peripheral target, 3) after the set cue period the peripheral target disappears, 4) the subject holds the home target for the set centre hold time (i.e. until it disappears), which will be longer than the cue period, 5) the disappearance of the home target instructs the subject to slide their finger on the vertical tablet in the direction opposite that of the remembered target location in order to guide the cursor towards the remembered target location (i.e. cursor feedback is rotated 180°), 6) once the cursor reaches the appropriate location of the peripheral target, the target is displayed to provide the subject with feedback and must be held for the set target hold time before disappearing again and ending the trial, 7) the next trial begins with the presentation of the home target after the set inter trial interval... this sequence continues for the set number of trials per target.
- Vertical arbitrary (A – condition #5) – 1) presentation of home target on the vertical tablet, which is one of four images symbolizing the direction that the subject is

required to move (see images and associated directions below), 2) subject touches home target on the vertical tablet which changes its colour, 3) after holding the home target for the set centre hold time it disappears instructing the subject to slide their finger in the appropriate direction on the vertical tablet, 4) If the direction is correct, a peripheral target (same targets as in the other conditions) will appear providing the subject with feedback, this target must be held for the set target hold time after which it disappears and the trial ends, 5) the next trial begins after the set inter trial interval with the presentation of the next home target image (pseudo-randomized such that all four images appear for the set number of trials)... this sequence continues for the set number of trials per target.

Left Up Right Down

- Horizontal (H – condition #6) – 1) presentation of home target on the vertical tablet, 2) subject uses horizontal tablet to direct a cursor (cross-hair) to the home target on the vertical tablet, once the cursor enters the home target it changes colour, 3) after holding the cursor in the home target for the set centre hold time a peripheral target is presented on the vertical tablet and the home target disappears instructing the subject to slide their finger along the horizontal tablet in the direction of the target such that

the cursor is directed towards the target on the vertical tablet, 4) once the cursor is held in the peripheral target for the set target hold time the target disappears and the trial ends, 5) the next trial begins with the presentation of the home target after the set inter trial interval... this sequence continues for the set number of trials per target.

- Horizontal memory (HM – condition #7) – 1) presentation of home target on the vertical tablet, 2) subject uses horizontal tablet to direct a cursor (cross-hair) to the home target on the vertical tablet, once the cursor enters the home target it changes colour and the presentation of a peripheral target on the vertical tablet is initiated, 3) after the set cue period the peripheral target disappears, 4) the subject holds the cursor in the home target for the set centre hold time (i.e. until it disappears), which will be longer than the cue period, 5) the disappearance of the home target instructs the subject to slide their finger along the horizontal tablet in the direction of the remembered target such that the cursor is directed towards the remembered target location on the vertical tablet, 6) once the cursor reaches the appropriate location of the peripheral target, the target is displayed to provide the subject with feedback, and the cursor must be held there for the set target hold time, after which the target disappears again ending the trial, 7) the next trial begins with the presentation of the home target after the set inter trial interval... this sequence continues for the set number of trials per target.
- Horizontal rotated (HR – condition #8) – 1) presentation of home target on the

vertical tablet, 2) subject uses horizontal tablet to direct a cursor (cross-hair) to the home target on the vertical tablet, once the cursor enters the home target it changes colour, 3) after holding the cursor in the home target for the set centre hold time a peripheral target is presented on the vertical tablet and the home target disappears instructing the subject to slide their finger along the horizontal tablet in the direction opposite that of the target such that the cursor is directed towards the target on the vertical tablet (i.e. cursor feedback is rotated 180°), 4) once the cursor is held in the peripheral target for the set target hold time the target disappears and the trial ends, 5) the next trial begins with the presentation of the home target after the set inter trial interval... this sequence continues for the set number of trials per target.

- Horizontal rotated memory (HRM – condition #9) – 1) presentation of home target on the vertical tablet, 2) subject uses horizontal tablet to direct a cursor (cross-hair) to the home target on the vertical tablet, once the cursor enters the home target it changes colour and the presentation of a peripheral target on the vertical tablet is initiated, 3) after the set cue period the peripheral target disappears, 4) the subject holds the home target for the set centre hold time (i.e. until it disappears), which will be longer than the cue period, 5) the disappearance of the home target instructs the subject to slide their finger along the horizontal tablet in the direction opposite that of the remembered target such that the cursor is directed towards the remembered target location (i.e. cursor feedback is rotated 180°), 6) once the cursor reaches the

appropriate location of the peripheral target, the target is displayed to provide the subject with feedback, and the cursor must be held there for the set target hold time, after which the target disappears again ending the trial, 7) the next trial begins with the presentation of the home target after the set inter trial interval... this sequence continues for the set number of trials per target.

3.3 Experimental configurations

The following configurations must be accessible and manipulable by the experimenter through a dialog box that can be opened prior to initiating the cognitive-motor assessment.

a) Monitor settings:

- Monitor dimensions
- Monitor resolution

b) Stimulus settings

- Nb_Trials per target (default 5)
- Home target (t1) location (default at centre of monitor)
- Exit t1 threshold (default 40 mm diameter) – this setting creates an invisible threshold around the home target once it has been touch which is used to determine when the finger exits the home target; this will allow us to minimize false leave too early errors (i.e. we want to make sure that they actually left the home target too early and that

their finger didn't just slip out of target)

- Peripheral target (t2) locations (default 75 mm left, above, right, and below centre)
- Target sizes (default 20 mm diameter)
- Target colours (default yellow changing to green upon touch for home target, red for peripheral targets)

c) Timing settings:

- Inter_Trial Interval (default 2000 ms)
- Pre-Entry Time (default 10000 ms) – error outcome 1 = failure to enter t1 in set amount of time; save error outcome and restart trial (i.e. extra trials will be saved if this error occurs)
- Centre_Hold Time (default 4000 ms) – error outcome 2 = left t1 too early; save error outcome and start next trial
- Cue period (default 2000 ms) – memory conditions only – error outcome 2 = left t1 too early; save error outcome and start next trial
- Early_Reaction Time (default 150 ms) – error outcome 3 = reaction time too short; save error outcome and restart trial (i.e. extra trials will be saved if this error occurs)
- Late_Reaction Time (default 8000 ms) – error outcome 4 = reaction time too long; save error outcome and start next trial
- Max Movement Time (default 10000 ms) – error outcome 5 = movement time too long; save error outcome and start next trial

- Target_Hold Time (default 500 ms) – error outcome 6 = failure to hold peripheral target for set amount of time; save error outcome and start next trial – *THT begins after being in target for 100ms*
- If no timing errors, outcome = 0

3.4 Data file saving and conversion

- Text file – below is a snippet of saved data from the old application illustrating the format in which data should be saved (note: all variable names must be consistent with the old application in order to allow seamless loading into the MATLAB graphic user interface developed for data analysis).

18/02/2011 10:28:17 AM

Exp_without_M: Nb_Trials 5, Cond_Order 1, Pre_entry 10000, C_Hold 4000

Cue_Period 2000 E_Reaction 150, L_Reaction 5000, Max_Move 10000, T_Hold 1000,

Inter_trial 2000 Cond 1, Trial 1, Outcome 0, Target#3 x 976, y 374, LenOfData 90,

Entry_t1 1250, Entry_t2 6193

1170,592,304

1186,596,305

1193,597,306

1202,599,307

1209,602,310

1225,606,313

...

Cond 1, Trial 2, Outcome 6, Target#1 x 308, y 374, LenOfData 108, Entry_t1 731, Entry_t2 5525

308,982,355

340,979,355

347,977,356

356,972,356

372,968,356

379,964,357

...

- Conversion of text files into binary MATLAB files for data analysis is also required (file naming – kh_1_c)

3.5 Data analysis

The following is a list of outcome measures currently computed in MATLAB using the data acquired from the cognitive-motor assessment.

- Velocity and finger position profiles
- Peak velocity

- Beginning and end of first ballistic movement using 10% peak velocity
- Reaction time (RT)
- Movement time (MT)
- Total movement time (TMT)
- Corrective movement time (CMT)
- Constant error (CE)
- Variable error (VE)
- Path length
- Corrective path length

Appendix B – Mean kinematic measures and discriminant analysis for imaging study participants

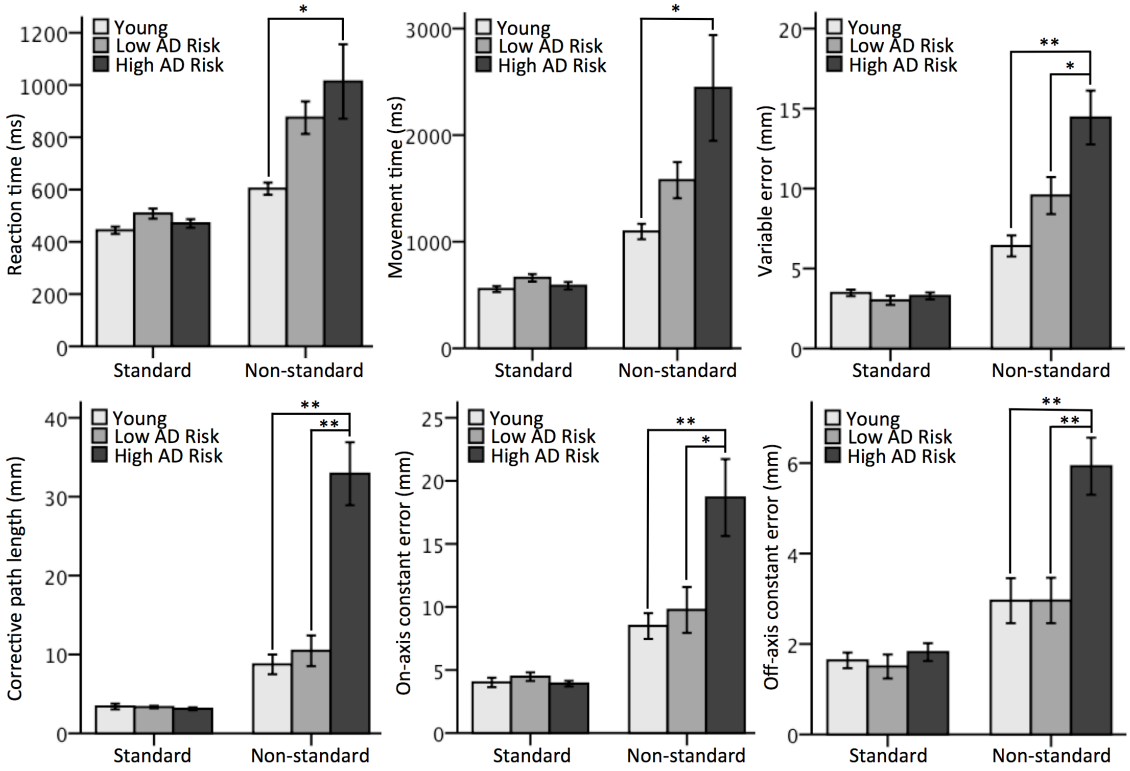

Figure B.1. Results of group (young: light grey bars, low AD risk: medium grey bars, high AD risk: dark grey bars) by condition (standard, non-standard) mixed ANOVAs on task dependent measures. Means +/- 1 SEM, * = < .05, ** = < .01.

Discriminant analysis: A discriminant analysis between the high and low AD risk participants included in our imaging studies was conducted in order to examine whether or not we could reproduce the results from study #1. Corrective path length and off-axis constant error from the PD+FR task were entered as predictor variables (i.e. the two variables that discriminated best between family history negative and family history positive participants in study #1). The resulting discriminant function was significant (Wilks' Lambda = .384, $p < .001$), with a canonical correlation of .79. The structure matrix indicated that corrective path length was the strongest predictor ($r = .94$) and off-axis constant error also added predictive power ($r = .68$). The resulting canonical discriminant function was D = (.08 x corrective path length) + (.204 x off-axis constant error) - 2.643 and the grouping of cases resulted in an overall classification accuracy of 90%, with a sensitivity of 80% and specificity of 100%. These results are consistent with study #1 and support the use of error measures from our cognitively demanding PD+FR visuomotor task in discriminating between high and low AD risk participants. Furthermore, we also found that the two participants from the high AD risk group who were "misclassified" as low AD risk were the only two participants from this group who were not ApoE4 carriers, while the two participants from the low AD risk group who were ApoE4 carriers had the highest discriminant scores (i.e. the largest error scores) in this group (see Figure B.2).

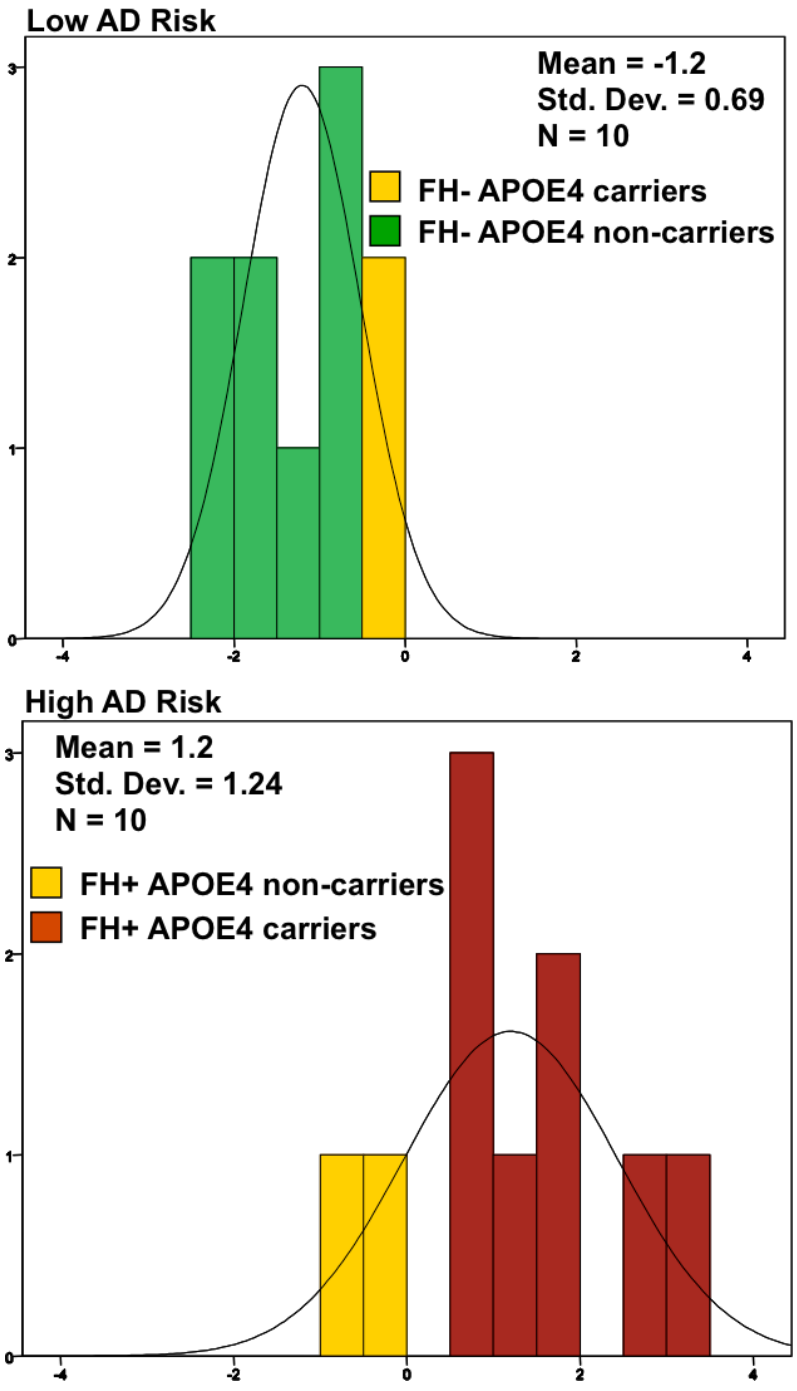

Figure B.2. Discriminant analysis classification results for imaging study participants.

Appendix C – Mean hippocampal volumes for imaging study participants

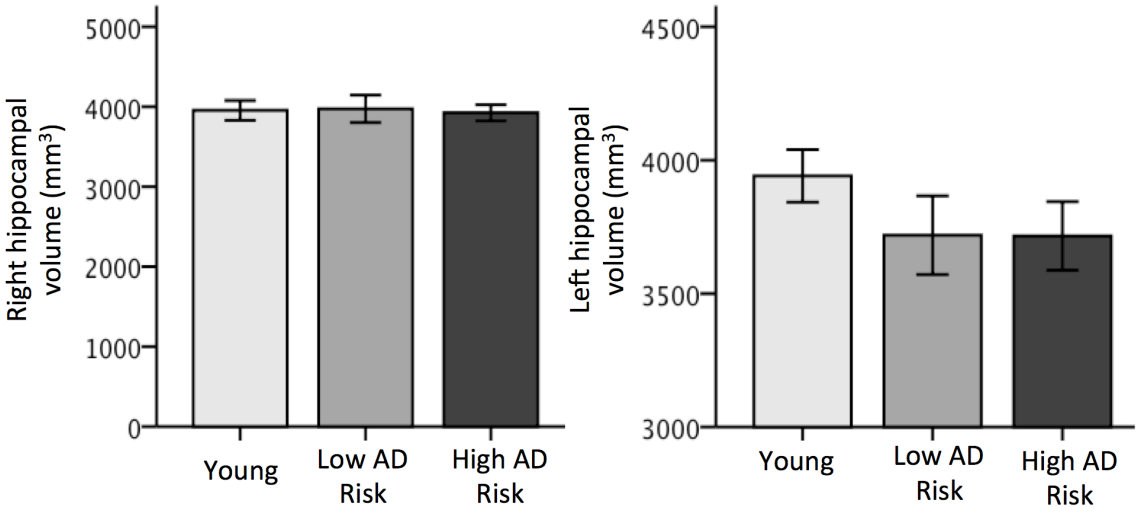

Figure C.1. Right and left mean hippocampal volumes compared across groups (young: light grey bars, low AD risk: medium grey bars, high AD risk: dark grey bars). No significant differences were found between groups in a one-way ANOVA test. Means +/- 1 SEM.

Appendix D – Methodology and correlational results for diffusion tensor imaging atlas-generated tracts of interest

Methods: In order to calculate mean diffusivity measures within major white matter (WM) tracts, tracts of interest (TOIs) were also identified using the Johns Hopkins University's (JHU) WM probabilistic atlas. Specifically, the diffusivity maps determined using DTIFIT were nonlinear registered to a standard space template (FMRIB58_FA) using tract-based spatial statistics (TBSS). These images were then smoothed to 2 mm Full Width Half Maximum (FWHM) using fslmaths, and TOI target masks for each subject were generated using the JHU WM probabilistic atlas in fslview. The tracts included in our analysis were the forceps major, forceps minor, superior longitudinal fasciculus (SLF), inferior frontal occipital fasciculus (IFOF), inferior longitudinal fasciculus (ILF), hippocampal cingulum bundle (hCG), and the corticospinal tract (CST). Average fractional anisotropy (FA), mean diffusivity (MD), radial diffusivity (DR), and axial diffusivity (DA) measures were calculated for each TOI using fslstats. In order to correlate WM integrity with cognitive-motor performance, mean diffusivity measures extracted from each TOI were correlated with kinematic measures from the non-standard task using Pearson's r in SPSS. Statistically significant correlations are reported at $p < .05$.

Results: The isolated TOIs from which mean diffusivity measures were extracted for correlational analyses are displayed in Figure C.1. MD and DA were not significantly correlated with any of the kinematic measures, however significant correlations were found for measures of FA and DR. Specifically, significant negative correlations were found between FA and RT (Fig. C.2A), MT (Fig. C.2B), and VE (Fig. C.2C) within several TOIs. Accordingly, significant positive correlations were also found between DR and RT (Fig. C.2A), MT (Fig. C.2B), and VE (Fig. C.2C), as well as on-axis CE (not shown in Fig. C.2). Statistics for these TOI-based FA and DR correlations are listed in Tables C.1 and C.2, respectively.

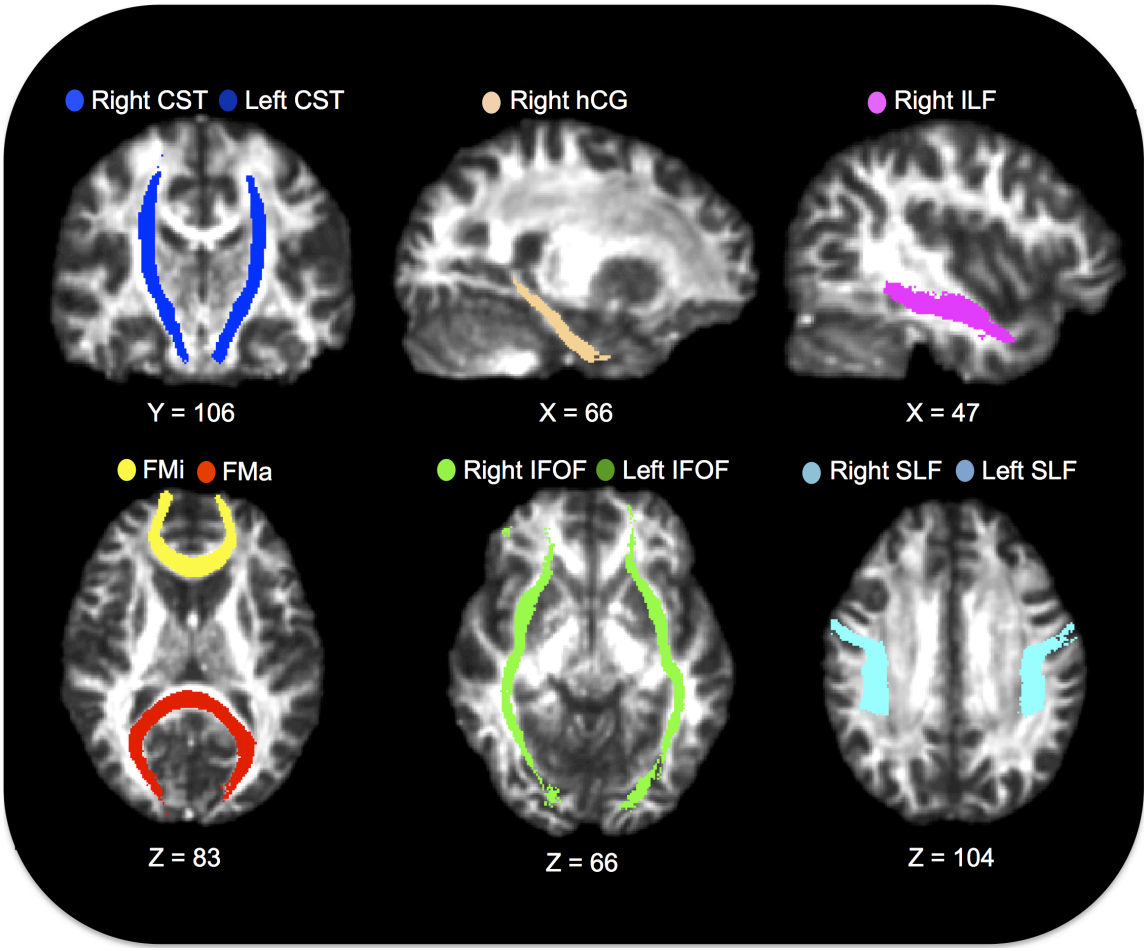

Figure D.1. Example tract of interest (TOI) target masks generated using the Johns Hopkins University's (JHU) white matter probabilistic atlas and color-coding for correlation scatterplots. CST: corticospinal tract; hCG: cingulum (hippocampal region); ILF: inferior longitudinal fasciculus; FMi: forceps minor; FMa: forceps major; IFOF: inferior fronto-occipital fasciculus; SLF: superior longitudinal fasciculus.

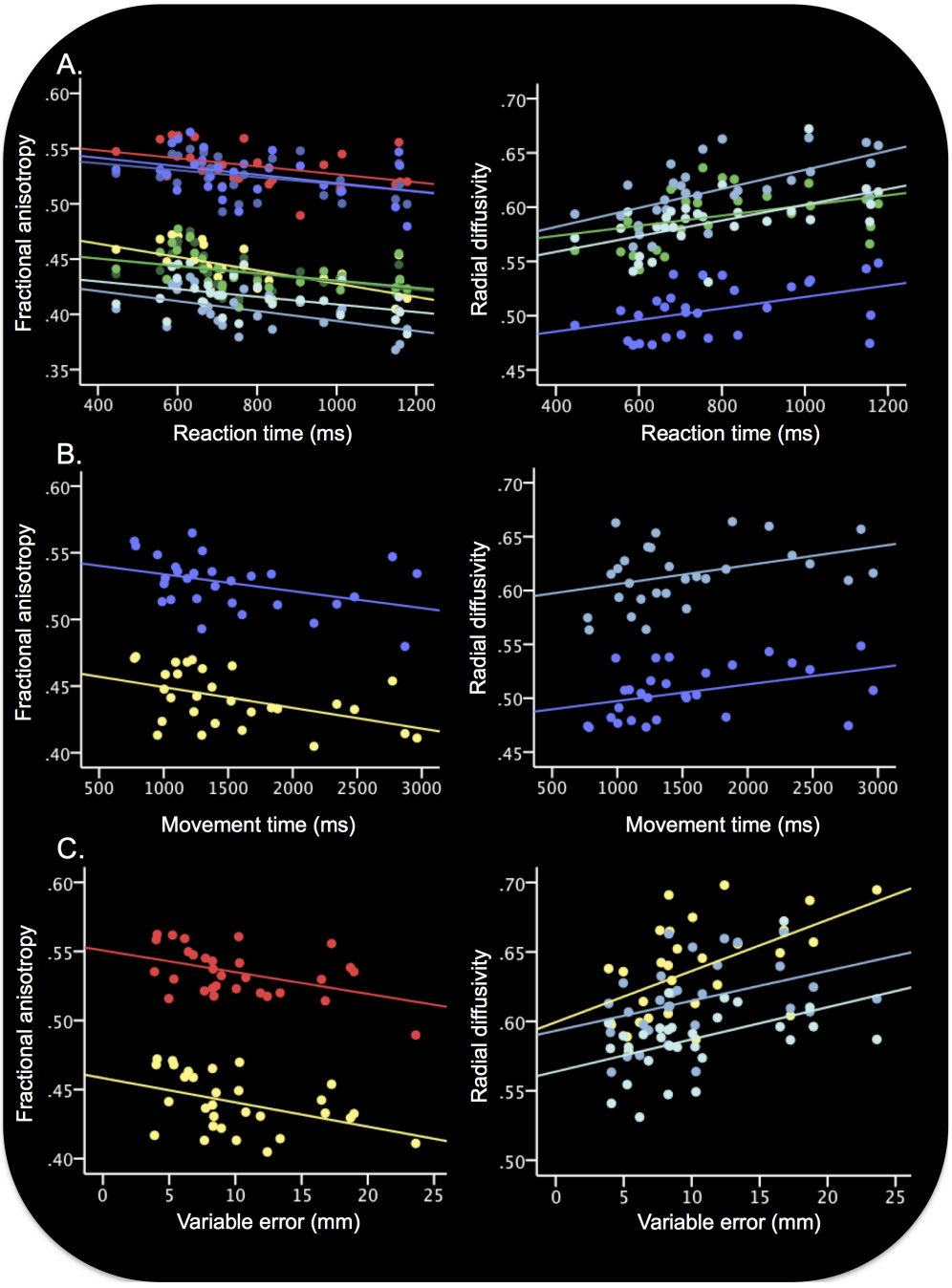

Figure D.2. Scatterplots of significant correlations between diffusivity measures (FA/DR) and **A.** reaction time, **B.** movement time, and **C.** variable error. Correlation statistics listed in Tables C.1 and C.2.

Table D.1

Mean FA correlations with cognitive-motor kinematics

Kinematic measures	TOI	*r*	r^2	*p* (2-tailed)
Reaction time	Forceps minor	-0.58	0.34	0.001
	Left SLF	-0.54	0.29	0.003
	Left IFOF	-0.43	0.19	0.019
	Forceps major	-0.41	0.17	0.026
	Right SLF	-0.41	0.17	0.027
	Right IFOF	-0.39	0.15	0.038
	Right CST	-0.39	0.15	0.039
	Left CST	-0.38	0.15	0.041
Movement time	Forceps minor	-0.47	0.22	0.011
	Right CST	-0.40	0.16	0.034
Variable error	Forceps major	-0.46	0.21	0.011
	Forceps minor	-0.43	0.19	0.018

TOI, tract of interest; see Figure D.1 for other abbreviation definitions.

Table D.2

Mean DR correlations with cognitive-motor kinematics

Kinematic measures	TOI	*r*	r^2	*p* (2-tailed)
Reaction time	Left SLF	0.62	0.39	0.000
	Right SLF	0.54	0.29	0.002
	Right CST	0.45	0.20	0.015
	Right IFOF	0.37	0.14	0.049
Movement time	Right CST	0.40	0.16	0.031
	Left SLF	0.38	0.15	0.041
Variable error	Forceps minor	0.54	0.29	0.002
	Right SLF	0.43	0.19	0.017
	Left SLF	0.39	0.15	0.035
On-axis constant error	Forceps minor	0.40	0.16	0.028
	Rights CST	0.36	0.13	0.050

TOI, tract of interest; see Figure D.1 for other abbreviation definitions.